BLENDING APPROACH FOR SOIL MOISTURE RETRIEVAL USING MICROWAVE REMOTE SENSING

Thesis submitted to the Andhra University, Visakhapatnam
in partial fulfillment of the requirement for the award of
Master of Technology in Remote Sensing and GIS

ANDHRA UNIVERSITY

Submitted By:
S. Anudeep

Supervised By:

Dr. Bhaskar R. Nikam
Scientist/Engineer 'SD',
Water Resources Department,
Indian Institute of Remote Sensing,
Dehradun

Dr. Praveen K. Thakur
Scientist/Engineer 'SE',
Water Resources Department,
Indian Institute of Remote Sensing,
Dehradun

Indian Institute of Remote Sensing, ISRO,
Dept. of Space, Govt. of India Dehradun – 248001
Uttarakhand, India
August, 2013

CERTIFICATE

This is to certify that this thesis work entitled "***Blending Approach for Soil Moisture Retrieval Using Microwave Remote Sensing***" is submitted by Mr. S. Anudeep in partial fulfillment of the requirement for the award of ***Master of Technology in Remote Sensing and GIS*** by the Andhra University. The research work presented here in this thesis is an original work of the candidate and has been carried out in Water Resources Department under the guidance of Dr. Bhaskar R. Nikam, Scientist/Engineer 'SD' and Dr. Praveen Kumar Thakur, Scientist/Engineer 'SE' at Indian Institute of Remote Sensing, ISRO, Dehradun, India.

Dr. Bhaskar R. Nikam
Scientist/Engineer 'SD',
Water Resources Department,
Indian Institute of Remote Sensing,
Dehradun

Dr. Praveen Kumar Thakur
Scientist/Engineer 'SE',
Water Resources Department,
Indian Institute of Remote Sensing,
Dehradun

Dr. Shiv Prasad Aggarwal
Head,
Water Resources Department,
Indian Institute of Remote Sensing,
Dehradun

Dr. Y.V.N. Krishna Murthy
Director,
Indian Institute of Remote Sensing,
Dehradun

Dr. S.K. Saha
Dean (Academic),
Indian Institute of Remote Sensing,
Dehradun

Dedicated to the most lovable and dearest parents.
To my dad and maa.

Acknowledgement

First and foremost I would like to extend my full thanks to Dr. Bhaskar R. Nikam for being an excellent supervisor throughout since the time of synopsis till the end. His expertise knowledge in this field and his vast experience has led me to complete my research project with a great success. His comments, updates and his constant support was by far the best to successfully take my project to completion and helped me to bygone all the hurdles during the path way.

I would also like to extend my sincere thanks to Dr. Praveen K. Thakur for being a supportive co-supervisor who helped me in undertaking this respective project work.

I extend my thanks to Dr.Vaibhav Garg, Course Coordinator, too for providing and accessing with any help and support during my course work and project work in IIRS.

I would like to thank and express my gratitude to my head of department Dr. S.P.Aggarwal for staying throughout the time as a motivation and helped us complete the project without any trouble. His comments, suggestions are always treasured for the constant development of the project work.

I would also like to express my gratitude to Mr. Kamal Pandey for his help in understanding the IDL code for extracting the soil moisture data from the gridded ASCAT data.

I thank Dr. Y.V.N.Krishna Murthy, Director, IIRS and extend my sincere gratitude towards him for his support and encouragement throughout my research period at IIRS with timely suggestions about the improvement of the research work and about the innovation which can be added further for a better end product. His constant support has led me to a very encouraging and optimistic mindset to complete the project with high user end applications.

I would like to extend my thanks to Andhra University for providing the Masters of Technology degree.

I would like to extend my farthest thanks to Stefan Kern from Integrated Climate Data Centre (ICDC), CliSAP/Klima Campus, and University of Hamburg, Hamburg, Germany for providing me the necessary dataset with my request. I also extend me greatest thanks to Dr. Wolfgang Wagner, Head, Institute of Photogrammetry and Remote Sensing (I.P.F.) Vienna University of Technology (TU Wien) for providing me the ASCAT data globally and have been a very important part for my success of the project.

I also extend my heartiest thanks to Dr.Yi Liu, Wouter Dorigo, Richard Kidd, and Matthew McCabe for their constant replies for various queries and have provided solutions to various problems, without which the task of completion would have been a tough task.

I would like to extend a whole hearted thanks to my very dear friend and roommate Suman Kumar Padhee for his immense help in programming. His knowledge and skills on programming has provided me a great help and the realization of code and its simulation was successfully performed. I would also like to thank Mr. Arpit Chouksey for his friendly support and optimistic view of the problems.

I would like to thank all my dearest friends Raju, Suman, Gaurav, Vineet, Tarul, Bikram, Akarsh, Dinesh, Prateek dada, Kirthiga, Surya IFS, Priyanka and Suruchi for their continuous support and encouragement throughout the time in IIRS. I would like to thank M.Sc friends Deepak sir, Shankar, Pavan Kolluru, Ravi Maurya too. I would also like to thank my junior friends, Shishant Gupta and Kirtika Kothari and Ponraj. They have been a solid pillar for me at every moment and their encouragement had led me to a success. Every rough time and happy moments with them will be remembered forever and will be nourished for a long time.

I extend my biggest and whole hearted thanks to my most loving and dearest parents and my brother Anurag, without whom I would have not accomplished any success and triumph. Their belief and trust had made me establish new endeavors. Dad's continuous encouragement and maa's constant love and concern are always over whelming and led me to a great accomplishment.

Date: 19th August 2013 ***S. Anudeep***

ABSTRACT

Soil moisture is an important element in hydrology having wide impact on all other elements of hydrological cycle. It also plays a very major role in the development of weather patterns. Soil moisture is highly dynamic in both temporal and spatial domains. Measuring or mapping soil moisture using field based techniques is not only laborious and time extensive but also has disadvantage of spatial and temporal coverage. To overcome these limitations remote sensing techniques along with modeling techniques are being utilized in recent times.

Soil moisture mapping using remote sensing techniques is mainly classified in two main categories based on type of data used, i.e., active and passive remote sensing based techniques. There are number of operational missions available globally for mapping soil moisture using passive microwave remote sensing, but this techniques lacks in spatial resolution of soil moisture product. Active microwave remote sensing data has additional advantage of high spatial resolution and all weather capability but it lacks in spatial coverage and temporal resolution. Hence the technique of blending the data from various passive and active microwave remote sensing sensors becomes essential to achieve high resolution (temporally and spatially) soil moisture product at regional, national or global levels. An attempt of blending of the soil moisture products derived from various sources of data (active and passive microwave) has been done in present study. The blended soil moisture product has higher spatial and temporal resolution.

In present study, the AMSR-E brightness temperature data is used for the year 2009, to map the soil moisture over India by parameterizing the various surface variables (soil and vegetation) in AMSR-E soil moisture retrieval algorithm. The parameters of AMSR-E algorithm were obtained from various sources as AIRS, USGS and other data sources. The roughness coefficients, height parameter (h) and polarization mixing parameter (Q) are calibrated as per the local vegetation and surface conditions which mainly depend on soil type, soil texture and plant type. The formula proposed by Dobson *et al.*, (1984), correlating the emissivity, volumetric water content to sand and clay fraction is used to estimate the brightness temperature. *Levenberg-Marquardt algorithm* is applied to estimate the value of volumetric water content. The errors pertaining in the estimated soil moisture map from the brightness temperature map of AMSR-E due to RFI and unavailability of the ground soil moisture data for the validation has forced to use the original satellite soil moisture product.

Soil moisture data product derived from Advanced Scatterometer (ASCAT), onboard MetOP (Meteorological operation satellite), is aptly used for year 2009 for blending process using the cumulative distribution function (CDF) matching technique. The soil moisture data derived from passive and active microwave are rescaled to the scale of GLDAS-Noah model by CDF matching, to derive the high spatial and temporal blended soil moisture product. Rescaling the soil moisture product keeping GLDAS-Noah data as the reference is performed by segmenting the cumulative distribution frequency (CDF) curve at definite intervals. Slope and intercept for

each segment is estimated to derive a linear equation. All the original soil moisture values present in a specific segment are rescaled to the reference data with the use of the linear equations developed. The blended soil moisture data is obtained by merging i.e. by taking the average of the two dataset. Blending process is performed initially pixel wise for various locations and then for the complete study area.

The blended soil moisture dataset has a good correlation of 0.6 with that of the in-situ soil moisture data. The blended soil moisture data follows a similar trend as per the rainfall, whereas AMSR-E or ASCAT lacks this trend. The spatial gaps available in the soil moisture dataset, where there is unavailability of data is eliminated by the blended product. The main benefit of this blending approach is the improvement in temporal resolution and good spatial coverage.

Table of Contents

List of Figures

List of Tables

CHAPTER -1
INTRODUCTION

The soil moisture is defined as the volume fraction of water held in the soil and is an important part of the hydrological cycle. A soil can be visualized as the structured skeleton of solid particles enclosing continuous voids. All soils are permeable materials which mean that water is freely allowed to flow through the interconnected network of pores between the solid particles. The relatively thin layer of soil on the surface of the earth is a porous material of extensively varying properties.

1.1 SOIL CHARACTERISTICS

The earth surface that is marked by the zone of aeration is the region in which pore spaces are filled with both air and water. The water present in that zone, pertaining the pores of rocks and soil is known as suspended or vadose zone or commonly it is also known as the soil moisture. The moisture present in the zone of aeration is present as gravity water in larger pore spaces and capillary water in subsequently smaller pores, as hygroscopic moisture holding to the soil grains as a water vapor. After a rainfall, the water may move downward in the larger pores, which disperses into capillary pores or pass through the zone of aeration to the groundwater or to the stream channel. The hygroscopic water is held by molecular attraction and it is not removed normally from the soil under usual climatic conditions. The soil moisture thus is highly variable in space and time depending upon various conditions prevailing.

The soil characteristics depends on the kinds and sizes of individual particles it beholds and importantly also on the arrangement and the bonding pattern of these particles. Generally they occur as the collection of the individual grains as that of sand, but they are linked into clusters or aggregates of varying stability. The properties of the consisting materials or particles are masked by the clustering which has a profound effect on the soil behavior. In between the particles, there exists an intricate system of pore spaces which is the main factor for the storage and movement of water and air.

1.2 APPLICATION OF SOIL MOISTURE

Soil moisture is highly variable both spatially and temporally in the environment, due to the heterogeneity of soil properties, topography, land cover, rainfall and evapotranspiration. Soil moisture has a wide range of applications and uses in hydrology, agriculture and meteorology. It influences all the major hydrological, meteorological and agricultural processes. Soil moisture is a prime source of water for evapotranspiration over the continents, and is involved in both the water and the energy cycles. Soil moisture affects the transfer of water vapor into the atmosphere. Dry soil can contribute very little to no moisture to atmosphere through the process of evaporation/evapotranspiration whereas, saturated soils can contribute hugely to atmosphere, as land surfaces that become flooded can create their own closed-loop as the evaporated

moisture forms local clouds that continue to add to the system through continuing precipitation. Thus soil moisture is a key component in the land surface schemes in global climate models because it is linked to evaporation and to the distribution of heat fluxes from the land to the atmosphere. Though, soil moisture has no direct significance in surface energy balance equation but strongly influences several terms such as evapotranspiration and specific heat capacity. Soil moisture has a huge role in estimating water budgets (Wagner, 2008). Soil moisture value is also important as to quantify the amount and variability of regional water resources in water limited regions on seasonal and annual time scale. The water conservation and management strategies need the information on the use and flow of water. The soil moisture patterns aid in the delineation of hydronomic zones (Molden *et al.,* 2001). Some of the major application areas of soil moisture are discussed below;

1.2.1 Numerical Weather Prediction

In Numerical Weather Predication (NWP) models it has been reported by researches that near surface parameters get influenced by soil moisture and they affect the heat and water between the soil layer and the lower atmosphere. Prior knowledge of soil moisture distribution is mandatory to raise the quality of forecast for numerical weather predictions. Taking precipitation into consideration, the feedback process between increase of evapotranspiration and precipitation is the main interest field (Ferranti and Viterbo, 2006, Dharssi *et al.,* 2011).

1.2.2 Runoff Forecasting

Precise food forecasts mainly depend on estimated current hydrological conditions during the time of forecast. Soil moisture acts as one of the key variables in flood forecasting models, as these models provides the information of rainfall portioning into infiltration and runoff when reaching the ground surface. The space borne remote sensing sensors provide an integral value of soil water content over an area for forecasting other hydrological parameters rather than a point values observed traditionally and the remote sensing derived data is generally available at global scale. Another subsequent use of remote sensed soil moisture data to support runoff predictions is by estimation of antecedent soil moisture (Brocca *et al.,* 2009, Matgen *et al.,* 2012).

1.2.3 Vegetation and Crop Growth Monitoring

The moisture content in the soil profile is one of the most essential parameters for monitoring and predicting the growth of natural vegetation and also non-irrigated agricultural crops. The root zone soil moisture is the main factor limiting plant growth, especially in arid, semi-arid and temperate climatic zones. The most significant use of soil moisture data is for improving the spatial crop yield modeling, the utilization of the information on spatial variability of top soil moisture as crop input model improves the crop yield simulations spatially as compared to the use of point information by single weather station (Verstraeten *et al.,* 2010).

1.2.4 Epidemic Risk Assessment

Mosquito borne diseases have constantly been a serious public health issue for all the people and also the livestock in tropical, subtropical and semi arid countries like India. The soil moisture data can be used for modeling of the infectious diseases forced due to weather and environmental parameters, mainly mosquito-borne diseases (Montosi *et al.,* 2012).
Soil moisture has an immense application in various fields like environment, atmospheres, and land surface process and in various societal risk assessments too.

1.3 REMOTE SENSING FOR SOIL MOISTURE MEASUREMENTS

New and improved methods of remote sensing have tremendously increased the understanding of land surface and its parameters. The mapping of soil moisture using the remotely sensed data has been done since a long time. The soil moisture is subject to rapidly change in time and shows significant variability with depth and space. A complete and obsolete description of soil moisture behavior requires frequent and three-dimensional measurement. The visible section of the electromagnetic spectrum has been used to map the soil moisture widely in the past, as it is simple to operate and applicable at various spatial and temporal scales but the biggest disadvantage lies, as the estimation requires the cloud free condition and high sensitivity towards soil and vegetation parameters which visible or optical remote sensing lacks, which has led the estimation to be done in microwave domain (Christopher Scott *et al.,* 2003).
Microwaves have the capability to penetrate clouds so they can operate in all weather conditions. These are highly sensitive to the moisture content. They are capable of penetrating into the ground itself. The depth of penetration is function of moisture content in the soil. The microwaves are sensitive to the presence of moisture in the soil as well as vegetation. The Sensitivity of the microwaves with response to soils and soil moisture coupled with relative transparency of the atmosphere makes the microwave remote sensing very well suited for soil moisture estimations. To understand the process of soil moisture estimation/mapping using microwave remote sensing it is prerequisite to understand the properties of soil, soil moisture and their interaction with microwave pulse.

Soil moisture mapping has been performed using optical, thermal infrared and microwave remote sensing. The method of using optical remote sensing has as advantage that it is simple to operate and it is applicable at a range of spatial and temporal scales. Thermal infrared remote sensing technique of estimation soil moisture has a benefit that it provides an integrated soil moisture value for the root zone and the technique is always cost effective. Though these are beneficial techniques they have certain limitations, for proper soil moisture retrieval cloud free condition is required which optical and thermal remote sensing lacks. A disadvantage in thermal remote sensing is depth of the root zone which is variable across an image. Considering these limitations, microwave remote sensing provides soil moisture measurements in all weather conditions with a good physical basis. The penetration capability of microwave sensing is much higher than the visible and thermal remote sensing (Christopher *et al.,* 2003).

As in the study, wet soil medium is in general a mixture of soil particles, air voids, and liquid water. The water contained in the soil usually is divided into two fractions, bound water and free water. Bound water refers to the water molecules contained in the first few molecular layers surrounding the soil particles. The amount of water contained in the first molecular layer attached to the soil particles is directly proportional to the total surface area of the soil particles in a unit volume. Electromagnetically, a soil medium is a four component dielectric mixture consisting of air, bulk soil, bound water, and free water. The complex dielectric constants of bound and free water are each functions of the electromagnetic frequency, the physical temperature, and the salinity. The dielectric constant is also a function of the bulk soil density, the shape of the soil particles, and the shape of the water inclusions (Hallikainen *et al.*, 1985).

The variation of dielectric constant of dry material and that of water is considerably observable. The dielectric constant of dry soil varies between 2-3 depending upon the texture whereas the dielectric constant of pure water is around 80 at room temperature and at around 1 GHz. Thus the difference is vividly seen clearly in the case of wet and dry soil. The dielectric constant is one of the important factors in measuring the soil moisture. The dielectric constant is an electrical property of matter and is a measure of the response of a medium to an applied electric field. The dielectric constant is a complex number which contains a real value (ε') and an imaginary (ε'') part. The real part determines the propagation characteristics of the energy as it passes upward through the soil, while the imaginary part of the constant determines the energy losses.

1.4 CLASSIFICATION OF MICROWAVE REMOTE SENSING

Measurements in microwave remote sensing of soil moisture broadly follow two distinct approaches,

1. Employing passive radiometric measurement.
2. Using active backscattering measurement.

Both the approaches have shown a very acceptable and excellent correlation with the soil moisture content.

However there are significant observable differences in both the approaches of active and passive microwave remote sensing resulting in differing recommended operating frequencies for the measurement of the soil moisture parameter. The frequency difference in microwave remote sensing produces quite a significant difference in the penetration capability. The commonality in the use of both active and passive microwave remote sensing system in soil moisture measurement lies in the large disparity between the dielectric constant of water and dry soil.

1.4.1 Passive Microwave Remote Sensing

The passive microwave remote sensing has shown to be superior for the measurement of soil moisture at lower frequencies. They are limited to coarser spatial resolution of around 10-30 km at L-band and C-band respectively. The added advantage is that they have higher sensitivity

towards soil moisture and less towards the surface geometry. Passive data provide global monitoring of the earth with a daily temporal sampling which is well suited for various numbers of applications like NWP models. There are many passive microwave remote sensors for the measurement of soil moisture as, Advanced Microwave Scanning Radiometer for the Earth Observation (AMSR-E), Soil moisture and ocean salinity satellite (SMOS),Special Sensor Microwave Imager (SSM/I), Tropical Rainfall measuring Mission (TRMM), which are presently operational and providing the satellite data for the globe daily.

1.4.2 Active Microwave Remote Sensing

The active microwave remote sensing system has the capability to provide high spatial resolution imagery that is in the order to meters to some kilometers, but they lack in higher temporal resolution. The data is not retrieved daily as in the case of passive sensors. They are in comparison with passive system, more sensitive to surface roughness, topographic features and vegetation. Over the vegetation cover, the active microwave data have shown a very good capability for the discrimination of vegetation type and forest biomass retrieval. Currently, the active microwave remote sensing through the sensor, Advanced Scatterometer (ASCAT) onboard MetOp provides soil moisture with higher spatial resolution.

1. 5 BLENDING OF PASSIVE AND ACTIVE MICROWAVE DATA

With varied advantages of active and passive microwave remote sensing individually, soil moisture is estimated time to time with higher accuracy and improved dataset. Due to higher needs we combine information derived from both passive and active satellite based microwave sensors which has the potential to offer improved estimates of surface soil moisture at global scale (Liu *et al.,* 2011) with higher spatial and temporal resolutions. The enhancement of information by combining both passive and active microwave products helps in understanding land surface atmosphere interactions these regions (Liu et al., 2012a). One of the approach used practically for combining soil moisture derive from active and passive microwave datasets is the blending approach. Blending is the process of combining two different dataset providing similar information with different units, scale and resolution, after performing the recalling for the satellite derived products. It is a method to merge soil moisture estimates from two different sensors that is from passive and active microwave soil moisture dataset into a single dataset. It has been done previously by Dr.Yi.Liu from University of New South Wales, Sydney, Australia, using six sensors. This technique has an added advantage of improved spatial and temporal soil moisture dataset as compared individually with passive or active soil moisture product.

1.6 PROBLEM STATEMENT

Various techniques and methods/algorithms have been applied to estimate soil moisture using the passive and active microwave remote sensing since a very long time with timely modification of the algorithms for the betterment of the soil moisture values by considering the

ground parameters and other land and atmospheric parameters which are necessary for precise soil moisture measurement at defined spatial and temporal resolution.
Active and passive sensors have their own advantages but they have caveats too due to which the method to estimate soil moisture using only by active or passive is unacceptable. The present hydrological and climatic modeling techniques demands soil moisture information at higher spatial as well as temporal scale. The non-availability of higher spatial and temporal resolution soil moisture data force the researches to relay on model derived soil moisture values which cannot be validated on global scale due to non-availability of observed data. This gap area in soil moisture mapping can be bridged through combining the active and passive soil moisture data products derived using data of various sources (sensors) to enhance the temporal and spatial resolution.

1.7 RESEARCH OBJECTIVE AND RESEARCH QUESTION

Considering the various above said limitations the major aim of the research is to develop a technique or an algorithm to estimate soil moisture which has higher spatial and temporal resolution with acceptable soil moisture values for the particular region. The subsequent objective is to estimate soil moisture from passive microwave remote sensor, by acquiring the brightness temperature value from the passive sensor. This is performed to estimate the quantitative value of soil moisture as per the local conditions prevailing.

1.7.1 Research Objectives

- To parameterize the different medium and sensor parameters used in the soil moisture estimation from passive microwave remote sensing data.
- To develop an algorithm for blending the soil moisture products derived from active and passive remote sensing to obtain higher spatial and temporal resolution.

1.7.2 Research Questions:

- How to estimate soil moisture using passive microwave remote sensing and how to reduce the impediment factors which attenuates the soil moisture estimation?
- How to implement blending of soil moisture products derived using microwave that is active and passive remote sensing data?

CHAPTER - 2
REVIEW LITERATURE

2.1 INTRODUCTION

Soil moisture defined as, a level of saturation in the upper soil layer relative to the soil field capacity, and is functioned by rainfall and evapotranspiration. The two parameters have an important role in the evolution of the soil moisture state and considered significant in the soil water balance equation too. The soil moisture value is generally expressed in volumetric units or in percentage. There are various conventional and remote sensing techniques to estimate soil moisture over the land surface. The microwave remote sensing techniques give large scale spatially distributed and frequent coverage of the phenomenon and combining that information with the *in-situ* measurements provides a quality study of soil moisture.

2.2 SOIL MOISTURE ESTIMATION FROM INDICES

Indexes extract information about the surface characteristics by amplifying the incident signal which allows greater sensitivity in predicting ecological and environmental variables (Khanna *et al.*, 2007). Various indices are there to estimate soil and vegetation moisture based on NIR (858 nm) and SWIR (1240 and 1640 nm). Various indices have been developed as indicators of the soil and vegetation moisture (Fensholt and Sandholt, 2003, Gao, 1996, Moran *et al.*, 1994). The indices like Crop Water Stress Index (CWSI) and Water Deficit Index (WDI) are used to detect soil moisture status based on the thermal bands.

The fundamental absorption for the liquid water is at 3 μm, with several absorptions in short wave infrared (SWIR) band at 1300 to 2500 nm. Gao, (1996) formulated the Normalized Difference Water Index (NDWI) which has become the most commonly used index for plant moisture determination. A new approach was introduced by Palacios-Orueta *et al.*, (2006) where they have parameterized the general shape of the spectrum by measuring the angle formed by three consecutive bands. They have developed two indices, based on the above approach, SASI and ANIR.

2.2.1 Short Wave Angle Slope Index (SASI)

The Short Wave Angle Slope Index (SASI) is a combination of NIR and SWIR bands. The SWIR region could be fitted by an inverted Gaussian function that was highly correlated to moisture content in soils (Whiting *et al.*, 2004). The important point to be noted is, since SASI is sensitive to moisture and not photosynthetic activity, revealing a complete different dynamics than NDVI.

2.2.2 Angle at NIR (ANIR)

The ANIR is combination of reflectance values in red, NIR, and SWIR bands. The soil reflectance increases monotonically from visible through SWIR when the soil is dry. The ANIR has a disadvantage that it is less sensitive to soil moisture level and it is also less a potential tool for discriminating dry plant matter from soil with multiple-band data. In a greener zone, ANIR values are smaller than those in dry plant matter or soils and as dry matter content increases ANIR also decreases. Its range of ANIR is from 0 to 2π radians.

2.2.3 Soil Wetness Variation Index (SWVI)

On the basis of change detection methodology from multi temporal satellite data analysis, a normalized SWI index called as Soil Wetness Variation Index (SWVI) is formulated, which decimates the variation related to the different soil water contents and variations determined by vegetation and roughness effect (Lacava *et al.*, 2005). SWVI is only sensitive to SWI variations, mainly depending on the soil moisture and not to its absolute values related to the surface roughness and vegetation cover. The SWI and SWVI are used for an intensive inter-comparison analysis.

The indices have been a very efficient technique to measure soil moisture and vegetation effect on that respectively. The indices like NDVI, NDWI, SASI, ANIR, SWVI and WDI have been widely used to estimate various measures as the amount of vegetation, soil moisture, and surface conditions. They provide data that is ground dependent and can be used for calibration and validation purposes.

2.3 GROUND BASED SOIL MOISTURE ESTIMATION METHODS

The ground based techniques involve the soil moisture estimation where the instrument is in direct contact with soil particles and provides more precise data (Dobriyal *et al.*, 2012). The point measurements are taken at any time scale by these instruments which can be accurately calibrated and give depth wise measurements of soil moisture.

2.3.1 Gravimetric Method or Thermostat-Weight Technique

Soil moisture content estimation is done widely by this technique (Schmugge *et al.*, 1980).This technique involves oven drying a soil sample of known volume at 105^{o}C for 24h. The resultant water content is calculated by subtracting the oven dry weight from initial field soil weight. The main advantage of the technique is that it is cost efficient, easy and accurate too. Although the disadvantage is, it is laborious, time intensive and difficult when soil is rocky (Stafford, 1988).

2.3.2 Neutron Probe Technology

In this instrument, it consists of a probe and an electron counting scalar connected by an electronic cable. A very high energy, fast moving neutrons are ejected into the soil by a

radioactive source. The released neutrons are slowed down by the collision with the nuclei of the hydrogen atoms present in the molecules of water in the soil (Chanasyk and Naeth, 1996). They are accurate and irrespective of the state of the water. The output from this instrument is directly linked to the soil moisture. The only limitation is that it is expensive equipment and requires extensive soil specific calibrations. The depth of the resolution is inadequate, which eventually makes soil moisture measurement a difficult task.

2.3.3 Tensiometers

It measures the capillary or moisture potential on the basis of suction force exerted on water by soil (Schmugge *et al.*, 1980). This instrument is cost effective and technique is non-destructive. It is well capable of measuring the water content in both saturated and unsaturated conditions. It produces continuous measurement without disturbing the soil. The only limitation is that it is unsuitable in dry soils and this instrument requires high maintenance because of which it is not extensively used in the research.

The others ground based soil moisture measuring methods are, time domain reflectometry, capacitance and frequency domain reflectometry, gypsum block measurements, pressure plate method, ground penetrating radar method. They all have their own advantages and disadvantages for measuring soil moisture for different soil type and with different penetration with varying accuracy.

2.4 MICROWAVE REMOTE SENSING

Microwave remote sensing provides a unique capability for direct observation of soil moisture. Remote measurements from space provide us the possibility of obtaining frequent, global sampling of soil moisture over a large fraction of the Earth's land surface. As known, microwave measurements have the benefit of being largely unaffected by cloud cover and variable surface solar illumination.

The principle of microwave remote sensing of soil moisture is basically based on the sensitivity of soil permittivity to the amount of liquid water. The permittivity of a medium, like moist soil, characterizes electromagnetic wave propagation and attenuation in the medium. The soil brightness temperature is dependent on the soil permittivity value (Wardlow *et al.*, 2012). The difference between the dielectric constant of water (about 80 at frequencies below 5 GHz) and that of dry soil (about 3.5) is very large and significant, due to which the emissivity of soils varies from approximately 0.6 for wet (saturated) soils to greater than 0.9 for dry soils. These variations are observed both by passive and active microwave sensors. For a soil at a temperature of 300 K this variation in emissivity corresponds to a soil brightness temperature variation of 90 K (Njoku and Entekhabi, 1996). This arises from the tendency of electric dipole of the water molecule to align itself with the electric field at microwave frequencies (Schmugge *et al.*, 1993). Various empirical models have been developed in order to provide a relation between volumetric water content for different soil types to that of dielectric constant at microwave frequencies (Hallikainen *et al.*, 1985, Dobson *et al.*, 1985).

2.5 FACTORS INFLUENTIAL IN MICROWAVE REMOTE SENSING

The factors affecting the soil brightness temperature are mainly, soil surface roughness, attenuation and emission by vegetation cover, surface heterogeneity, some lesser degree to soil texture and variability in temperature of the soil and vegetation.
The low frequency microwave range of 1-3 GHz that is less than 5 GHz is considered the most suitable for soil moisture sensing (Jackson *et al.*, 2002). This wavelength is preferred owing to reduce the atmospheric attenuations and greater vegetation penetration, though it increases the errors due to radio frequency interferences.

2.5.1 Dielectric Constant

The measurements of dielectric constants as a function of soil moisture have been carried out over a wide microwave frequency range. The measurements were made for soils with different texture structures. Two distinct features associated with the relation between the soil dielectric constant and moisture content has emerged from the study (Spans, 1978).

1) The dielectric constant increases slowly with moisture content and after reaching a transition moisture value, the dielectric constant increases steeply with moisture content for all soils.
2) The transition moisture is found to vary with soil type or texture.

2.5.2 Surface Roughness

The surface roughness has a profound effect on the soil moisture. Surface roughness is an important variable and its knowledge is important for many models too. Roughness parameters are also very variable in space. For instance, in the agricultural fields where the crops are grown, the soil surface remain untilled from sowing till the harvest and during this period of time the surface roughness is assumed to be constant and soil moisture estimation technique is simplified that is soil moisture variation is a consequence of its dynamics. During the agriculture inactive period the assumption of constant roughness condition simplifies the soil moisture estimation. It is important to evaluate the variations of surface roughness occurring over the growing season and to assess their influence on the estimation of soil moisture from satellite data (Álvarez-Mozos *et al.*, 2009).

2.5.3 Bulk Density

Soil, bulk density and microwave have a distinct relationship. The microwave emission from the soil surface reduces as bulk density of soil increases. The increasing bulk density of soil affects the dielectric properties of dry and moist soil. It has been seen that, dielectric parameters of soil at microwave frequencies are mainly the function of various properties of soil such as texture, moisture, bulk density, temperature, and soil type (Gupta and Jangid, 2011).

2.6 PASSIVE MICROWAVE REMOTE SENSING

Wigneron *et al.*, (2003) have shown a very broad way to retrieve soil moisture considering the factor of vegetation canopy. The effect of vegetation has to be considered as vegetation absorbs and reflects part of microwave emission from the soil surface. The three main retrieval approaches are, statistical techniques, forward model inversion and use of neural networks.
In the statistical approach the land surface information is retrieved by directly manipulating the measured signals through the empirical relationship as:

$$X_j = F_j(T_{B,1}, T_{B,2}, \ldots T_{B,n}).$$

where $T_{B,i}$ corresponds to the sensor configuration and x_j is the respective land surface variable. Statistical method is done based on the classification on dual or multi configuration observations or the surface soil moisture is statistically related to combination of microwave emissivity and vegetation indices. The important aspect to be considered here is that, it is a site specific method which adds to its limitations.

The forward model inversion is used to simulate the microwave radiometric measurements as a function of land surface characteristics. Here the limitation observed is that, a prior knowledge of functional form of the process that is to be modeled is needed and multi-scattering effects are taken into account which further requires large number of inputs.

One of the forward model approach mentioned in the Wigneron *et al.*, (2003) is statistical inversion approach where the principle is to search for input parameters, consisting of geophysical parameters that minimizes the squared error between the brightness temperature measured from satellite data and actual output of the model.

The neural network (NN) method of estimation of soil moisture another widely used way in remote sensing for the soil moisture estimation. Here, an appropriate set of input-output data is generated, using the forward model. Then the copy of forward model is made by training the NN on the set of data. The advantage in this method is that, once the neural network is trained, parameter inversion can be accomplished quickly.

In Hui Lu *et al.*, (2009) the algorithm developed to retrieve the moisture content is based on a modified radiative transfer (RT) model, in which the volume scattering measurement inside the soil layer is calculated through dense media radiative transfer theory (DMRT) (Wen *et al.*, 1990) and the surface roughness effect is simulated by Advanced Integration Equation Model (AIEM) (Chen *et al.*, 2003). Using the optimized parameter value, The forward model is executed to generate the lookup table, which relates the soil moisture content to the brightness temperature. Then, the soil moisture content is estimated by linearly interpolating the brightness temperature into inversed lookup table. In this, it has presented the structure of the soil moisture retrieval algorithm for the space borne passive microwave remote sensing.

Microwave remote sensing offers great possibility of quantifying the surface soil moisture condition over spatial extent (Champagne *et al.*, 2011). This research examines the use of surface soil moisture to derive the soil moisture anomaly. Four methods were used to spatially aggregate information to develop an anomaly. Two methods used soil survey and climatologically zones to define the region of homogeneity, while the other two methods used zones defined by data driven segmentation of satellite soil moisture data. This method is used to

assess the condition of the soil moisture at large spatial scale which can have further implications like drought assessment etc.

2.7 RELATIONSHIP BETWEEN DIELECTRIC CONSTANT AND VOLUMETRIC WATER CONTENT

It is very important to understand the relationship between the effective dielectric constant of the soils and the volumetric water content as it used to determine the soil moisture content. Various empirical relations have been suggested for the relationship between the dielectric constant and the vol. water content. The most common one is that of Topp *et al.*, (1980) –

$$\varepsilon_{eff} = 3.03 + 9.3\theta + 146\theta^2 - 76.7\theta^3$$

It was suggested that another constant that is, bound water be added with lower dielectric constant than that of free water as in Dobson *et al.*, (1985).

While the function proposed by Dobson *et al.*, (1984) also takes into account the soil texture by allowing its coefficients to be dependent on the clay and sand percentages:

$$\varepsilon_{eff} = 2.37 + (- 5.24 + 0.55 \times \%sand + 0.15 \times \%clay)\theta + (146.04 - 0.75 \times \%sand - 0.85 \times \%clay)\ \theta^2$$

The models relating the volumetric soil moisture and the dielectric constant are needed in the study (Peplinski *et al.*, 1995).

The review of all the literature and journals had given the conclusion that passive microwave remote sensing has the pronounced ability to detect and map the surface soil moisture due to its penetrating ability and due to its ability to detect the vegetation canopy, surface roughness and other surface parameters at all weather conditions. The added advantage of the passive microwave remote sensing for the soil moisture retrieval is that, it provides the data with good temporal resolution. The data is available on the daily basis and the only demerit is that of the spatial resolution. The spatial resolution is not so fine; the soil moisture is available at a coarser resolution and from the top layer only (Christopher Scott *et al.*, 2003)

2.8 ACTIVE MICROWAVE REMOTE SENSING

Several algorithms have been developed to infer the soil moisture using active microwave remote sensing. The information on multiple radar channels, usually multiple polarization, are required to separate the effect of surface roughness and surface dielectric constant to extract the soil moisture information (van Zyl and Kim, 2001). The high sensitivity of active microwave sensors with respect to soil moisture is the key element in the active microwave remote sensing (Ulaby and Batlivala, 1976, Ulaby *et al.*, 1978, Dobson and Ulaby, 1986), The backscattering coefficient (σ_o) describes the amount of average backscattered energy compared to the energy of the incident field. The intensity of σ_o is a function of electrical and physical properties of the target, wavelength, polarization and incidence angle of the radar. Vegetation and surface roughness are another prominent factors affecting the incident microwave radiation (Barrett *et al.*, 2009).

The first-order small perturbation model used to estimate the soil moisture is used to describe scattering from slightly rough surfaces. Using this model, it is seen that the ratio of the two co-polarized radar cross section in the linear basis is independent of the surface roughness. The model has the disadvantage that it is only applicable to smooth surfaces. The first-order small perturbation inversion will tend to underestimate the surface dielectric constant in the presence of significant roughness (van Zyl and Kim, 2001).

Based on the algorithm proposed by Oh *et al.*, (1992), they have developed an empirical model in terms of the RMS surface height, the wave number and the relative dielectric constant. Here the roughness and the soil dielectric constant are explicitly given in terms of co-polarization ratio (p) and cross-polarization ratio (q). Expression is developed in terms of surface dielectric constant from the above said parameters.

Dubois *et al.*, (1995) have developed an empirical model that requires only the measurement of co-polarized radar cross section, between the frequency 1.5 and 11 GHz to retrieve mainly surface RMS height and soil dielectric constant from the bare soil. This algorithm is only applicable to the surfaces with roughness coefficient value less that 3.0 and angle of incidence to be in between 30^{o} to 70^{o}.

The above said models do not take into consideration the shape of the surface power spectrum which is related to the surface roughness correlation function and correlation length.

Although, In the algorithm proposed by Shi *et al.*, (1997) the backscattering coefficients are sensitive to soil moisture, surface RMS height and the shape of the surface roughness power spectrum.

All the empirical models developed from a limited number of observations might give site specific results because of the nonlinear response of backscattering to the soil moisture and surface roughness parameters.

The integrated equation model (IEM) (Fung *et al.*, 1992) which is a physically based radiative transfer model provides an alternate approach for the retrieval of soil moisture from the radar data. It is applicable for a wide range of surface roughness conditions; however the complexity of this model makes it difficult to infer soil moisture and roughness parameter. This model essentially quantifies the backscattering coefficient as a function of unknown soil moisture content and surface roughness and known radar configuration.

In the IEM, it is only applicable for single scattering terms where second order scattering is not considered. Thus for the consideration of multiple scattering terms improved IEM model (Fung *et al.*, 1996) is applied.

The various complexity and difficulty encountered in the application of theoretical models has led to the development of the empirical and semi-empirical models (Neusch and Sties, 1999). The backscattering models have been employed through simple retrieval algorithms. These types of models have the disadvantage that they are generally derived from specific data sets, valid only to that area which is under the investigation (Chen *et al.*, 1995). Here, large databases of study sites are important to ensure that developed models are quite robust and transferable to other datasets, irrespective of the sensor and surface conditions (Baghdadi *et al.*, 2008).

The semi empirical models provide a link between the complexity of the theoretical models and simplicity of the empirical models which may be applied with little information

about the surface roughness (D'Urso and Minacapilli, 2006,). The main advantage of these types of models is that they are site independent – a problem associated generally with empirical backscattering models.

The most recent technique of soil moisture retrieval is by using polarimetric parameters. The parameters are coherence, entropy and alpha angle (α). The polarimetric measurements (Raney, 2007, Dubois-Fernandez *et al.*, 2008) are used to study the dependence of polarimetric signature on surface parameters such as soil moisture and surface roughness.

The main characteristics of the polarimetric data are that, it allows the discrimination of various types of scattering mechanisms within an imaged cell. The major advantage is its ability to measure all the polarization characteristics of the surface.

The study of various literatures on the active microwave remote sensing had provided a conclusion that the estimation of soil moisture from active microwave remote sensing is a very profound way of measurement. The added advantage of high spatial resolution is the main reason to use the active remote sensing. Active microwave remote sensing can be done at any time irrespective of the atmosphere that is it can be done even if there is no cloud free condition also (Christopher Scott *et al.*, 2003). The added advantage of this is high sensitivity towards soil moisture content (Barrett *et al.*, 2009). The only demerit in active microwave remote sensing is the lower temporal resolution. The data is not available at the daily basis which is a big setback in the active microwave remote sensor.

2.9 COMBINED ACTIVE AND PASSIVE MICROWAVE REMOTE SENSING

Scatterometer, radar and radiometric responses have often been modeled by separate techniques individually with satisfactory results. However, a discrete scatter microwave model (Chauhan *et al.*, 1994) using both active and passive microwave data is used to retrieve the soil moisture (Chauhan, 1997). The model is according to the established sensor sensitivities to the soil and vegetation characteristics coupled with emission model to estimate soil moisture. The technique has been used to determine the optical thickness and RMS height by active remote sensing and this information is used as ancillary data for inferring soil moisture by passive technique. Here the determination of the parameters is based on the physically based discrete scatter model and thereof this technique holds good for all kinds of vegetation and surface conditions. In this model, the surface roughness inversion algorithm does not require a large database. The main caveat in this model is that it takes various assumptions into the consideration. The various assumptions lead to some quantifying error in the estimated value from the parameter which can only be rectified through ground measurements.

2.10 LEVENBERG-MARQUARDT ALGORITHM

The Levenberg-Marquardt (LM) algorithm is an iterative system that locates the minimum of a multivariate function that is expressed as the sum of squares of nonlinear real valued functions. It is one of the standard techniques for nonlinear least-squares problems. The algorithm is applied to nonlinear least squares minimization.

The function to be minimized is of the form,

$$f(x) = \frac{1}{2}\sum_{j=1}^{m} r_j^2(x)$$

where $x = (x_1, x_2, \ldots, x_n)$ is a vector and r_j is the function and it is assumed that $m \geq n$.
R can also be defined as:

$$r(x) = (r_1(x), r_2(x), \ldots, r_m(x))$$

and similarly f can be written as, $f(x) = \frac{1}{2}\|r(x)\|^2$.

Solving the above equation for the minimum value derives the required parameter estimation. Nonlinear least squares methods Levenberg-Marquardt (LM) algorithm involves an iterative improvement to parameter values in order to minimize the sum of the squares of the errors between the function and the measured data points(Lourakis, 2005, Ranganathan, 2004, McLauchlan, 2001, Henry, 2011).

This minimization function is used to estimate the soil moisture from brightness temperature as input and various other parameters required to estimate the value.

2.11 RADIATIVE TRANSFER (RT) METHOD

The important aspect in the radiative transfer method is the interaction between the radiation from the surface and matter which is explained using two processes, *extinction* and *emission*. The distinction between the two is, if the radiation traversing a medium is reduced in its intensity it is called extinction, and if medium adds energy of it owns it is defined as emission. Both the processes occur simultaneously (Ulaby *et al.*, 1981a).

The fundamental quantity in the formulation of the radiative transfer equation is the specific intensity $I_v(\mathbf{r})$. It is defined in terms of amount of power dP along the direction **r** within a solid angle dΩ through an area dA in a frequency interval (v, v + dv) as,

$$dP = I_v(\mathbf{r})\, \cos\theta dA d\Omega\, dv$$

The dimension of I_v is same as that of the spectral brightness. In the remote sensing domain the radiation at a single frequency is considered. In terms of intensity, the amount of power at a single frequency is written as,

$$dP = I(\mathbf{r})\, \cos\theta dA d\Omega.$$

$I(\mathbf{r})$ is replaced by B for brightness temperature, and the equation governs the variation of intensities in a medium that absorbs, emits and simultaneously scatters the incident radiation (Ulaby *et al.*, 1981b).

This algorithm is used to retrieve the land parameters from microwave remote sensing and specifically used in soil moisture retrievals due to the consideration of various factors and the preciseness of the value.

2.12 PRESENT STUDY

Considering the various advantages and disadvantages of the passive and active microwave remote sensing, where each of which have different sensitivities to soil moisture and vegetation cover, we have induced a technique to blend the passive and active soil moisture data for a higher spatial and temporal resolution in the present study. This process preserves the relative dynamics of the original satellite derived dataset and also establishes a new line of soil moisture data which has a better resolution for the Indian conditions. It provides the opportunity to generate a combined product that incorporates the advantages of both microwave techniques (Liu et al., 2012b, Liu et al., 2011, Wagner et al., 2013a). It moreover enhances the basic understanding of soil moisture in the water and energy cycle respectively.

CHAPTER - 3
STUDY AREA AND DATA USED

3.1 STUDY AREA

As discussed in earlier chapters the spatial resolution for which the soil moisture mapping is done in case of passive microwave remote sensing is of the order 10 to 30 km, hence to analysis the applicability of any algorithm developed for mapping/estimation of soil moisture using microwave remote sensing the study area should be of order thousands of square kilometers, which is a catchment or basin scale in terms of hydrology. Keeping this in mind Ganga River Basin, the largest river basin in India has been chosen as study area for present study. The location map of Ganga River Basin is shown in Fig. 3.1

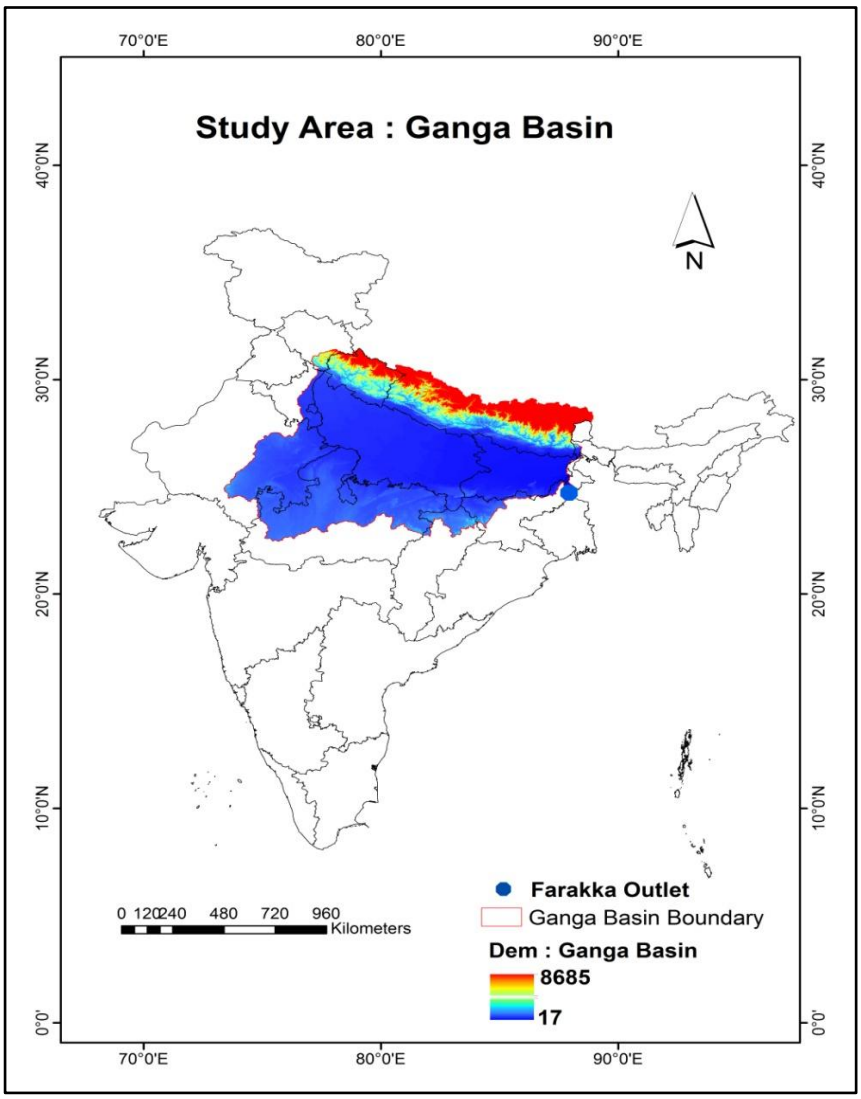

Fig. 3.1: Study Area

The Ganga basin extends its vast stretch over an area of 9,26,080.3734 sq. km, ranks among the largest in the world in drainage basin area and length and it primarily lies in India with Tibet, Nepal and Bangladesh as the other parts where Ganga basin touches, and the extent from 22.625^{o} to 31.375^{o} North and 73.375^{o} to 88.8750^{o} East. The basin is bounded on the north by the Himalayas, on the west by the Aravallis and the ridge separating it from Indus basin, on the southern part by the Vindhyas and Chhota nagpur plateaus and on the east by the Brahmaputra ridge. The outlet of the Ganges basin is considered at the Farakka barrage (24.80^{o} N and 87.93^{o} E).

The river has two main headwaters in the Himalayas - the Bhagirathi and the Alaknanda and others for each of its other tributaries. The Bhagirathi flows from the Gangotri glacier at Gomukh and the latter from a glacier near Alkapuri. Farther downstream, the river is joined by a number of other Himalayan rivers, the Yamuna, Ghaghara, Gomti, Gandak and Kosi. However, the Ganga and its major tributaries, the Yamuna, Ram Ganga, and Ghaghara are the only Himalayan rivers that have significant base and flood flows.

The basin engulfs semi-arid valleys in the rain shadow north of the Himalaya, densely forested mountains south of the highest ranges, the scrubby Shiwalik foothills and the fertile Gangetic Plains. Central highlands south of the Gangetic Plain have cloud touching plateaus, hills and mountains intersected by valleys and river plains. The annual surface water potential of the basin has been assessed as 525 km^3 in India, out of which 250 km^3 is utilizable water. There is about 5,80,000 km^2 of arable land, 29.5% of the cultivable area of India (Source: Ganga basin, Wikipedia).

The basin lies in the States of Uttar Pradesh, Madhya Pradesh, Bihar, Rajasthan, West Bengal, Haryana, Himachal Pradesh and the Union Territory of Delhi.

3.1.1 PHYSIOGRAPHY

The main physical sub-divisions are the Northern Mountains, the Gangetic Plains and the Central Highlands. Northern Mountains includes the Himalayan ranges comprising their foot hills. The Gangetic plains, situated between the Himalayas and the Deccan plateau, constitute the most fertile plains of the basin which is perfectly suited for intensive cultivation. The Central highlands lying to the south of the Great Plains consists of mountains, hills and plateaus intersected by valleys and river plains. They are largely covered by forests. Aravali uplands, Bundelkhand upland, Malwa plateau, Vindhyan ranges and Narmada valley lie in this region.

3.1.2 SOIL TYPE

Predominant soil types found in the basin are sandy, loamy, clay and their combinations such as sandy loam, loam, silty clay loam and loamy sand soils. The cultivable area of Ganga basin is about 57.96 M.ha which is 29.5% of the total cultivable area of the country (Source: Central Water Commission (CWC), India).

3.1.3 River System

The Ganga originates as Bhagirathi from the Gangotri glaciers in the Himalayas at an elevation of about 7010 m in Uttarkashi district of Uttarakhand and flows for a total length of about 2525 km up to its outfall into the Bay of Bengal through the former main course of Bhagirathi-Hooghly (Source: Central Water Commission (CWC), India). The principal tributaries joining the river are the Yamuna, the Ramganga, the Ghaghra, the Gandak, the Kosi, the Mahananda and the Sone. Chambal and Betwa are the two important sub-tributaries. Click for basin map of the sub-basin showing the river system and other features.

3.1.4 Climate and Hydrology

The water supply in the Ganga basin depends partly on the rains brought by the south westerly monsoon winds from July to October, and on the flow from melting Himalayan snows in the hot season from April to June. Precipitation in the river basin accompanies the southwest monsoon winds, but it also comes with tropical cyclones that originate in the Bay of Bengal between June and October. Only a small amount of rainfall occurs in December and January. The average annual rainfall varies from 762 mm at the western corner of the basin to more than 2,290 mm at the eastern. In the upper Gangetic Plain in Uttar Pradesh, rainfall averages about 760-2290 mm whereas in the Middle Ganges Plain of Bihar, from 1016 to 1524 mm and in the delta region, between 1524 and 2540 mm. The delta region experiences strong cyclonic storms both before the commencement of the monsoon season, from March to May, and at the end of it, from September to October.

3.1.5 Important Projects

The Ganga and Yamuna canal systems irrigate vast areas utilizing the perennial flow of the river. Important storages constructed in the basin include Matatila, Sarda Sagar, Ramganga, Mayurakshi reservoirs. Some other important projects are Rajghat on Betwa, Bansagar on Sone and Tehri on Bhagirathi. The hydropower potential of the basin is 10,715 MW at 60% load factor.

3.1.6 Mythological Scenario

The Ganga basin is the cradle of Hindu and Buddhist pilgrimage culture. Some of the most important centers of spiritual learning and healing have thrived for centuries along the Ganges banks. At the headwaters of the Ganga in the Himalayas, sacred shrines at Tapavan, Gomukh, Bhojbasa, and Gangotri mark the sources of illumination. The shrines of Kedarnath and Badrinath also celebrate their position in the upper reaches of the watershed and considered the important shrines of India and Indian culture preserving the deepest heritage of India. Farther downstream in the Himalayas are Uttarkashi and Rishikesh and along the plains lie Haridwar, Allahabad (Prayag), Banaras, Vindhyachal, Nadia and Kalighat. Along the river Yamuna, there are sacred places of Mathura and Vrindavan are located and inland within the Ganga basin, the

Hindu center of Vindyachal and the Buddhist sites of Gaya, Rajgir and Nalanda. In these pilgrimage centers and in countless other smaller sacred spots along her great traverse, pilgrims worship the Ganga and carry away her pure water for worship and purification.

3.2 DATA USED AND DATA PROPERTIES

The various satellite products used in the study are AMSR-E and ASCAT soil moisture product, GLDAS-Noah modeled soil moisture product. The data is chosen for the year 2009 as the AMSR-E has discontinued providing the soil moisture data after October 2010 and simultaneously ASCAT and Noah data is retrieved for the year 2009 only. AMSR-E soil moisture product is preferred for the present research work due to the following reasons:

1. AMSR-E sensor works at the frequency of 6.9 GHz and the Soil Moisture Ocean Salinity mission (SMOS), providing the soil moisture data too operates at the frequency of 1.4 GHz at which radio frequency interference (RFI), Faraday rotation and galactic noise become increasingly significant and is the main sources of error (Njoku and Entekhabi, 1996). Thus AMSR-E is preferred in this study.
2. The algorithm to retrieve soil moisture by using brightness temperature (Tb) of AMSR-E is less complex and in the algorithm it considers all the parameters related and required to estimate soil moisture and surface roughness, whereas SMOS algorithm is more complex and needs much understanding.
3. ASCAT sensor is chosen as the active sensor for the soil moisture which operates at the frequency of 5.3GHz (C-band) and this is closer to the frequency in which AMSR-E operates too, whereas SMOS operates at 1.4 GHz that is in L-band due to which it is not chosen for the present research.
4. A model data is needed for the rescaling purpose in the blending process and from various GLDAS models, mosaic, Community Land Model (CLM), VIC and Noah, Noah is considered best because of its similar spatial resolution as that of ASCAT, as accordingly AMSR-E is chosen having same spatial resolution as that of Noah land surface model.

Noah model is preferred as this model and VUA-NASA algorithm in AMSR-E uses a common soil property dataset (soil map by FAO). Indian Meteorological department (IMD) district wise rainfall data has also been taken from India Water Portal, to establish a correlation and analysis with the soil moisture. Temperature data have been taken from, National Oceanic and Atmospheric Administration - National Climatic Data Center (NOAA – NCDC) which is used in the analysis and comparison with the soil moisture. Ganga basin has been delineated from the DEM derived from GTOPO with spatial resolution of 1 km.

3.2.1 Advanced Microwave Scattering Radiometer – Earth Observation (AMSR-E)

Advanced Microwave Scattering Radiometer on-board Aqua is a twelve channel, six frequency total power passive microwave radiometer system. The data has been retrieved globally from National Snow and Ice Data center (NSIDC). It measures brightness temperatures at 6.925, 10.65, 18.7, 23.8, 36.5, and 89.0 GHz as in Table 3.1. Vertically and horizontally polarized measurements are taken at all channels. Aqua is one of a series of space based platforms that are central to NASA's Earth Science Enterprise (ESE), a long-term study of the scope, dynamics and implications of global change. The primary focus for the Aqua Project is the multi-disciplinary study of the Earth's Interrelated Processes (atmosphere, oceans, and land surface) and their relationship to earth system changes. It allows long-term change detection, identify its human and natural causes and advance the development of models for long-term forecasting (Source: AMSR-E Data Users Handbook, 4th Edition, March 2006,)

AMSR-E scans the Earth's surface by mechanically rotating the antenna and acquires radiance data of the Earth's surface. The aperture diameter of AMSR-E antenna is 1.6 m, and its spatial resolution is about 5 km in the 89 GHz band and about 60 km in the 6.9 GHz band of the largest wavelength. It conically scans and keeps an angle of incidence on the earth surface (55 degrees) to be constant and minimizes the effect of sea surface wind on the sea surface temperature and accomplishes a swath width of about 1450 km. Further, AMSR-E has a function to acquire radiance temperatures of deep space (about 2.7 °K) for calibrating observation data and high temperature calibration source.

Table 3.1: AMSR-E Main Characteristics

Items		Characteristics						
Observation Frequency		6.925 GHz	10.65 GHz	18.7 GHz	23.8 GHz	36.5 GHz	89.0 GHz	
							A	B
Spatial Resolution		50 km		25 km		15 km	5 km	
Band Width		350 MHz	100 MHz	200 MHz	400 MHz	1000 MHz	3000 MHz	
Polarization		Horizontal and Vertical						
Incident Angle		55°						54.5°
Cross polarization		less than –20 dB						
Swath Width		more than 1,450 km						
Dynamic Range		2.7-340 K						
Precision		1 K (1) as target						
Sensitivity		0.34K	0.7K	0.7K	0.6K	0.7K	1.2K	
Quantifying Bit Number		12 bit	10 bit					
Data Rate		87.392 Kbps						
Electric Power		350 ±35 W						
Weight		324 ±15 kg						
Size	Antenna Unit	1.95 x 1.7 x 2.4 m						
	Control Unit	0.8 x 1.0 x 0.6 m						

(Source: AMSR-E Data Users Handbook, 4th Edition, March 2006).

AMSR-E measures geophysical parameters supporting several global change sciences and monitoring efforts as shown in Table 3.2.

Table 3.2: Observation Targets and Purpose of AMSR-E

Target	Purpose
Precipitation	Precipitation has extremely important roles, through provision of water to the biosphere and as an air conditioning agent that removes excess heat from the surface (through evaporation) and making the Earth habitable. The AMSR-E measures rain rates over both land and ocean. Over the ocean, the AMSR microwave frequencies can probe through smaller cloud particles to measure the microwave emission from the larger raindrops.
Sea Surface Temperature	Over the ocean, AMSR-E provides sea surface temperatures (SST) through cloud cover of no precipitation, supplementing infrared-based measurements of SST that are restricted to cloud-free areas. SST fluctuations are known to have a profound impact on weather patterns across the globe, and the AMSR's all-weather capability could provide a significant improvement in our ability to monitor SST's and the processes controlling them.
Water Vapor	The total integrated water vapor of the atmosphere is measured over the ocean, which is important for the understanding of how water is cycled through the atmosphere. Since water vapor is the Earth's primary greenhouse gas, and it contributes the most to future projections of global warming, it is critical to understand how it varies naturally in the Earth system.
Wind Speed	Ocean surface roughness is also measured by AMSR-E, which is converted into a near-surface wind speed. These winds are one important component of how much water is evaporated from the surface of the ocean.
Cloud Liquid Water	AMSR-E cloud water estimates over the ocean help studies of whether clouds, and their ability to reflect sunlight, increase or decrease under various conditions. This could be an important feedback mechanism that either enhances or mitigates global warming, depending on whether clouds increase or decrease with warming.
Sea Ice	Monitoring of sea ice parameters, such as ice type and extent, is necessary to understand how this frozen blanket over the ocean acts to change climate through its ability to insulate the water against heat loss to the frigid atmosphere above it, and through its ability to reflect sunlight that would otherwise warm the ocean.
Snow Cover	In much the same way as the AMSR can see large ice particles in the upper reaches of rain systems, it also measures the scattering effects of snow cover. These measurements are empirically related to snow cover depth and water content based upon field measurements. Like sea ice, snow cover has a large influence on how much sunlight is reflected from the Earth. It also acts as a blanket, keeping heat from escaping from the underlying soil, and allowing deep cold air masses to develop during the winter. It further provides an important storage mechanism for water during the winter months, which then affects how much surface wetness is available for vegetation and crops in the spring.
Soil Moisture	Wet soil can be identified in the AMSR observations if not too much vegetation is present. Surface Wetness is important for maintaining crop and vegetation health, and its monitoring on a global basis would allow drought-prone areas to be monitored for signs of drought.

(Source: AMSR-E Data Users Handbook, 4th Edition, March 2006).

a) Temporal Coverage

Temporal coverage is from 19th June 2002 to 3rd October 2010.
Each swath spans approximately 50 minutes. The data sampling interval is 2.6 m sec per sample for the 6.9 GHz to 36.5 GHz channels, and 1.3 m sec for the 89.0 GHz channel. A full scan takes approximately 1.5 seconds. AMSR-E collects 243 data points per scan for the 6.9 GHz to 36.5 GHz channels, and 486 data points for the 89.0 GHz channel. The number of satellite passes per day is a function of latitude as shown in AMSR-E Observation Times.

b) Spatial Coverage

Spatial Coverage Map of AMSR-E is shown in Fig. 3.2.This map shows a typical day of coverage with 28 half-orbits.

Fig. 3.2: Spatial Coverage of AMSR-E (Source: NSIDC)

Coverage is global between 89.24°N and 89.24°S, except for snow-covered and densely-vegetated areas. The swath width is 1445 km.

b.1) Spatial Resolution

Input brightness temperature data at 10.7 GHz, corresponding to a 38 km mean spatial resolution, are re-sampled to a global cylindrical 25 km EASE-Grid cell spacing. The effective spatial resolution is thus slightly higher than the inbuilt 38 km resolution (Source: NSIDC).

b.2) Grid Description

Level-2A brightness temperatures are re-sampled to a global cylindrical EASE-Grid (1383 columns by 586 rows) with a nominal grid spacing of 25 km (true at 30°S). In the case of the Level-2B soil data, each geophysical variable value has a corresponding EASE-Grid row and column index (Source: NSIDC).

3.2.2 Advanced Scatterometer (ASCAT)

The Advanced Scatterometer (ASCAT) onboard MetOp is an active microwave remote sensing instrument that was designed EUMETSAT, with high radiometric accuracy, and its multiple-viewing capabilities to make it an attractive sensor for measuring soil moisture (Wagner et al., 2013b). The data have been provided by Integrated Climate Data center (ICDC). In ASCAT the incidence angle range is extended to 25°–65°. ASCAT covers two 550 km swaths separated by approximately 360 km from the satellite ground track. It uses two sets of three antennae, one on each side of the satellite ground track.

The ASCAT Level 2 soil moisture products are generated and distributed in near real time. The main geophysical parameter derived from ASCAT data is soil moisture index, which represents the degree of saturation of the topmost soil layer (< 5 cm) and is given in percent,

ranging from 0 (dry) to 100 (wet). Level 2 soil moisture products are generated by European Organization for the exploitation of Meteorological Satellites (EUMETSAT) using the so-called Water retrieval package (WARP-NRT) software, originally developed by the Institute of Photogrammetry and Remote Sensing of the Vienna University of Technology, based on the L1b averaged products on 12.5 and 25 km swath grids, as well as on a long term historical database of geo-located scatterometer soil moisture values around the globe.

ASCAT is indeed a suitable sensor for soil moisture retrieval for various reasons, its operation frequencies of 5.3 GHz is in the range of microwave frequencies (< 10 GHz) where the inclusion of liquid water to soil content strongly increases the soil dielectric constant. Therefore, when the soil moisture content increases, so does the dielectric constant at the air-soil boundary and therefore the backscatter value. This dependence of the backscattering intensity on the soil moisture content implies that ASCAT backscatter (σ_o) measurements provide a relatively direct measurement of the soil moisture content over bare soils. In the presence of vegetation, the value of σ_o changes, making it vital to correct the model or algorithm considering the effect of vegetation on the overall backscatter. Even, the roughness factor has an important effect on the backscatter measurements (Wagner et al., 2013b). Fig 3.3 shows the ascending and descending pass of ASCAT sensor.

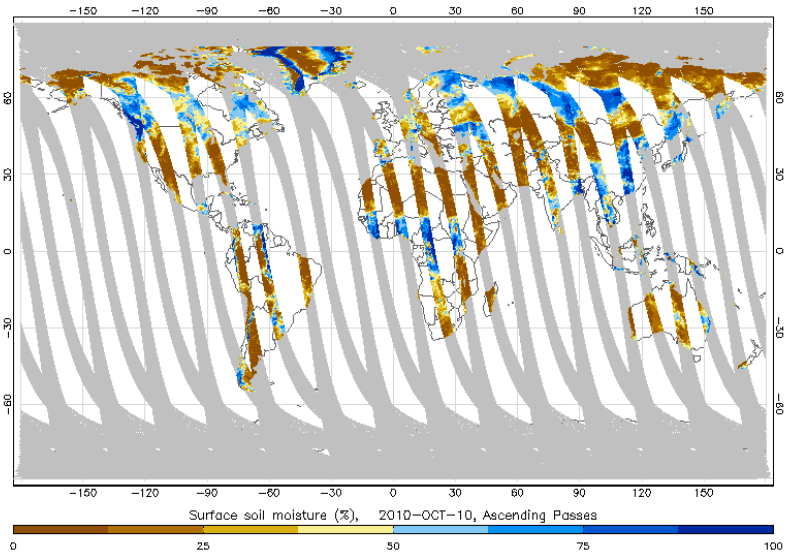

Fig. 3.3: ASCAT Soil Moisture Index (Ascending Pass) (Source: ASCAT Factsheet, EUMETSAT)

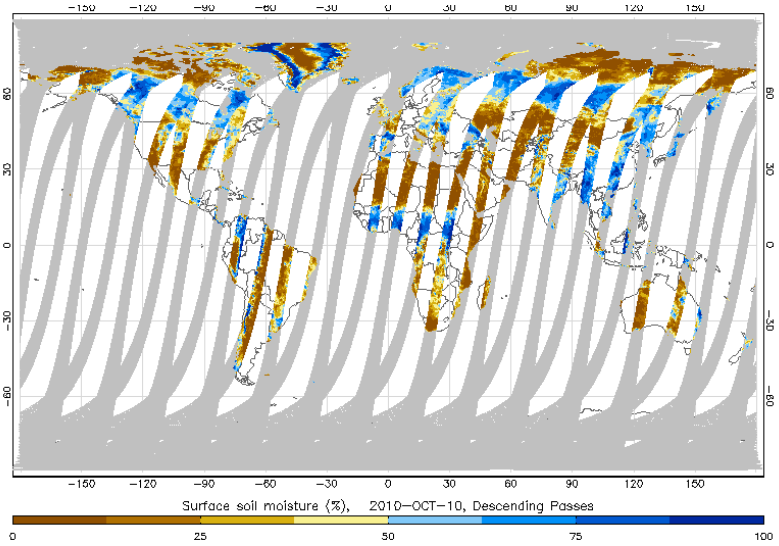

Fig. 3.4: ASCAT Soil Moisture Index (Descending Pass) (Source: ASCAT Factsheet, EUMETSAT)

The Fig 3.3 & 3.4 shows soil moisture index values derived from ASCAT on MeTop during October 10th, 2010 for ascending and descending passes respectively. The operational generation and dissemination of these products has started in December 2008 by Vienna University of Technology. The grid spacing of this ASCAT soil moisture product is 25 km, covering the two ASCAT swaths, which are each 550 km wide and are located at a distance of approximately 350 km on either side of the sub-satellite ground track (Source: ASCAT Factsheet, EUMETSAT).

3.2.3 Global Land Data Assimilation System – Noah (GLDAS-Noah)

Land surface temperature and wetness conditions affect and also get affected by numerous climatological, meteorological, ecological and geophysical phenomena. It is important to derive accurate, high-resolution estimates of terrestrial water and energy storages as these variables are very vital for predicting climate change and for executing wide array of studies in ecological and environmental studies. Furthermore, since soil moisture, temperature, and other necessary parameters are location based induces errors in the representation of these in different climate models and thus it leads to incorrect predictions. The discrepancies are also generated due to biases in the land surface forcing data and parameterization.

Thus, a Global Land Data Assimilation System (GLDAS) has been developed jointly by scientists at NASA, GSFC, NOAA to make use of new generation of ground based and space-based observation systems. The data is taken from Goddard Earth Science Data and Information Services center (GES DISC). In the GLDAS model, the constraints are applied in two ways that is, by forcing the land surface models (LSMs) with observation based meteorological fields and by employing data assimilation techniques.

Table 3.3: GLDAS Forcing and Output Field Information.

GLDAS forcing and output fields.	
Required forcing fields	**Summary of output fields**
Precipitation	Soil moisture in each layer
Downward shortwave radiation	Snow depth, fractional coverage, and water equivalent
Downward longwave radiation	Plant canopy surface water storage
Near-surface air temperature	Soil temperature in each layer
Near-surface specific humidity	Average surface temperature
Near-surface *U* wind	Surface and subsurface runoff
Near-surface *V* wind	Bare soil, snow, and canopy surface water evaporation
Surface pressure	Canopy transpiration
	Latent, sensible, and ground heat flux
	Snow phase change heat flux
	Snowmelt
	Snowfall and rainfall
	Net surface shortwave and longwave radiation
	Aerodynamic conductance
	Canopy conductance
	Surface albedo

(Source: Rodell *et al.*, 2004)

GLDAS comprises of land surface model that is, National centers for Environmental Prediction/Oregon State University/ Air Force/ Hydrologic Research Lab Model (Noah) which provides a temporally and spatially consistent characterization of the hydrological cycle. GLDAS model derived estimates are mainly 3-hourly products with 0.25^{o} spatial resolution, while satellite based observations offer twice-daily instantaneous retrievals at similar spatial scales (Liu.Y.Y *et al.*, 2009). The GLDAS forcing and output field information is provided in Table 3.3.

The fine scale variability of the observation based precipitation is reflected in the fines scale patterns of soil moisture in the derived forcing run because soil moisture shows a high degree of variability at all scales (Famiglietti *et al.*, 1999). The fine scale soil moisture variability is evident in the derived forcing run results. This may be preferable from a weather forecasting perspective. However, the broader patterns of soil moisture are not necessarily more accurate in the derived forcing run.

While, deriving the soil moisture content map, porosity and the percentages of sand, silt and clay were horizontally re-sampled to the 0.25^{o} GLDAS grid and interpolated to 0-2, 2-150, 150-350 cm depths from the original depths. These depths were chosen as to facilitate future assimilation of surface soil moisture fields derived from AMSR-E satellite measurements.
GLDAS is a global, high resolution terrestrial modeling system that incorporates both satellite and even ground based observations to generate optimal fields of land surface states and fluxes in real time (Rodell *et al.*, 2004).

3.2.4 Ground Soil Moisture Data

The ground (*in-situ*) soil moisture data is taken from International Soil Moisture Network (ISMN) for the China location, as the ground data for the Indian region was unavailable for the present time period chosen. The MAQU network in China consisting of 20 ground stations located at the eastern edge of the Tibetan plateau in central China at an average altitude of 3000m MSL. Out of the 20 stations in the network, the most suitable was CST-02 located at latitude 33 40'N and longitude 102 09'E at 3449m MSL with dominant land class as grass. The soil moisture is measured at the depth of 5 cm using ECH20 EC-TM (Tenshiometer). The ground soil moisture measured at 5:00 am is taken for the validation purpose.

CHAPTER - 4
METHODOLOGY

4.1 INTRODUCTION

The methodology implied in this research work mainly focuses on the blending of soil moisture data acquired from the passive and active microwave dataset, using a reference dataset having same spatial and temporal resolution as that of the microwave data. The methodology also involves the retrieval of soil moisture from the brightness temperature (T_b) data observed through passive microwave remote sensing. Fig 4.1 represents the overall flowchart of the methodology.

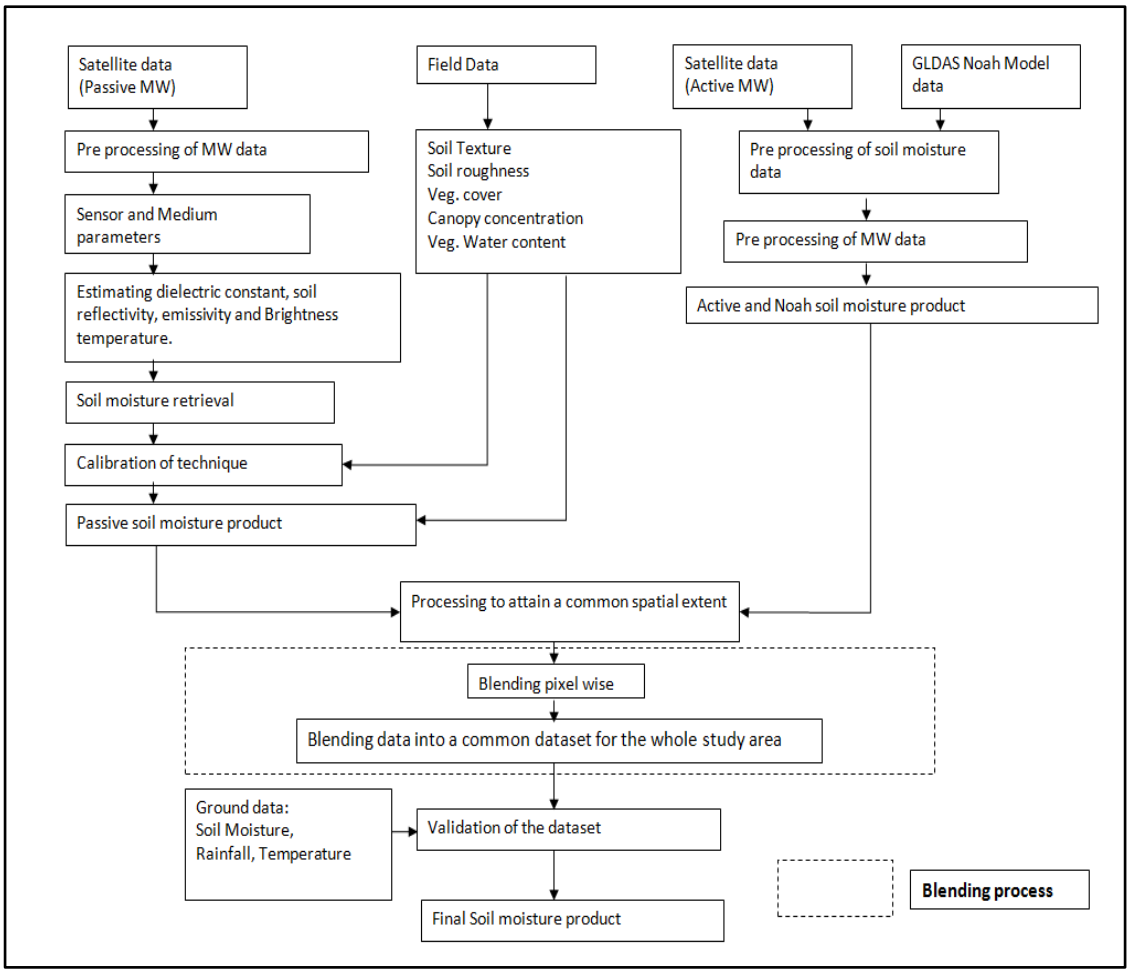

Fig. 4.1: Flow Chart Depicting the Overall Methodology

The methodology is mainly divided into following sections:

1. Acquiring the required datasets for the study time period.
2. Preparation and preprocessing of the datasets for the study area.
3. Retrieval of soil moisture from the passive microwave data.
4. Cumulative distribution function matching approach for rescaling.
5. Blending the microwave dataset all together.

4. 2 DATA ACQUISITION AND SOFTWARE USED

The primary data acquired is the soil moisture data for the time period 01st January 2009 to 31st December 2009 i.e., for a complete one year time span, from various sensors and sources for the purpose of blending. The dataset is classified according to the type of microwave sensor and the selected reference data.

4.2.1 Satellite Data Acquired

a) ***AMSR-E data***

The passive microwave data is acquired from Advanced Microwave Scanning Radiometer - Earth Observing System Sensor on the NASA's Aqua Satellite for the year of 2009. The Level-2B land surface product (AE_Land) of AMSR-E includes daily measurements of surface soil moisture, vegetation/roughness water content interpretive information, and quality control variables. Ancillary data includes time, geolocation, and quality assessment. Input brightness temperature data at 10.7 GHz, corresponding to a 38 km mean spatial resolution, are re-sampled to a global cylindrical 25 km Equal-Area Scalable Earth Grid (EASE-Grid) cell spacing. The data is acquired from National Snow and Ice data Centre (http://nsidc.org/data/amsre/). The data is in the units of m^3 / m^3.

b) ***ASCAT data***

The Advanced Scatterometer onboard MetOp provides the active microwave data from its scatterometer sensor. The data is acquired in two forms, image form and the non-image form.

I. **Image form:** The image form of the ASCAT data for the Indian region is received from Integrated Climate Data Centre (ICDC), CliSAP/Klima Campus, University of Hamburg, Hamburg, Germany on request basis. The soil moisture data is available as 5-Day composites for the year 2009 at 25 km spatial resolution.

II. **Non-Image form:** The non-image form of data is acquired from Institute of Photogrammetry and Remote Sensing (IPF), Vienna Institute of Technology (TU Wien), Vienna, Austria from Dr. Wolfgang Wagner, for the time duration 01 January 2007 to 31 May 2012. The data is in the form of discrete global grid (DGG). The grid is defined such that the spacing is approximately 12.5 km. The total grid consists of 32,64,391 points, where 8,39,826 points are defined over the land. The grid is sub-divided globally into 2,592 cells which cover 5^o X 5^o each.

The data is in the units of percentage that is from 0-100%. Fig 4.2 gives the basic idea of the cells with their index and number of grid points contained in it (Product Sheet: ASCAT Surface Soil Moisture 25 km Time Series).

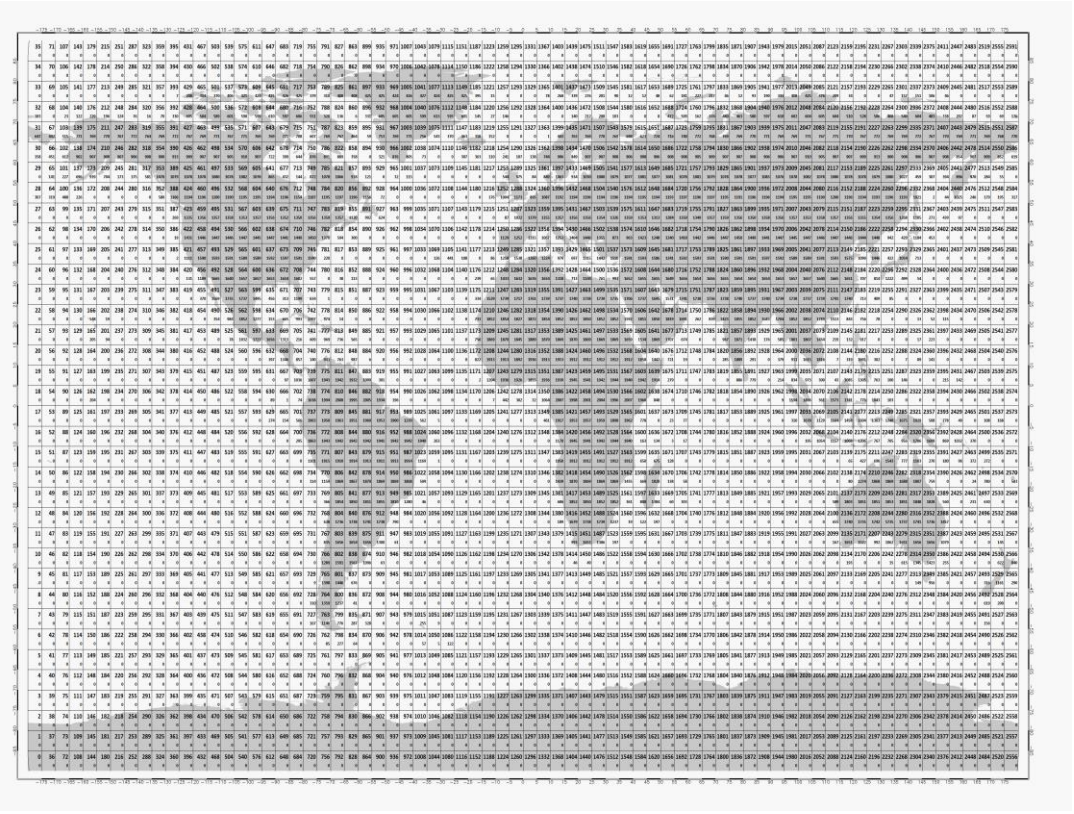

Fig. 4.2: Cell Structure of Discrete Global Grid (DGG) (Source: TU Wein University, ASCAT soil moisture product).

c) **GLDAS-Noah Data**

The Global Land Data Assimilation System (GLDAS) - Noah land surface model data product, version 1 with 3-h time interval and 0.25^{o} spatial resolution. The data is acquired for the entire year 2009. Noah model uses a four-layered soil description with a 10-cm thick top layer and takes into account the fractions of sand and clay. Out of the four layered soil moisture value provision, the value of the top layer that if for 0-10 cm soil moisture value is taken into consideration in the research. The data is in the units Kg / m^2. The data is acquired from the open portal, Goddard Earth Sciences Data and Information Service Center (GES DISC), (http://disc.gsfc.nasa.gov/hydrology/data-holdings).

4.2.2 Software Used

The software packages and programming languages used to complete this study are listed below,

- ERDAS Imagine 9.3
- Arc GIS 10.0
- ILWIS 3.3
- ENVI 4.3
- IDL 6.3
- Panoply 3.1.8

4.3 PREPARATION AND PREPROCESSING OF THE DATASETS

The dataset acquired from passive microwave remote sensor that is AMSR-E is first extracted for the study area and then multiplied with the scale factor 0.001 (National Snow and Ice Data Center, Detailed data description) to acquire the true value of soil moisture. The soil moisture data and brightness temperature is available at 6.9 GHz for horizontal and vertical polarization in ascending and descending mode. The data at both modes are averaged to finally get the required soil moisture and brightness temperature value at 6.9GHz frequency.

The image form of ASCAT data was available in Network Common Data Form (NetCDF) i.e. .nc format which has to be converted to compatible image format specifically either in .img (Image format) or .tiff (tagged information file format) format which has to be further processed. The conversion was done with the aid of customized code developed in Python 2.7 programming language (Annexture-1). The data is then extracted for the study area by masking it with the vector layer (shape file) of the Ganga basin.

The GLDAS-Noah data is a combination of various parameters providing information of various land variables. There are total 22 geophysical parameters subsisted in the GLDAS data set. The Noah data too was in .nc (NetCDF) format which is again converted to the image format by specifically extracting only the soil moisture data out of total parameters available. The soil moisture data is available for four different depths, out of which the extraction is performed for the top most layer (0-10 cm) only as the AMSR-E soil moisture data also represents the top 0-5 cm layer only. The soil moisture dataset is again extracted by mask to retrieve data for the study area.

The original unit of Noah soil moisture data is kg/m^2 which has to be converted to m^3/m^3, so that it would be similar with the AMSR-E data units. The conversion is done by considering the top soil layer depth as 10 cm.

During the preprocessing, it is important to make sure that all the data set has same spatial extent, similar row and column number that mean same cell size and similar projection system. Due to the voluminous data, the extraction and conversion from .nc to image format has been done using programming in Python language. Coding was performed in Python 2.7.3 and 2.6.5 programming language using Arcpy and GDAL modules.

All the above mentioned dataset have snow covered area in the upper reaches of Ganga basin, the snow cover have to removed by masking it with the snow extent provided by the MODIS data for the year 2009, as presence of soil moisture over the snow area is not acceptable.

4.4 RETRIEVAL OF SOIL MOISTURE FROM THE PASSIVE MICROWAVE DATA

The retrieval of soil moisture from passive microwave sensor using the brightness temperature is the main task and the algorithm flow chart depicting the same is given in Fig. 4.3,

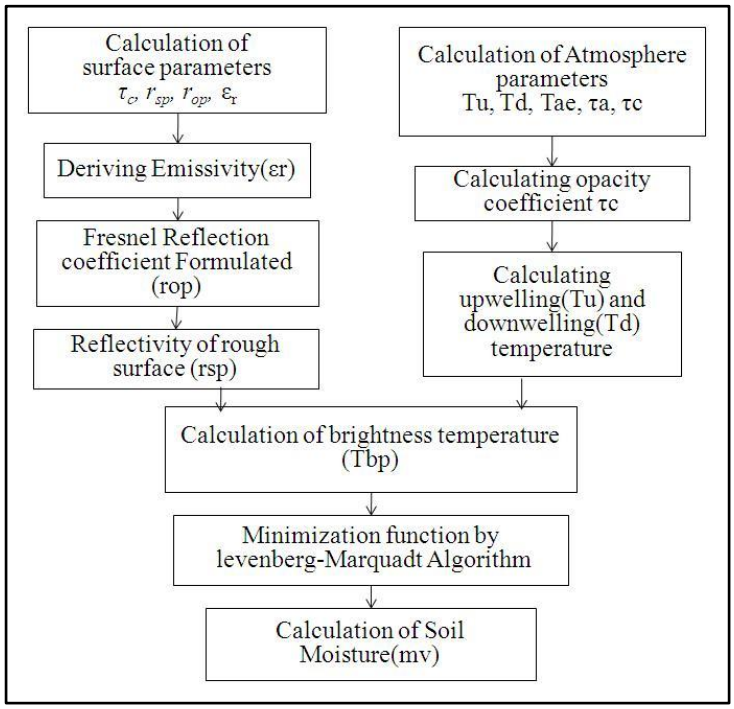

Fig. 4.3: Flow Chart Depicting Soil Moisture Retrieval Using Passive Microwave Data

The retrieval algorithm for soil moisture (m_e) uses a physically-based radiative transfer model (Njoku, 1999) and for the estimation of soil moisture the T_e and W_e values needs to be calculated. The baseline algorithm (AMSR Land Surface Parameters, Algorithm Theoretical basis document version 3.0, Eni G. Njoku) used in present study uses the two lowest AMSR frequencies (6.9 and 10.7 GHz) as the Surface roughness and vegetation scattering effects increasing complexity above ~10 GHz, and the uncertainty in derived products is greater above ~10 GHz. These frequencies also have better vegetation penetration and soil moisture sensitivity though with the decreased spatial resolution.

In general parameter retrieval algorithms the land surface is modeled as absorbing vegetation layer above soil in Fig 4.4.

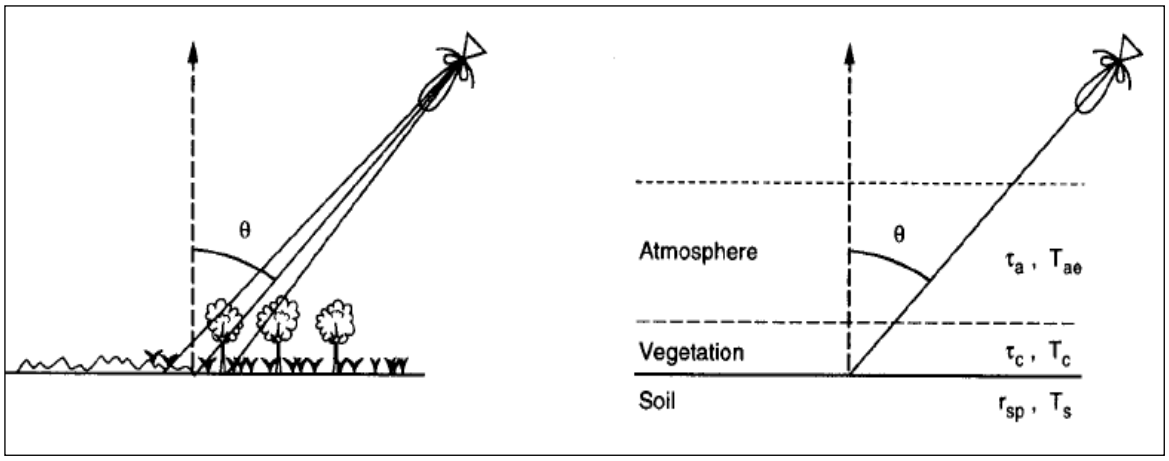

Fig 4.4: Model Representation of a Space-Borne Radiometer, viewing a heterogeneous earth surface (Njoku, 1999)

The brightness temperature TBp observed at the top of the atmosphere at a given incidence angle and at a given frequency can be expressed by the radiative transfer equation (Njoku, 1999).

$$TBp = T_u + exp(-\tau_a)\,[\{T_d\, r_{sp}\, exp(-2\tau_c)\} + \{esp\, T_s\, exp(-\tau_c) + T_c\,(1 - \tau_p)\,[1 - exp(-\tau_c)]\,[1 + r_{sp}\, exp(-\tau_c)]\}] \quad \text{- [1]}$$

where,
T_u - Upwelling atmospheric radiation (watt/m^2).
T_d - Downwelling atmospheric radiation (watt/m^2).
T_a - Atmospheric Opacity.
T_c - Vegetation temperature (K).
τ_c - Vegetation opacity.
r_{sp} - Soil reflectivity.
T_s – Effective soil temperature (k).
ω_p – vegetation single scattering albedo.

The assumption in the above equation is that, a specular soil surface with no reflection at air-vegetation boundary.

Another simplifying approximation is that the vegetation and underlying soil are at close to the same physical temperature T_e. This approximation does not degrade the moisture retrieval accuracy, but will result in the retrieval of a mean or effective radiating temperature of the composite soil/vegetation medium.

Substituting $T_s \approx T_c = T_e$ in Equation (1) we obtain:

$$T_{Bp} = T_u + exp\,(-\tau_a)\,[\{T_d\, r_{sp}\, exp\,(-2\tau_c)\} + T_e\,\{(1 - r_{sp})\, exp\,(-\tau_c) + (1 - \omega_p)\, [1 - exp\,(-\tau_c)]\,[1 + r_{sp}\, exp\,(-\tau_c)]\}] \quad \text{- [2]}$$

Atmosphere as the parameter -

The expressions for T_u and T_d are obtained from the literature (Hofer and Njoku, 1981). T_u and T_d can be expressed using the effective radiating temperature approximation as;

$$T_u \approx T_d \approx T_{ae}\,[1 - exp\,(-\tau_a)] \quad \text{- [3]}$$

where, T_{ae} is the mean temperature of the microwave-emitting region of the atmosphere. This expression is valid for most atmospheric water vapor and cloud conditions. T_{ae} is frequency dependent and also depends on the distributions of temperature, humidity, and liquid water. T_{ae} may be expressed simply as a function of the surface air temperature T_{as} and a frequency dependent offset δT_a:

$$T_{ae} \approx T_{as} - \delta T_a \quad \text{- [4]}$$

The effect of uncertainty in T_{ae} on the observed TBp is sufficiently small. The opacity τ_a along the atmospheric path is dependent on the viewing angle q and the precipitable water q_v and vertical-column cloud liquid water q_l. It can be expressed as:

$$\tau_a = (t_o + a_v q_v + a_l q_l) / cos\theta \quad \text{- [5]}$$

where, τ_o is the oxygen opacity at nadir, and a_v and a_l are frequency-dependent coefficients. Values for these coefficients are derived for water vapor and droplet absorption in the atmosphere (Rayleigh absorption is assumed for the cloud droplets) from various literatures and journals (Njoku and Li, 1999).

Surface as the parameter -

The dependence of τ_c on vegetation columnar water content follows an approximately linear relationship, written as (Njoku, 1999):

$$\tau_c = b\, w_e / cos\theta \quad \text{- [6]}$$

where, cosθ accounts for the slant path through the vegetation. The coefficient b depends on canopy structure and frequency. Theory and experimental data suggest that for given vegetation type (b,) is approximately proportional to frequencies below ~10 GHz (Jackson and Schmugge, 1991, Le Vine and Karam, 1996).

This indicates that at higher frequencies the frequency dependence of b decreases and its dependence on canopy structure eventually increase. This provides rationale for restricting the physically-based retrieval algorithm to be in between 6.9 and 10.7 GHz.

The reflectivity of rough soil, r_{sp}, is related to that of smooth soil r_{op}, by the semi-empirical formulation (Njoku and Li, 1999),

$$rsv = [(1 - Q)\, rov + Q\, roh\,]\, exp\,(-h) \quad \text{- [7]}$$

$$rsh = [(1 - Q)\, roh + Q\, rov\,]\, exp\,(-h) \quad \text{- [8]}$$

Expression for h and Q are:

$$Q = 0.35[1 - exp\,(-0.6.\sigma^2.\lambda)] \quad \text{- [9]}$$

$$h = \left(\frac{4\pi\sigma\, cos\theta}{\lambda}\right)^2 \quad \text{- [10]}$$

where, λ is frequency of radiometer and σ is the surface rms height.

The Fresnel expressions relate the reflectivities r_{ov} and r_{oh} of a smooth, homogeneous soil to the complex dielectric constant of the soil e_r:

$$r_{ov} = \left|\frac{\varepsilon r\, cos\,\theta - \sqrt{\varepsilon r - sin^2\theta}}{\varepsilon r\, cos\theta + \sqrt{\varepsilon r - sin^2\theta}}\right|^2 \quad \text{- [11]}$$

$$r_{oh} = \left|\frac{cos\,\theta - \sqrt{\varepsilon r - sin^2\theta}}{cos\theta + \sqrt{\varepsilon r - sin^2\theta}}\right|^2 \quad \text{- [12]}$$

From the above equation, θ is the incidence angle relative to the surface normal. For a given frequency, the dielectric constant depends on the volumetric soil moisture content m_e and to a lesser extent on soil type.

This relationship can be expressed as:

$$\varepsilon_r = f\,(m_e\,;\, \rho_b,\, s,\, c) \quad \text{- [13]}$$

The most common one is that of Topp *et al.,* (1980) providing the relationship between the effective dielectric constant and soil moisture is –

$$\varepsilon_{eff} = 3.03 + 9.3\theta + 146\theta^2 - 76.7\theta^3 \quad \text{- [14]}$$

While the function proposed by (Dobson *et al.,* 1984) takes into account the soil texture by allowing its coefficients to be dependent on the clay and sand percentages:

$$\varepsilon_{eff} = 2.37 + (-5.24 + 0.55 \times \%sand + 0.15 \times \%clay)\theta + (146.04 - 0.75 \times \%sand - 0.85 \times \%clay)\,\theta^3 \quad \text{- [15]}$$

The high sensitivity of brightness temperature to soil moisture is the principal advantage of using microwave radiometry for soil moisture sensing (Njoku, 1999).

Various parameters used in the algorithm proposed by (Njoku, 1999) is shown in the Table 4.1,

Table 4.1: Parameters of the Microwave Model

Parameters	Description
1.Media and Sensor parameters	
• Atmosphere	
τ_o	Oxygen nadir opacity
av ,al	Water vapor and liquid water opacity coefficient
δTa	Lapse rate temperature differential (K)
• Vegetation	
ω_p	Single scattering albedo
b	Opacity coefficient
• Soil	
h,Q	Roughness Coefficients
s,c	Sand and clay fractions
• Sensor	
θ	Viewing angle (deg)
v	Frequency (GHz)
p	Polarization
2.Media Variables	
• Atmosphere	
q_v	Precipitable water (cm)
q_l	Cloud liquid water path (mm)
K	Surface air temperature (K)

(Source: Njoku, 1999)

Retrieval of Soil Moisture-

In the iterative procedure, the values of the geophysical parameters to be retrieved x = {me, we, and Te} are adjusted to minimize the weighted-sum of squared differences X^2 between observed, T_{Bi} observed, and computed, Φ(x), brightness temperatures. The Levenberg-Marquardt algorithm is used for the minimization (Press *et al.*, 1989).

$$X^2 = \sum_{i=1}^{n} \left(\frac{T_{bi}obs - \Phi(x)}{\sigma_i} \right)^2 \quad \text{- [16]}$$

At each retrieval point, the algorithm starts with a-priori values of the geophysical variables x_o and adjusts these iteratively until X^2 convergence to the minimum value of less than 1. σ_i represents the measurement noise in channel i. The model $\Phi(x)$ is mathematically sound and hence convergence is normally fast, except where the model cannot adequately represent the surface emission, or where the sensitivity to the parameters is too low. The atmospheric variables of the model q_v, q_l, T_{as}, and δT_a are given an initial values derived from climatology. The atmospheric parameters t_o, a_v, and a_w, are known constants. The parameters b, h, Q, ω_p, ρ_b, s, and c are given fixed values based on the model.

This algorithm is applied in present study to estimate the soil moisture from the brightness temperature considering various surface and atmospheric parameters and basic
The soil moisture retrieved from the passive microwave sensor (AMSR-E) lacks the spatial resolution i.e. coverage of many areas is lacking due to the sensor orbit and the swath width. To overcome this limitation it is combined with the active sensor (ASCAT) keeping the GLDAS-Noah as the reference. Rescaling is performed for both AMSR-E and ASCAT as the spatial extent, scale and units are not common and rescaling is done to get the data in a similar format as that of the refereed data chosen.

4.5 CDF MATCHING APPROACH

This section describes the process of rescaling the microwave dataset using piece wise linear cumulative distribution function matching technique. Fig 4.5 shows the flow chart of the process.

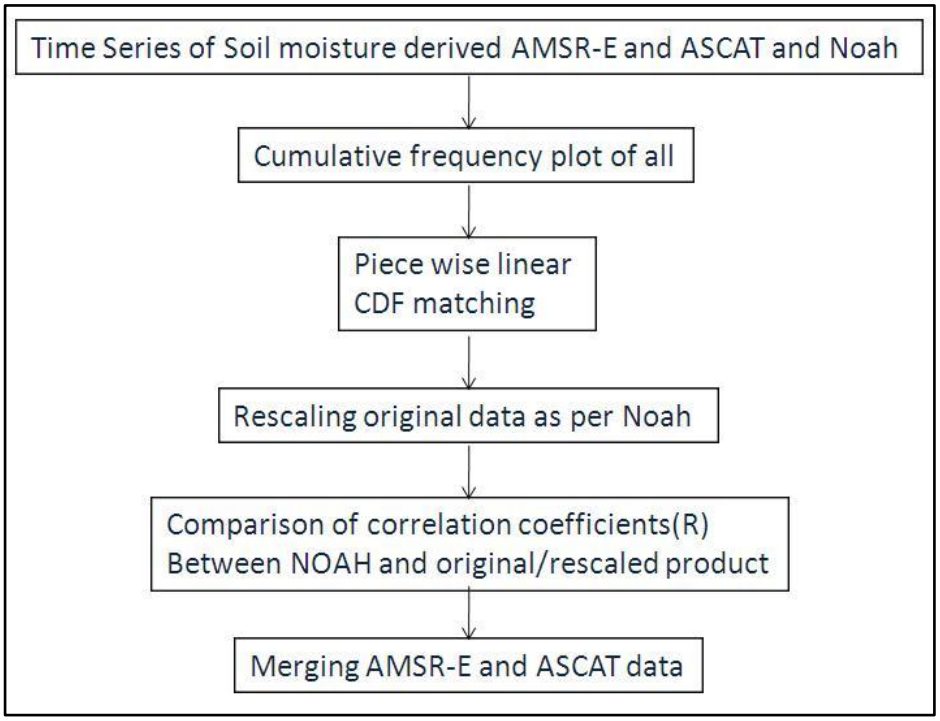

Fig. 4.5: Flow Chart Depicting Cumulative Distribution Matching (CDF) approach

The important task in the blending approach is to determine an appropriate threshold of correlation coefficient above which an improved soil moisture product can be produced by combining both products. Thus, to determine the threshold value, both microwave products (having units of m^3/m^3 and % respectively) were adjusted to a common range and then compared the results with the initial input data.

Combining AMSR-E and Tu-Wien ASCAT soil moisture products requires adjustment against reference dataset. The reference data set chosen in present study is GLDAS-Noah soil moisture data which has a spatial and temporal resolution similar to AMSR-E and ASCAT products (25 km resolution and daily interval) with a year long time record and appropriate for all land cover types. The Noah model and the NASA algorithm use a common soil property dataset, based on Food and Agriculture Organization (FAO) soil map of the world. This added property provided another reason for choosing the GLDAS-Noah as the reference dataset (Liu *et al.*, 2011).

The cumulative distribution function (CDF) matching approach is used to rescale microwave satellite observed against the Noah simulated soil moisture. Various studies in the past have followed the similar technique to establish a relative relationship for the calibration of radar or satellite data (Reichle, 2004, Lee, 2004).

A piece-wise linear CDF matching was applied to each grid cell individually. Time series is plotted for each pixel of soil moisture estimates from Noah, AMSR-E and ASCAT. The points at which all the three data are available are noted. The cumulative distribution frequencies are plotted for all the dataset individually. The CDF matching process mainly involves, initially dividing the CDF into several segments and then performing linear regression analysis for the each segment and finally using the linear equation to rescale the data falling into the different segments.

In the present study, twelve segments are defined by breaking at 0, 5, 10, 20, 30, 40, 50, 60, 70, 80, 90, 95 and 100 percentiles of the cumulative distribution frequency plots. The division of the CDF curve is done into 10-12 segments as this number turned out the most robust while it is still able to resolve well the tails of the CDF (as suggested by Yi.Liu, email conversation). The thirteen percentile values are noted from all three dataset for AMSR-E, ASCAT and Noah. Once the values are noted for each break point, the cumulative distribution frequency curves are plotted against Noah, AMSR-E curve is plotted against Noah and similarly ASCAT is plotted against Noah. The linear equations for the each segment are established between the two data plotted against each other as suggested by Liu *et al.*, (2011).

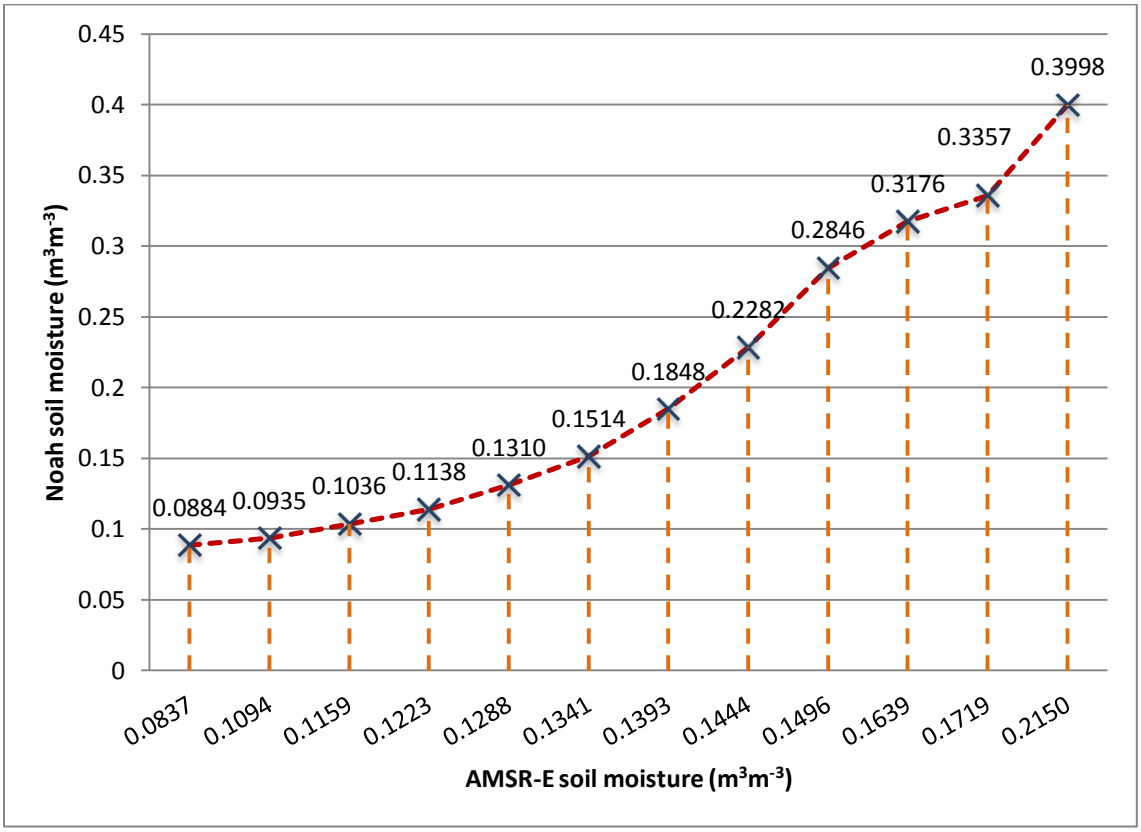

Fig. 4.6: Regression line of AMSR-E against Noah depicting 11 segments.

The data in different segments visible in Fig. 4.6 have different adjusting equations. The equations provide the information of slope and intercept. The rescaling is done using the linear equations which have the slope and intercept information along with it. The rescaling is done for AMSR-E and ASCAT against that of Noah.

In detail, the rescaling is done as, in the above plot, P5 and P10 of AMSR-E is 0.084 and 0.109, and P5 and P10 of Noah is 8.842 and 9.349, so the slope and intercept is Noah =19.75*AMSRE+7.188. For all AMSR-E soil moisture between 0.084 and 0.109, we use this linear equation. As an example, if AMSR-E is 0.09, then after rescaling it will be (19.75*0.09) +7.188 = 8.9655. Similarly we will calculate all the values for AMSR-E and ASCAT according to the Noah using this approach (Liu *et al.*, 2009).

4.6 BLENDING OF MICROWAVE DATASET

Once, the rescaling of the original soil moisture dataset is done the final blended soil moisture product is retrieved from the rescaled passive and active microwave data by the process of averaging, when both the rescaled AMSR-E and Noah dataset have coincident values available, otherwise only one appropriate rescaled product is chosen (Liu et al., 2012a). This process is merging the two dataset into one.

The above mentioned complete process is performed cell by cell wise and to derive the complete blended product for the entire image, a customized computer program is developed in python 2.6.5 using gdal, arcpy, os ad glob libraries.
Thus the final blended product is available with finer spatial and temporal resolution which can be further used for various applications.

4.7 VALIDATION

Validation is performed either directly on parameters derived from AMSR observations or in conjunction with the ground data (*in-situ*). Validation should include inter- comparisons of similar data products developed by different instruments and models. Validation will be performed in collaboration with end users of the AMSR land products.

4.7.1 Validation and Calibration of Soil Moisture Value Retrieved

The soil moisture retrieved from the brightness temperature of the AMSR-E follows an algorithm and the soil moisture obtained needs to be validated. The validation is performed by comparing it with the soil moisture product (AE_Land.2) of the AMSR-E sensor. This technique will allows checking the closeness and the correlation of the derived soil moisture and the soil moisture product of AMSR-E.

The calibration of various parameters involved in estimating the soil moisture is done using the parameters obtained from the SMEX 02 soil climate analysis network (SCAN) station, IOWA (Source: http://nsidc.org/data/amsr_validation/soil_moisture/smex02/). The dataset include hourly and daily recordings of precipitation, air temperature, solar radiation, wind speed, relative humidity, soil moisture, and soil temperature. The station has numerous sensors that automatically record data. Sensors include global precipitation sensor, thermistor, thin film capacitance-type sensor, anemometer, pyranometer, pressure sensor, and a frequency-shift dielectric measuring device.

Various parameters are obtained from this experiment that includes ground soil moisture parameters, vegetation parameters, and meteorological parameters, land surface information which are all mandatory for calculating the soil moisture and for validating the value by calibrating the algorithm from these parametric data.
The validation and calibration is performed using the python programming language to estimate the soil moisture with higher precision and accuracy.

4.7.2 Validation of Merged Soil Moisture product

The merged soil moisture product is validated with the ground soil moisture data available for the China location at MAQU network as mentioned in chapter 3. The ground soil moisture data is provided by International Soil Moisture Network (ISMN).

CHAPTER - 5
RESULTS AND DISCUSSION

Using the framework designed for soil moisture estimation and blending, the following results were obtained. All the results are presented and discussed below:

5.1 PRE-PROCESSING

The global data providing the soil moisture and brightness temperature available from various sources (i.e. AMSR-E, ASCAT and Noah) as shown in the Fig 5.1, 5.2, 5.3 and 5.4 are initially preprocessed for spatial extend of the study area (Fig 5.5) to obtain common spatial and temporal resolution.
The input global data acquired are –

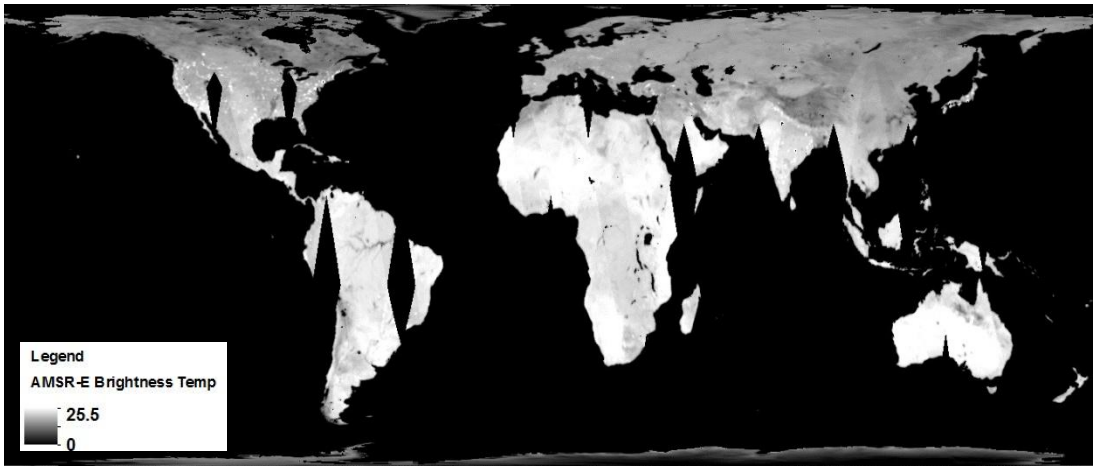

Fig. 5.1: Global Map of AMSR-E Brightness Temperature (K)

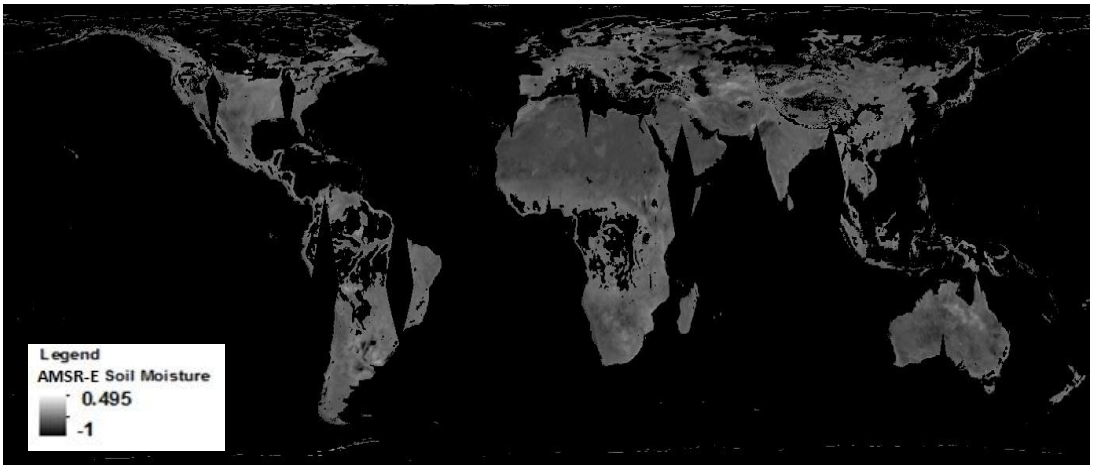

Fig. 5.2: Global Map of AMSR-E Soil moisture (m^3m^{-3})

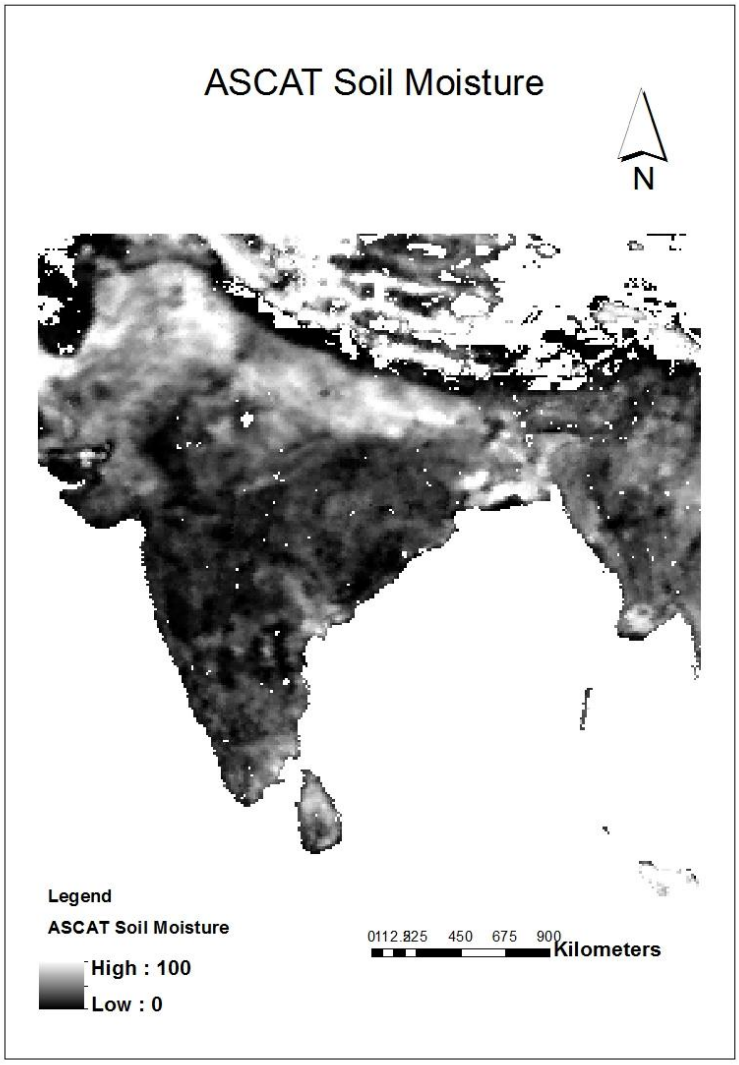

Fig. 5.3: ASCAT Soil moisture Map for India region (%)

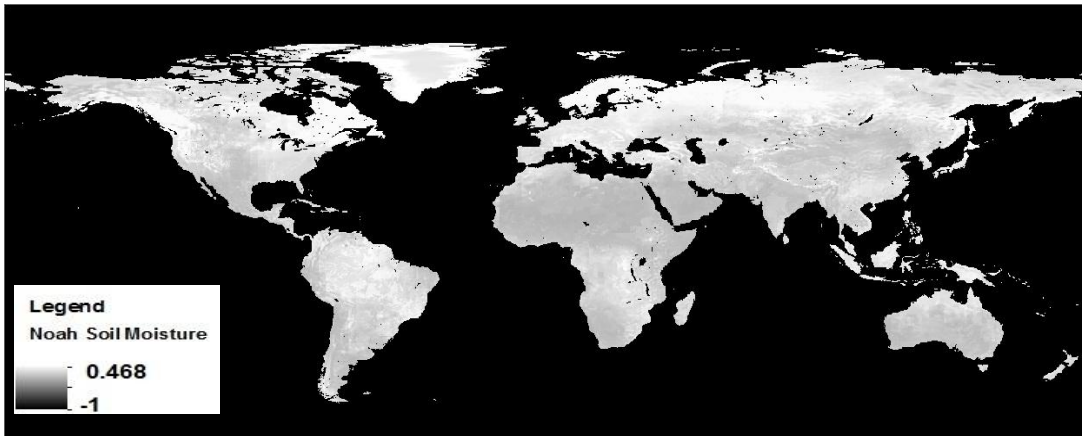

Fig. 5.4: Global Map of Noah Soil moisture (m^3m^{-3})

The preprocessed dataset for the study area are shown in Figs 5.5 where '-2' value represents the snow cover value and '-1' value represents 'no-data'.

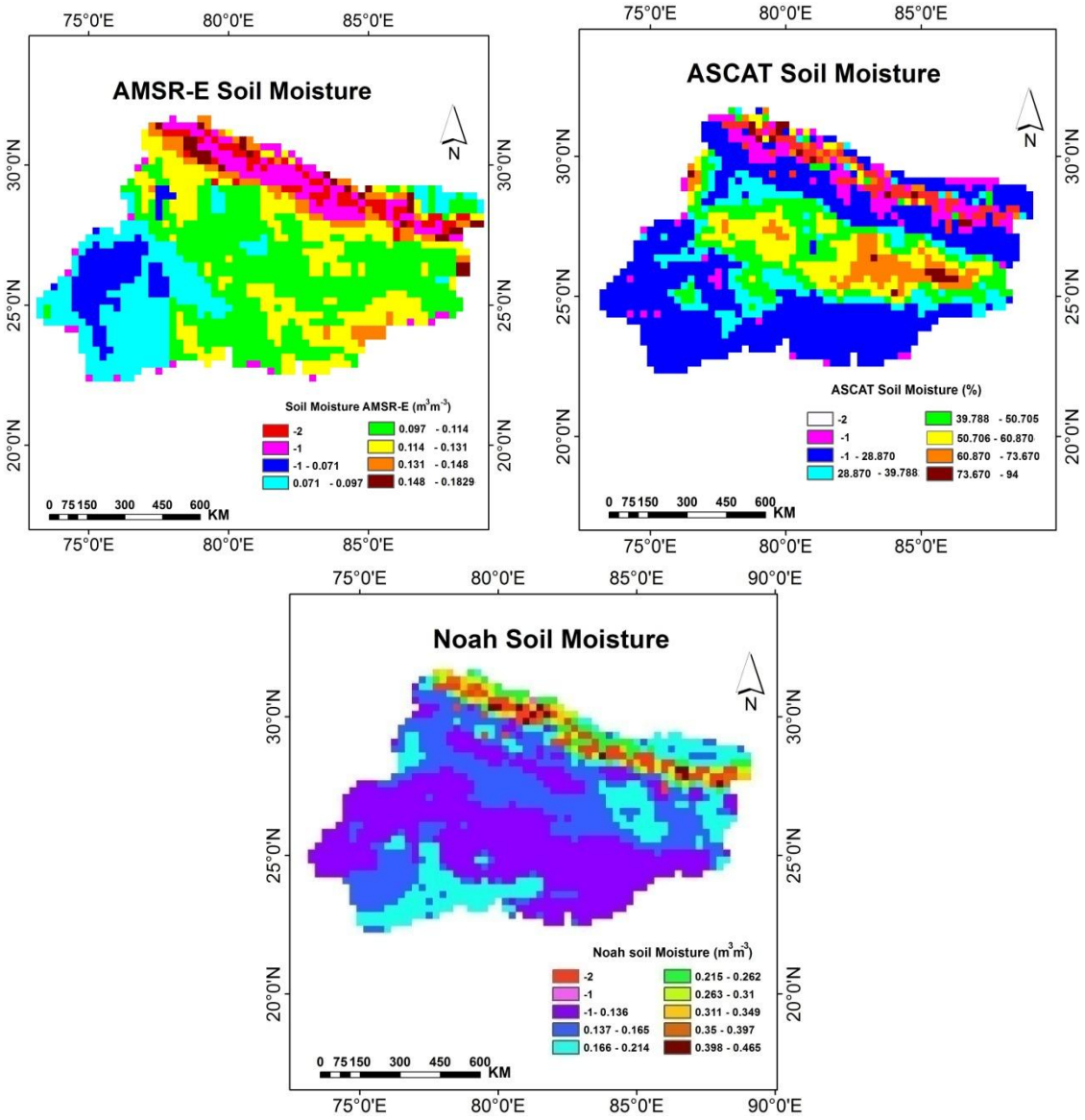

Fig. 5.5: Three different soil moisture dataset for the study area.

5.2 RETRIEVAL OF SOIL MOISTURE FROM AMSR-E BRIGHTNESS TEMPERATURE DATA

Brightness temperature (T_b) data is used to retrieve the soil moisture using reference values of various parameters from standard literatures. This is executed using the python coding for the whole 365 images for the year 2009 as the data was voluminous and the Fig 5.6 shows the soil moisture image for May 6th 2009.

The soil moisture map derived from the Tb image is as follows in Fig 5.6 –

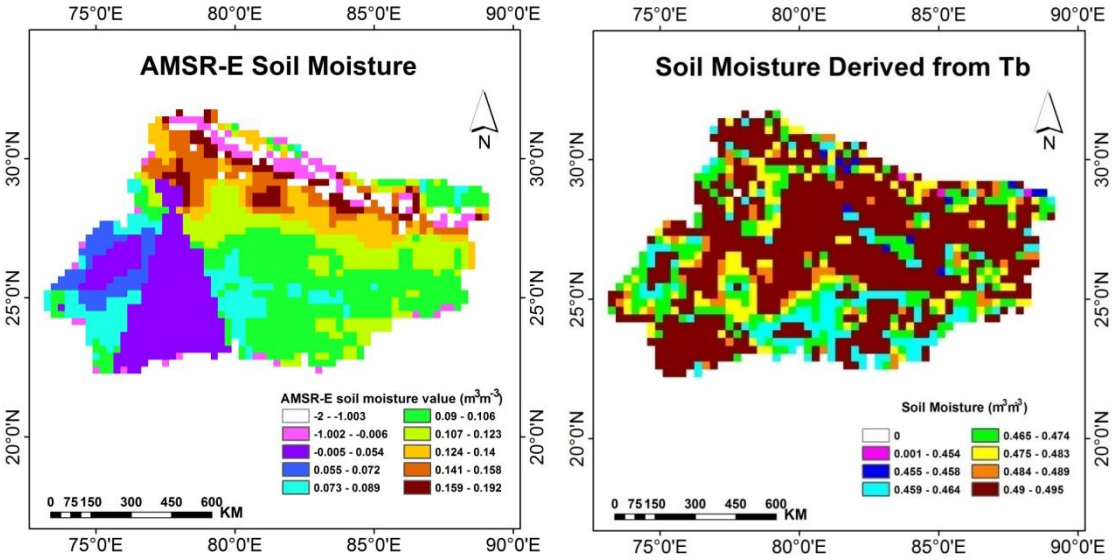

Fig. 5.6: Soil Moisture map derived from AMSR-E brightness temperature (Tb) and original AMSR-E soil moisture

Soil moisture derived from the algorithm is not used for further blending process as, the errors created due to radio frequency interference (RFI) is not removed. The errors due to heterogeneity are also not eliminated since it requires a complex processes and further ground data which was unavailable for the respective study area and thus could not be processed in the present study.

The derived soil moisture is not recommended too because the validation of the derived soil moisture could not be done, due to the ground soil moisture data unavailability. Thus the soil moisture product by AMSR-E is only used for the blending process.

Soil moisture is now merged with ASCAT soil moisture product keeping the GLDAS Noah data as the reference and CDF matching is performed for rescaling the microwave data.

5.3 CDF MATCHING

CDF matching approach for the rescaling of AMSR-E and ASCAT data as per Noah reference dataset is performed initially by pixel wise, choosing various pixels having different characteristics at varied locations of India with different rainfall and different climatic conditions prevailing. The final blending technique is processed for the whole Ganga basin chosen as the study area.

Those points were at location:

i. Mahendargarh in Haryana.
ii. Sova, Bikaner in Rajasthan.
iii. Hoshangabad in Madhya Pradesh.
iv. Bargarh in Orissa.
v. Haripur in Uttarakhand.

Mahendargarh in Haryana (28.22°N and 76.20°E) is chosen as this place in rich in Wheat production. The area has abundance of Wheat patches during the Rabi season starting in October till the next year April. The crop growing period for the wheat in Haryana is December end till April mid and harvesting is done during the mid April to April end.

- *Sova* in Bikaner district in Rajasthan having coordinates 27.78°N and 73.47°E is located in the middle of the Thar Desert and has a hot desert climate with very little rainfall and extreme temperatures as can be seen in the Table 5.1 and Fig. 5.7 for the year 2009:

Table 5.1: Temperature profile of Sova for the year 2009.

Month/Temp.	**Max Temp**	**Min temp**	**Mean temp**
January	24.59	9.63	17.11
February	29.19	13.62	21.41
March	34.62	18.33	26.47
April	38.14	22.15	30.15
May	44.25	29.07	36.66
June	42.44	29.35	35.89
July	40.1	28.17	34.13
August	38.65	28.26	33.45
September	39.69	25.38	32.54
October	37.34	22.03	29.68
November	30.74	14.42	22.58
December	26.63	11.02	18.83

(Source: NOAA-NCDC)

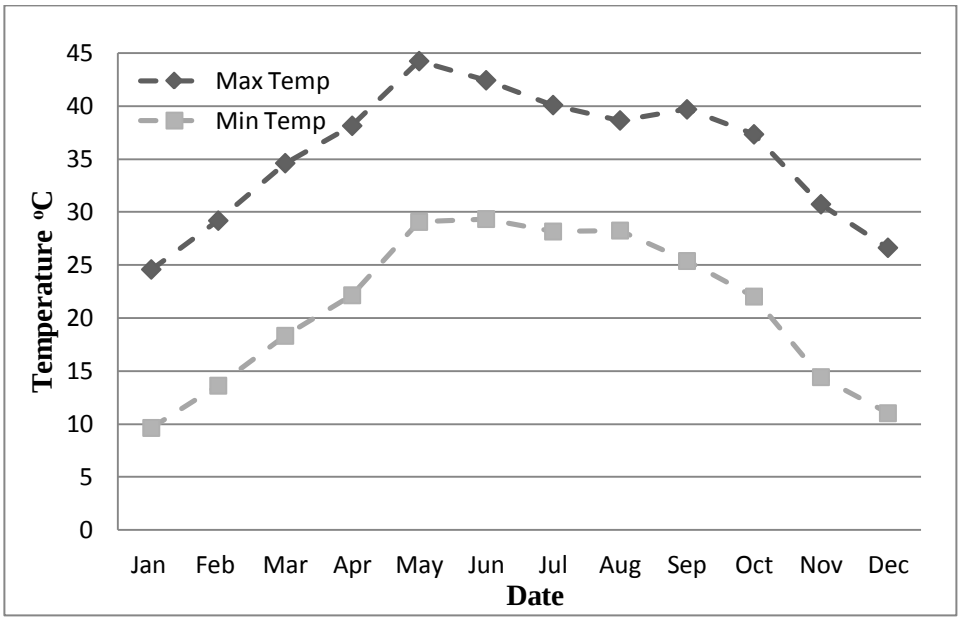

Fig. 5.7: Comparison of maximum and minimum temperature for the year 2009.

- *Hoshangabad* located in-between the the Indrasagar reservoir and Tawa reservoir in Madhya Pradesh with coordinates 22.76^{o}N and 77.70^{o}E respectively. It is located on the south bank of the Narmada River. The average maximum and minimum temperatures are 32^{o}C and 19^{o}C. In broader perspective, the climate of the area is neither hotter nor cooler. This area experiences all seasons.
- *Bargarh* located in the Bolangir district of western Orissa located at 21.50^{o}N and 83.48^{o}E lying along the Deccan plateau is rich in Rice production during the kharif season. Kharif season starts in June and goes until December. The transplanting of Rice/Paddy is done in the beginning of June till the start of August and eventually harvesting is done in beginning of December month.
- *Haripur* located in Haridwar district of Uttarakhand at 30.08^{o}N and 77.91^{o}E at an elevation of 330m MSL. This location is characterized by terrace farming at upland area and crop production according to the climatic condition on the plains. The maximum temperature goes upto 37^{o}C and minimum to 7^{o}C minimum in the winter period. The temperature profile is given in Table 5.2:

Table. 5.2: Temperature profile for the year 2009 in Haripur

Month/Temp	Max Temp	Min Temp	Mean Temp
January	23.00	7.92	15.46
February	25.34	9.45	17.40
March	29.38	13.29	21.33
April	35.27	17.42	26.35
May	36.18	21.00	28.59
June	37.97	23.31	30.64
July	32.67	23.46	28.06
August	31.68	22.90	27.29
September	31.48	21.74	26.61
October	30.03	13.56	21.79
November	26.34	10.54	18.44
December	22.69	7.00	14.85

(Source: NOAA-NCDC)

The rainfall variation for these locations can be viewed in Table 5.3,

Table 5.3: District wise rainfall data for the year 2009

State	Haryana	Rajasthan	Madhya Pradesh	Orissa	Uttarakhand
District	Mahendargarh	Bikaner	Hoshangabad	Bolangir	Hardwar
Location	Mahendargarh	Sova	Hoshangabad	Bargarh	Haripur
January	2	2	16.2	0	N.A.
February	0	7.9	0	0	N.A.
March	9	15.5	0	0	0.3
April	0	0	2.2	0	0
May	14	16.2	29.4	28.2	17.2
June	47.6	21.8	68.7	88.7	67.3
July	51.1	108.5	608.3	943.7	315
August	68.4	23.2	291.5	370.1	257.2
September	84.8	8.5	377.5	129.9	222.7

October	0	0.1	73.3	52.1	13.1
November	0	0	70.1	33.6	0
December	0	0.8	37.5	0	0
Annual Total	276.9	204.5	1574.7	1646.3	892.8

(Source: Indian Meteorological Department (IMD), India)

As mentioned in the methodology the CDF matching is done initially by deriving the time series for the each pixel for all the three datasets for the complete year 2009.

Keeping the Mahendargarh location as an example, the time series of soil moisture estimates for the AMSR-E, ASCAT and Noah are plotted in Figs 5.8, 5.9 and 5.10

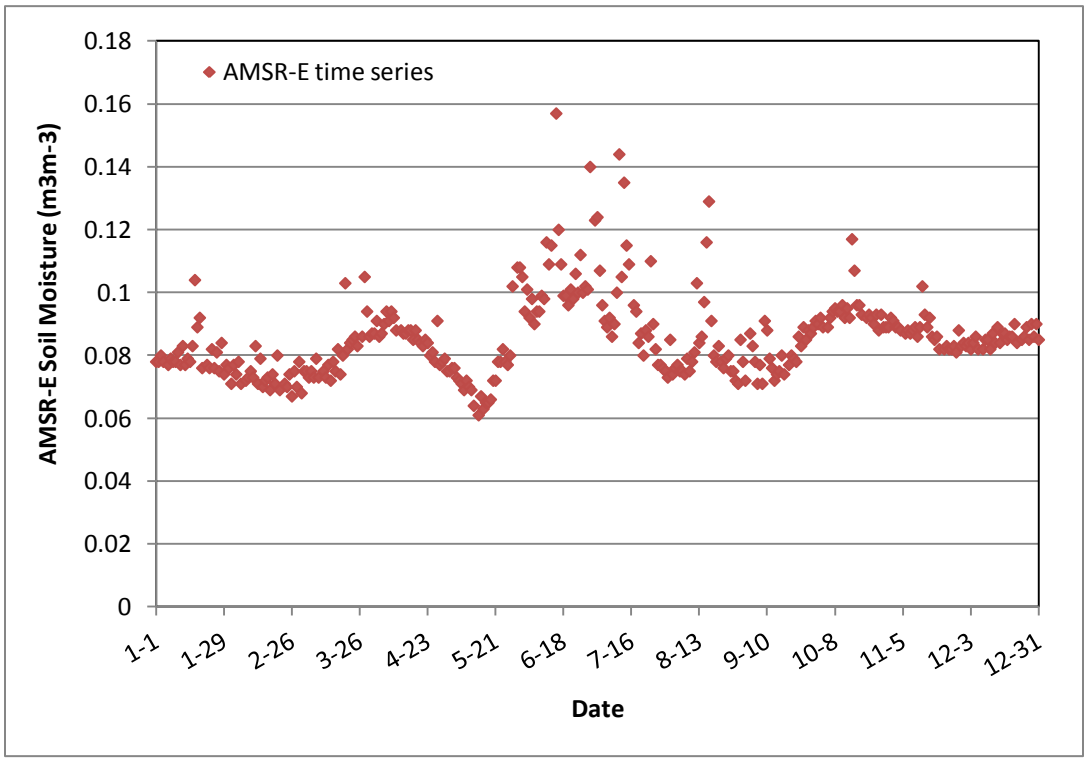

Fig. 5.8: AMSR-E time series map

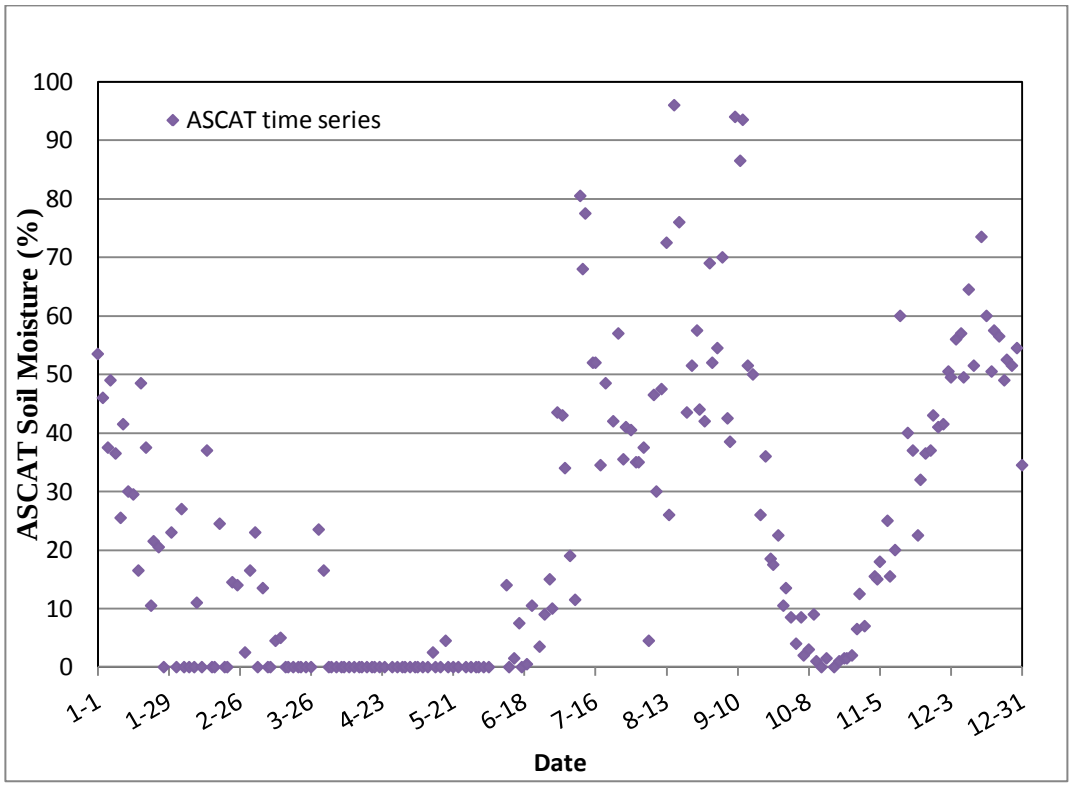

Fig. 5.9: ASCAT time series map

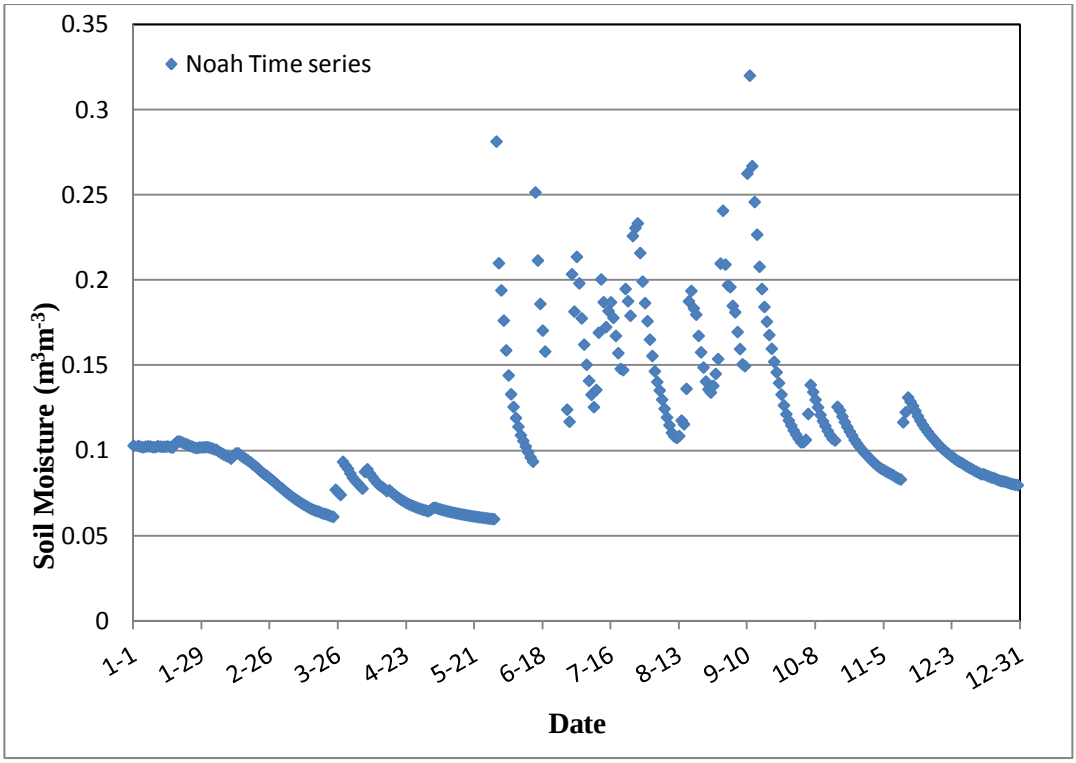

Fig. 5.10: Noah time series map

The cumulative distribution frequency (CDF) curves for these datasets are plotted, Figs 5.11, 5.12 and 5.13 for the respective time series data considering the same location.

The process of plotting the CDF curves for the yearly time series for each pixel requires programming and Python program is developed to estimate the cumulative values at various intervals and are plotted respectively. A text file is created for each pixel in the study area estimating the frequency of soil moisture value at defined interval.

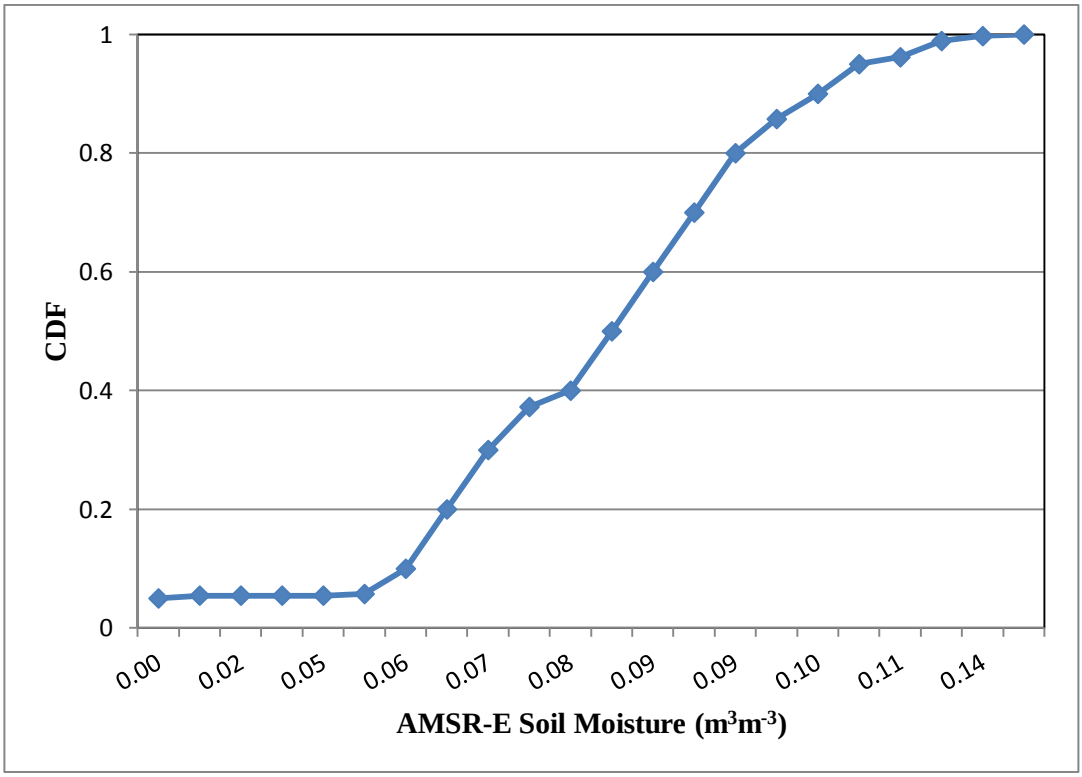

Fig. 5.11: CDF curve of AMSR-E soil moisture estimate

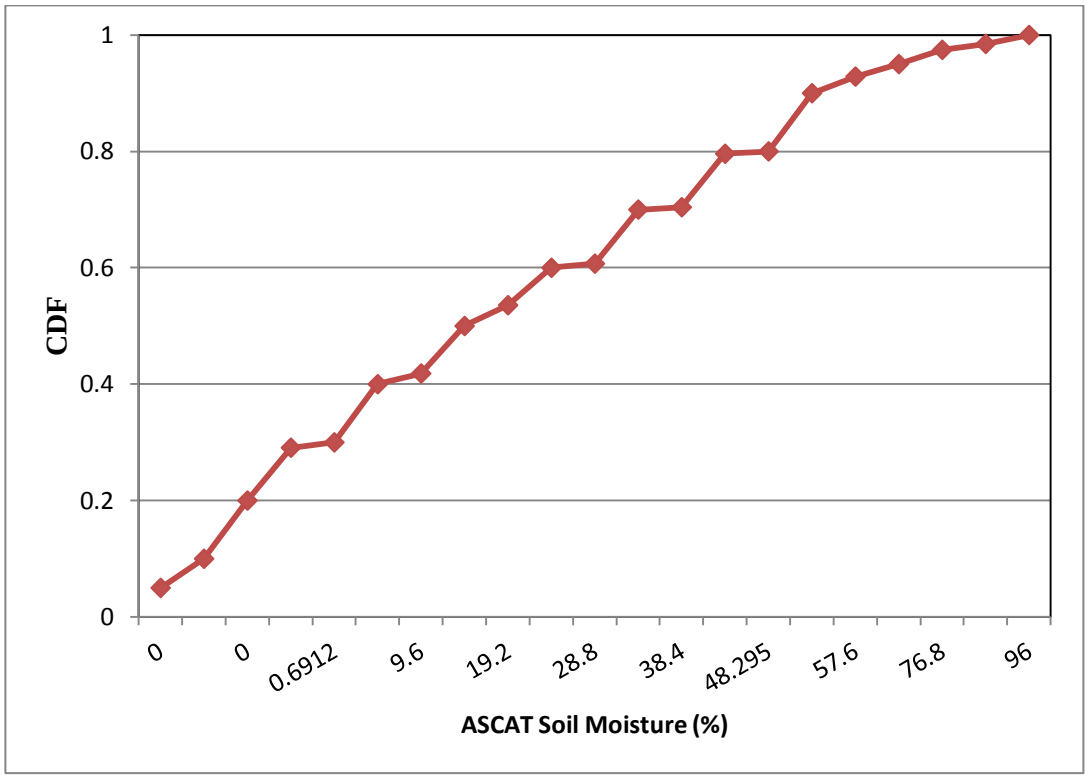

Fig. 5.12: CDF curve of ASCAT soil moisture estimate

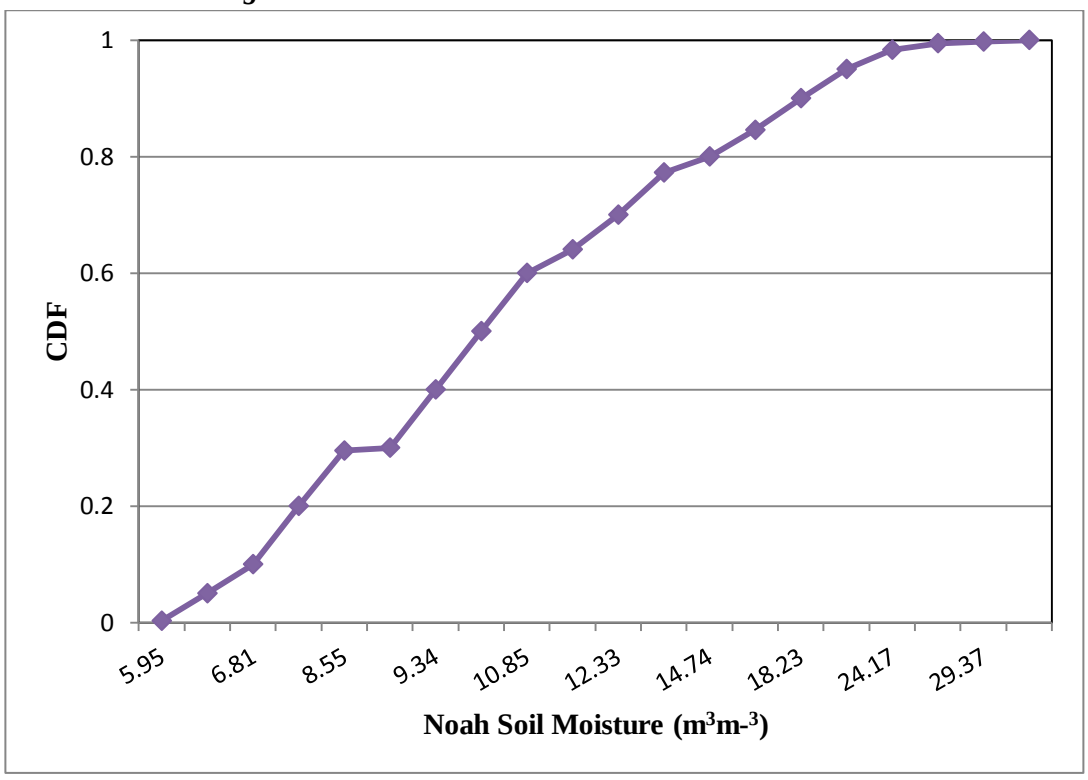

Fig. 5.13: CDF curve of Noah soil moisture estimate

Once the CDF curves are plotted each plot is divided into various segments and linear regression line of AMSR-E against Noah is plotted (Fig 5.14). The process is repeated similarly for ASCAT and Noah (Fig 5.15)

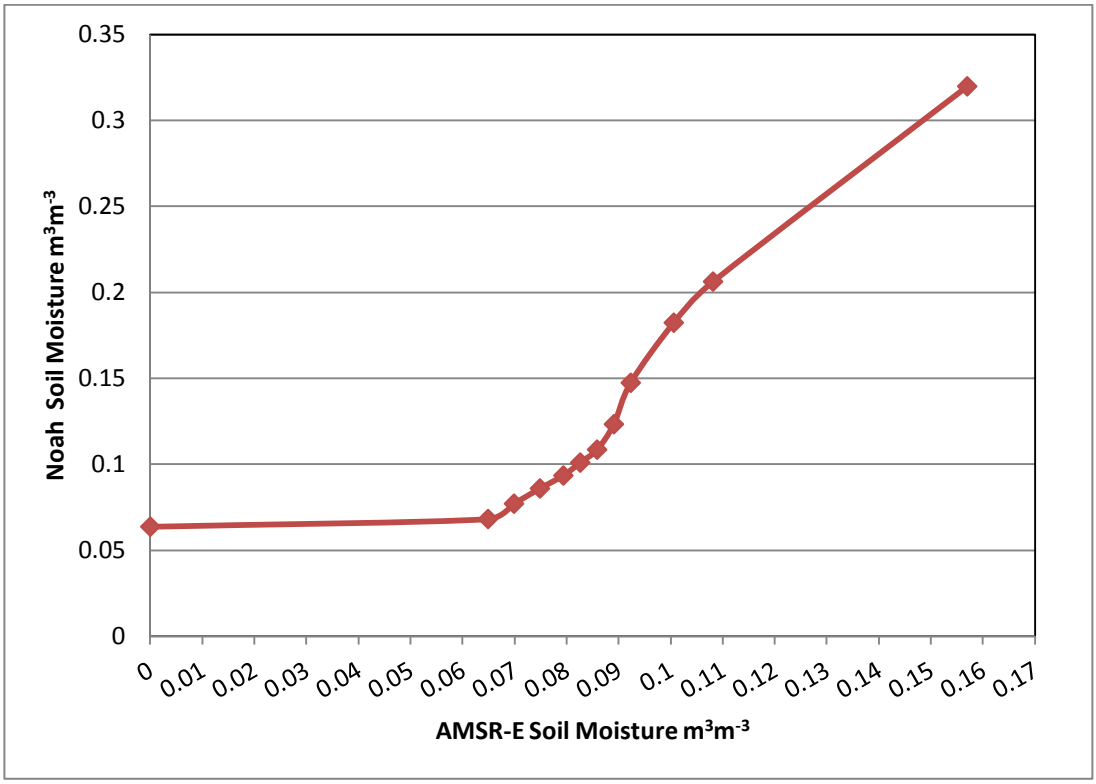

Fig. 5.14: CDF curve of Noah plotted against CDF curve of AMSR-E for 11 segments

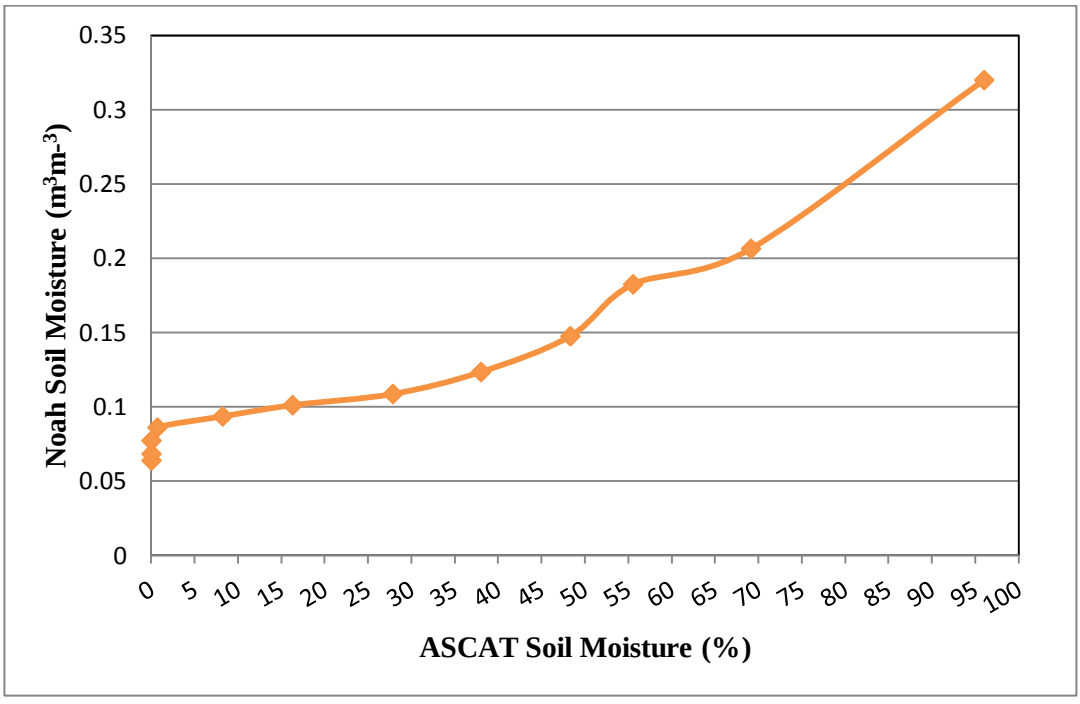

Fig. 5.15: CDF curve of Noah plotted against CDF curve of ASCAT for 11 segments

Rescaling of AMSR-E and ASCAT soil moisture data is carried out. The Slope (m) and intercept (c) values are estimated for each segment using the programming. For every pixel, a linear equation is deduced which is used for the rescaling purpose.
The equations for the various segments for the Mahendargarh location are derived from the slope and intercept and the linear equations for each segment are in Table 5.4 and 5.5.

Table 5.4: Linear equations for the segments between the graph Noah and AMSR-E

Segment No.	**Noah and AMSR-E slope (m)**	**Intercept (C)**	**Linear Equation**
1	6.863	6.37	**Y=3.863X+6.367**
2	178.826	-4.81	**Y=178.826-4.812**
3	177.429	-4.72	**Y=177.429X-4.717**
4	167.253	-3.96	**Y=167.253X-3.957**
5	232.72	-9.04	**Y=232.72X-9.044**
6	232.72	-9.22	**Y=232.72X-9.222**
7	456.816	-28.44	**Y=456.816X-28.438**
8	744.446	-53.93	**Y=744.446X-53.929**
9	422.473	-24.13	**Y=422.473X-24.131**
10	317.275	-13.82	**Y=317.275X-13.816**
11	232.448	-4.48	**Y=232.448X-4.482**

Table 5.5: Linear equations for the segments between the graph Noah and ASCAT

Segment No.	**Noah and ASCAT Slope (m)**	**Intercept (C)**	**Linear Equation**
1	0	6.37	**Y=6.367**
2	0	6.81	**Y=6.812**
3	1.279	7.70	**Y=1.279X+7.703**
4	0.1	8.52	**Y=0.1X-8.5179**
5	0.093	8.58	**Y=0.093X+8.577**
6	0.065	9.04	**Y=0.065X+9.036**

7	0.146	6.78	**Y=0.146X+6.783**
8	0.234	3.44	**Y=0.234X+3.436**
9	0.483	-8.59	**Y=0.483X-8.589**
10	0.176	8.46	**Y=0.176X+8.455**
11	0.422	-8.55	**Y=0.422X-8.547**

Using the above mentioned linear equations, rescaling process is performed for each value of AMSR-E and ASCAT for the year 2009 and since this task requires the need for programming. CDF matching and rescalling is performed with the help of Python programming. The rescaled Soil moisture value of AMSR-E has 0.902 correlation with that of original soil moisture value and similarly Noah rescaled value has the correlation of 0.92 with the original ASCAT soil moisture value.

Rescaling soil moisture values of AMSR-E and ASCAT is followed by CDF matching. CDF matching is performed by overlapping CDF curves of Noah, rescaled AMSR-E and rescaled ASCAT product (Fig 5.16).

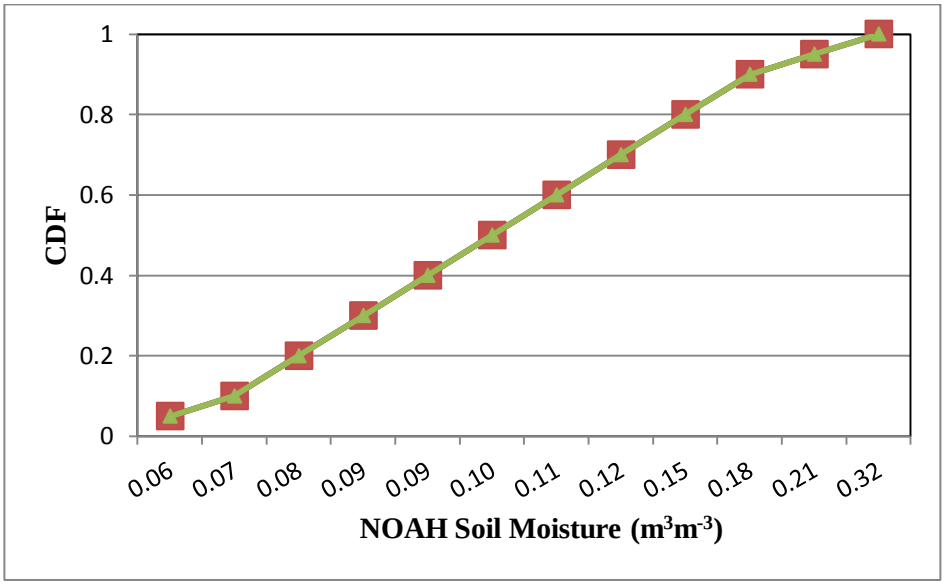

Fig. 5.16: CDF curve of Noah plotted against AMSR-E and ASCAT Soil moisture product.

5.4 BLENDED TIME SERIES PLOTS

Time series plot of blended soil moisture product is compared with that of AMSR-E and ASCAT soil moisture product for the respective locations as mentioned above for the year 2009.

5.4.1 Mahendargarh

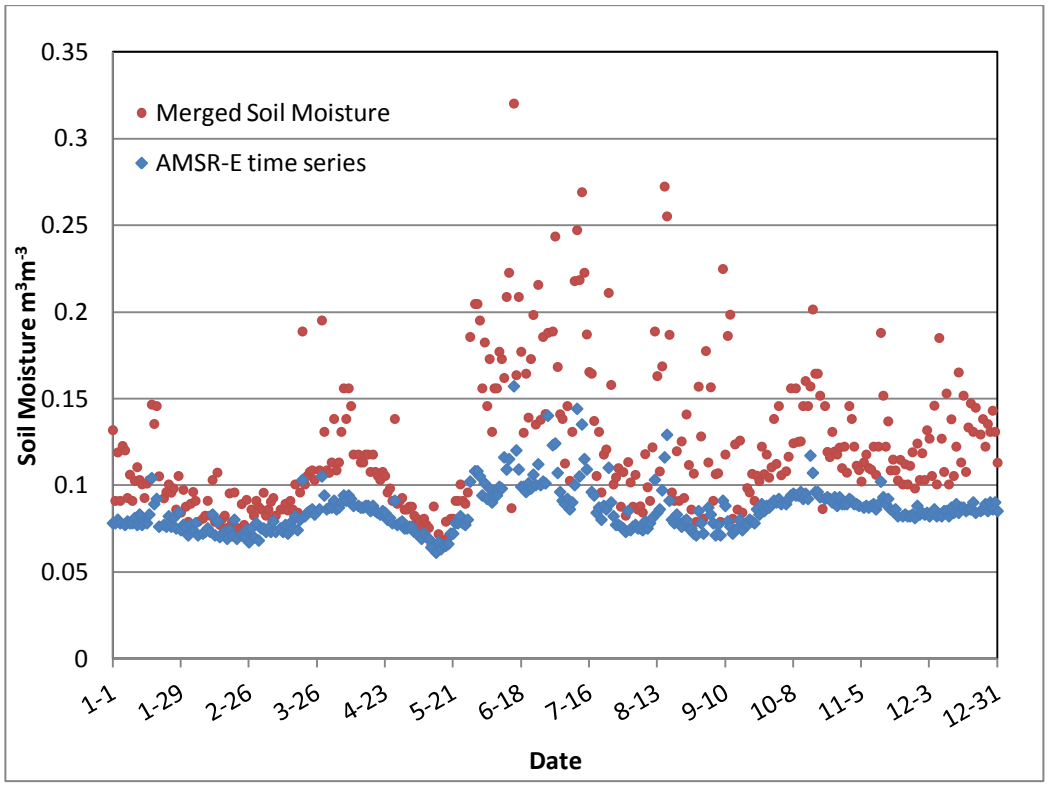

Fig. 5.17: Plot of time series between Blended soil moisture product and AMSR-E product

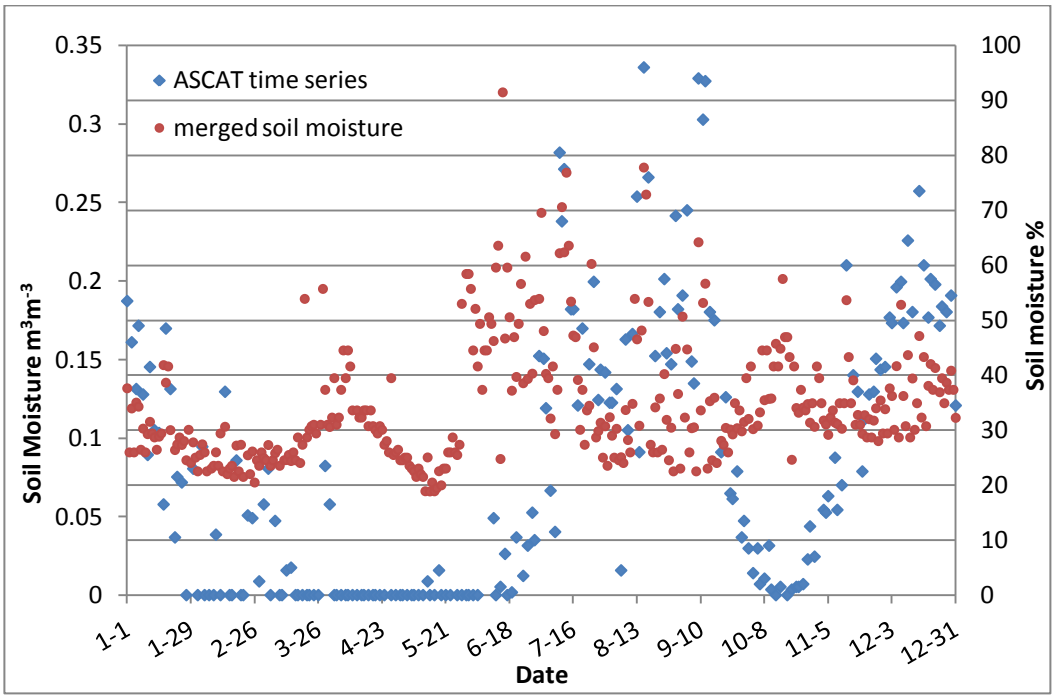

Fig. 5.18: Plot of time series between Blended soil moisture product and ASCAT product

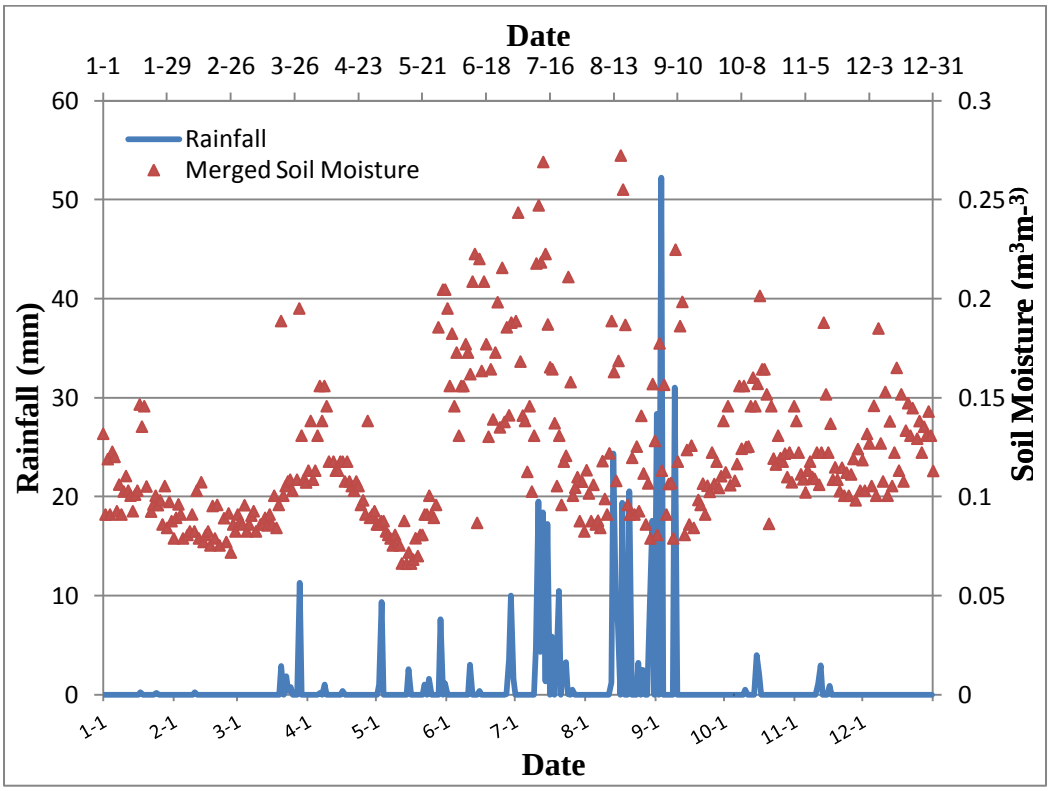

Fig 5.19: Plot of time series between Blended soil moisture product and rainfall

The plots depicting the soil moisture time series trends for AMSR-E, ASCAT and the merged soil moisture data clearly indicates that during the four month time period of June, July, August and September there is a high amount of soil moisture, which is typically the monsoon season in the area.

In India, southwest monsoon dominates the rainfall period and in also in the region of Mahendargarh, Haryana, 80% of rainfall occurs between July to September that is the monsoon period. With the progress of monsoon from June to September the soil moisture value is always high and reaches upto value 0.32 m^3m^{-3}. The minimum soil moisture during the monsoon period is 0.079 and goes upto 0.32 m^3m^{-3}. It is also clearly visible that just before the onset of rainfall that is in the month of May the soil moisture value is low, which could be the effect of harsh summer in the area.

By observing the plot of merged soil moisture data with that of the rainfall pattern, it is indicates that during the period of high rainfall, the soil moisture value is also touching high the theoretical saturation limit. Rainfall has a direct impact on the soil moisture value and this is clearly shown in the above graph (Fig. 5.19).

This Mahendargarh area is Wheat producing place where the sowing takes place in Oct-Dec months and harvesting takes place in April month. During the irrigation period of January to March extending until mid of April, the soil moisture is relatively high. Irrigation leads to relative higher soil moisture as compared to normal bare conditions.

The hottest months in this area are May and June and soil moisture values decline during this period. In between mid of April to the end of May, the soil moisture value declines in a linear trend reaching minimum value of 0.066 m^3m^{-3} as during these period two important phenomenon to observe are, harvesting of Wheat and simultaneously the increasing temperature.

Observing the Fig 5.17, the values are almost same and they follow a similar pattern due to the availability of data at the daily scale having the correlation value 0.7942, but in the Fig 5.18, it is clearly showing that ASCAT data is unavailable at various times of the year, as it is the active microwave data and it lacks temporal resolution. The non-availability of ASCAT data for many time steps itself justifies the attempt done in this study, the blended product generated at point scale using ASCAT, AMSR-E and Noah combines advantages of all three sources (i.e. temporal consistency, spatial resolution, value/unit standardization).

5.4.2 Sova

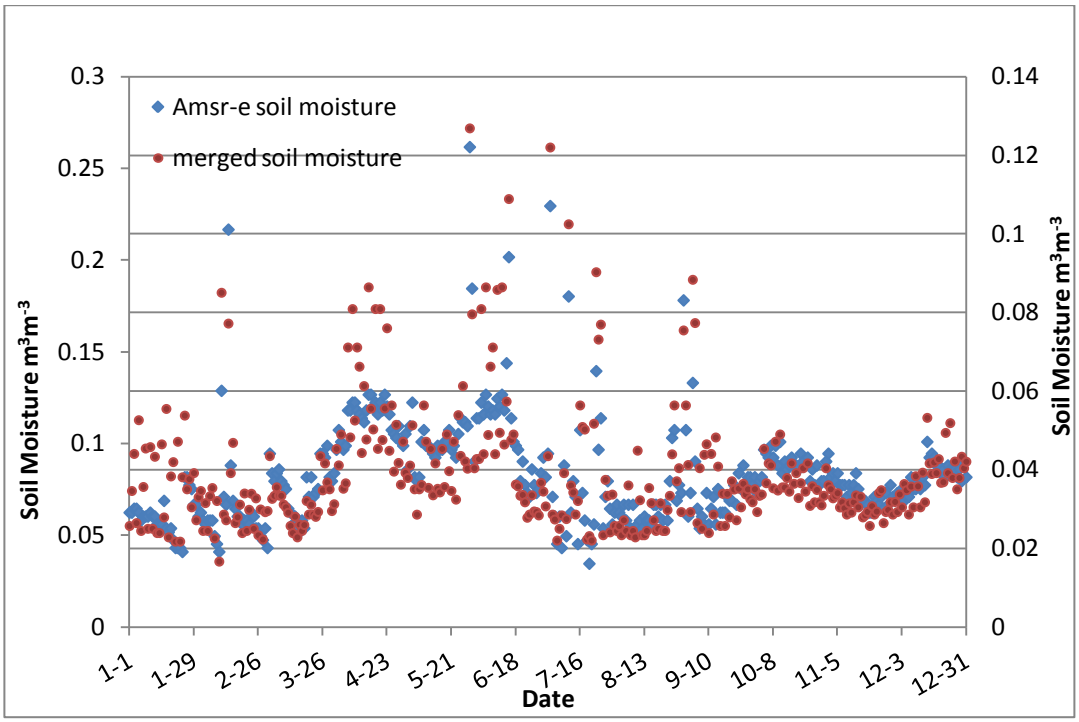

Fig 5.20: Plot of time series between Blended soil moisture product and AMSR-E product

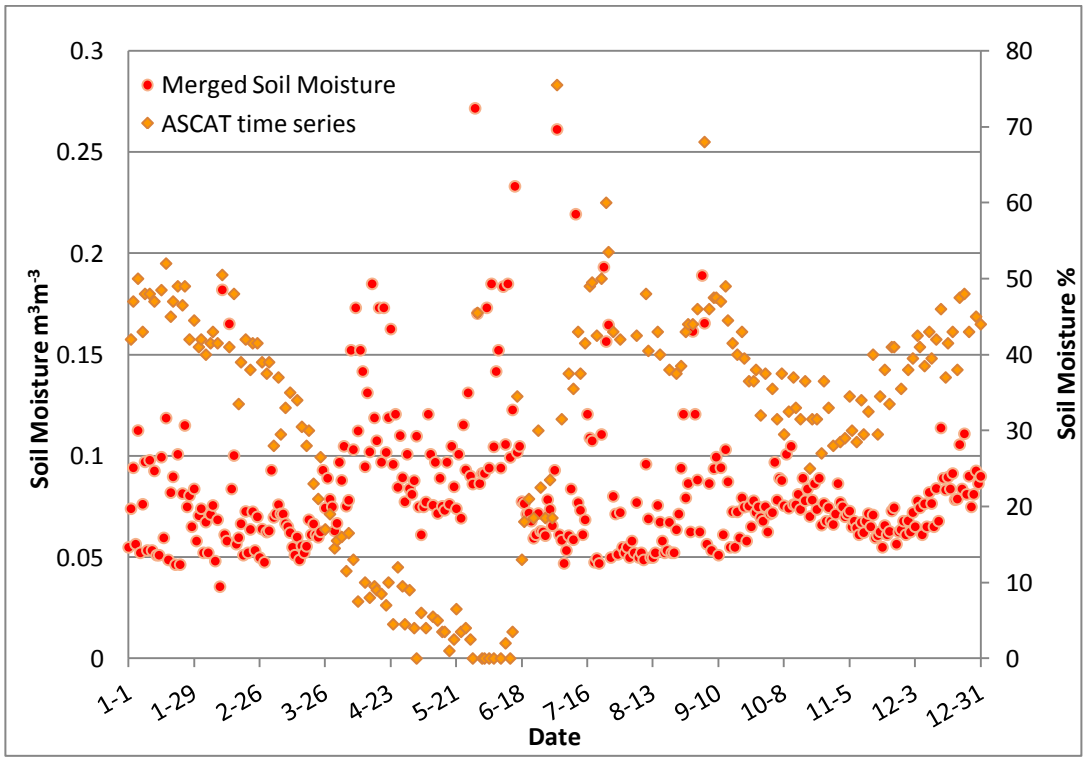

Fig. 5.21: Plot of time series between Blended soil moisture product and ASCAT product

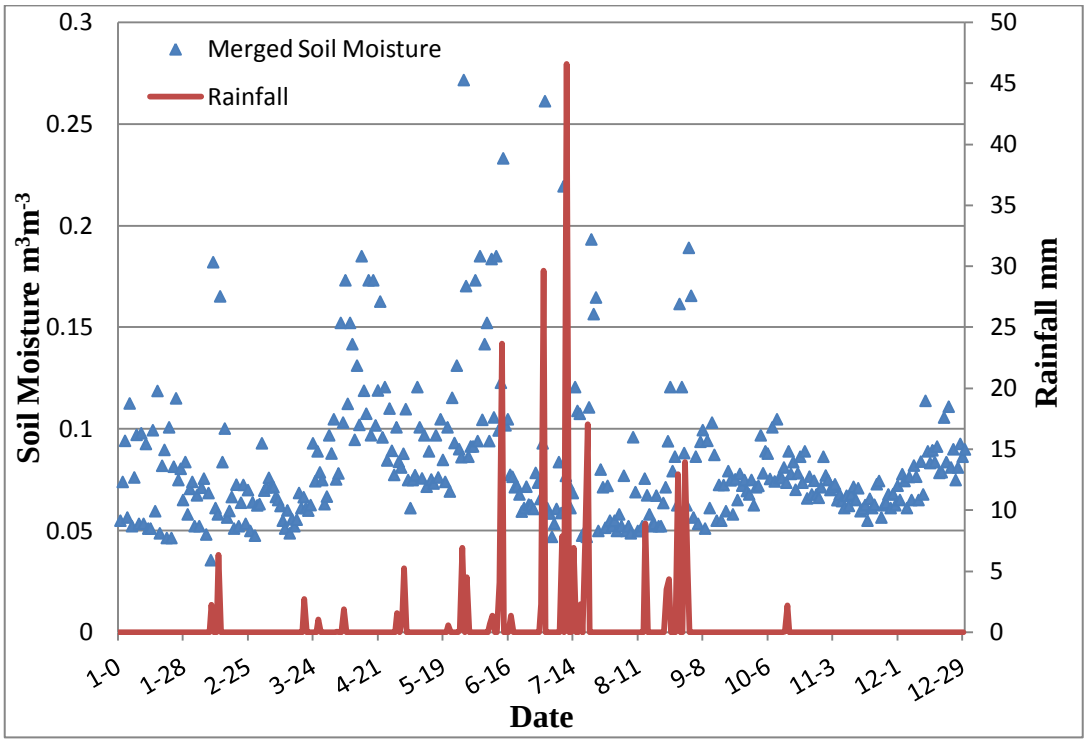

Fig. 5.22: Plot of time series between Blended soil moisture product and rainfall

The soil moisture obtained from the merged soil moisture product is distributed and the values are generally lying in the range of 0.05 to 0.125 m^3m^{-3}.

The monsoon period in the Sova region is between June to August with scanty rainfall in May too. It can be seen in Fig. 5.22 that soil moisture value reaches its peak in that duration only with value of 0.27 m^3m^{-3}. Since the rainfall is an uncommon event here and with the scanty of rainfall, the soil moisture is also not very high in this region.

Observing the rainfall trends, the peak rainfall is 46 mm in the month of July. The period of June to the start of August, there is a significant amount of rainfall. Even though the soil moisture is not constantly high during that period, this may be due to the low water holding capacity of sandy soil in the area; the soil moisture is relatively high in monsoon because of the rainfall events.

Other than rainfall, temperature plays a very vital role especially in an area like Sova in Bikaner. With temperature going high upto 44^oC in the month of June and constantly maintains a very high temperature during the period of April end to September, the soil moisture values do not goes to a very high figures. The minimum temperature is in the range of 28-30^oC during those four hot months. The maximum soil moisture during that period is 0.2716 m^3m^{-3}. Although there is a considerable rainfall in those months, the soil moisture values stays below the maximum due to the high temperature. The temperature has a very significant role in soil moisture.

The Sova region is in the desert area of Rajasthan with major soil type as sandy soil and brown loamy soil (Source: Agriculture Contingency Plan for District: Bikaner, ICAR), and this is the main reason for the high temperature and scanty rainfall leading to a very moderate value

of soil moisture over the entire year. The land use land cover as this region leads to the soil moisture value as optimal as 0.1 to 0.2 m^3m^{-3} and that is due to the cooler temperature in the nights.

The major filed crops cultivated in this region are Gram in Rabi and Groundnut and Beans in Kharif season. The sowing period for the Kharif crop is in the months of June and July and the harvesting is done in October and November and in between these months the soil moisture is comparatively a bit higher due to the irrigation upto the value 0.23 m^3m^{-3}.

5.4.3 Hoshangabad

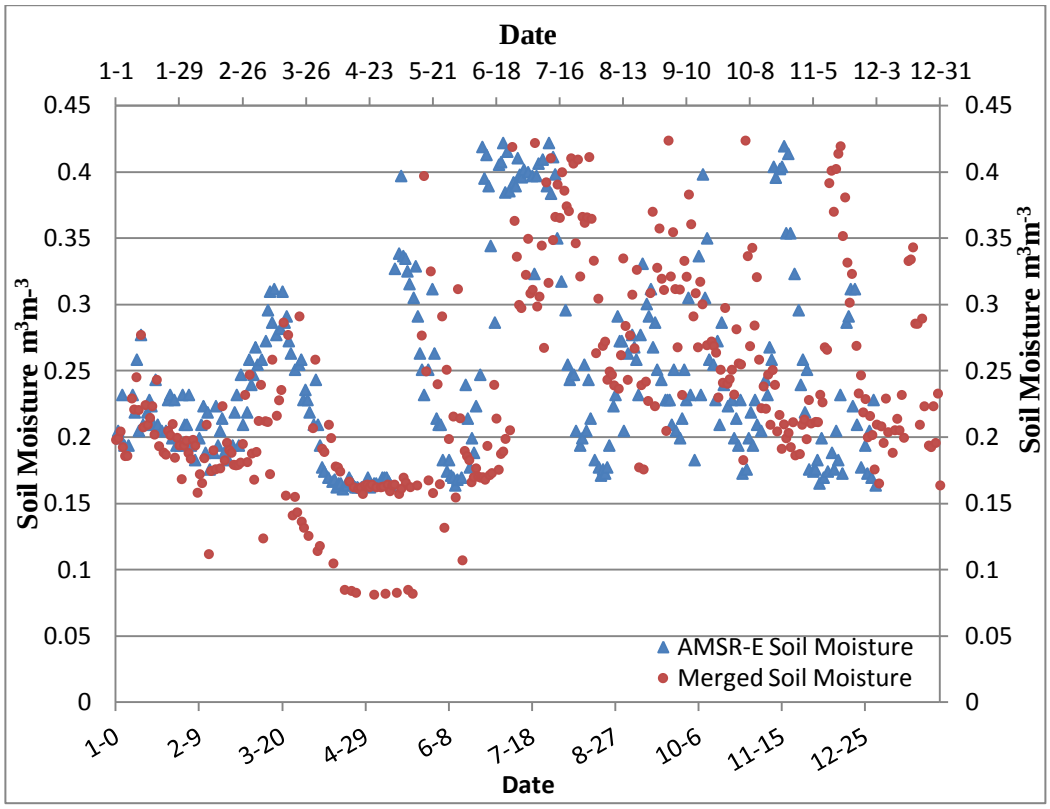

Fig. 5.23: Plot of time series between Blended soil moisture product and AMSR-E product

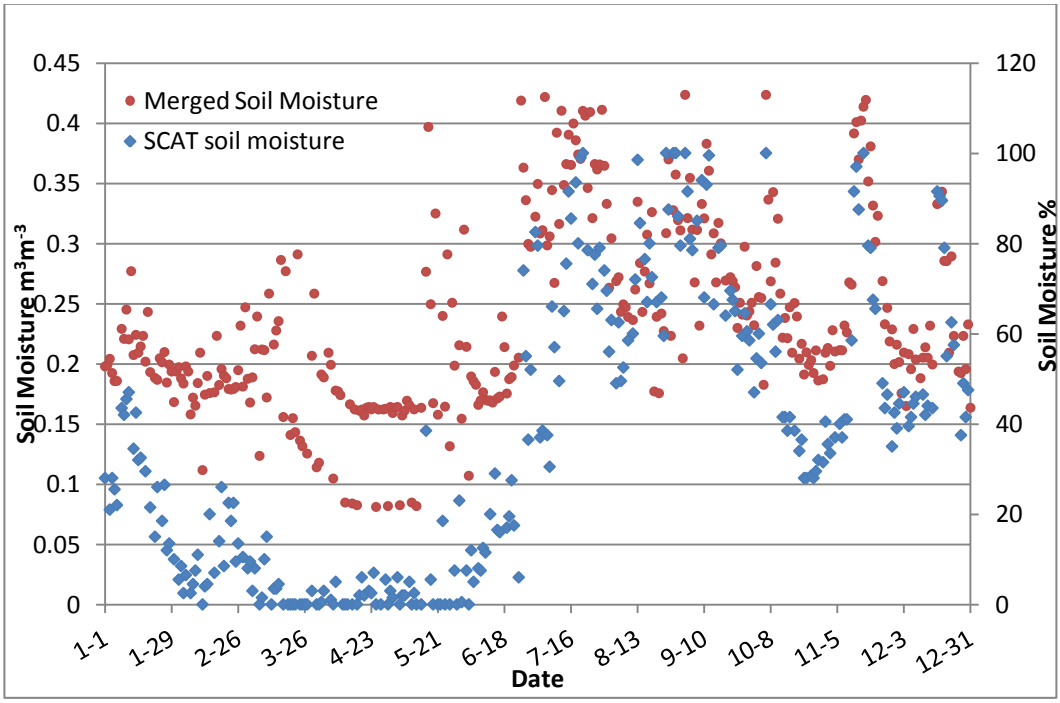

Fig. 5.24: Plot of time series between Blended soil moisture product and ASCAT product

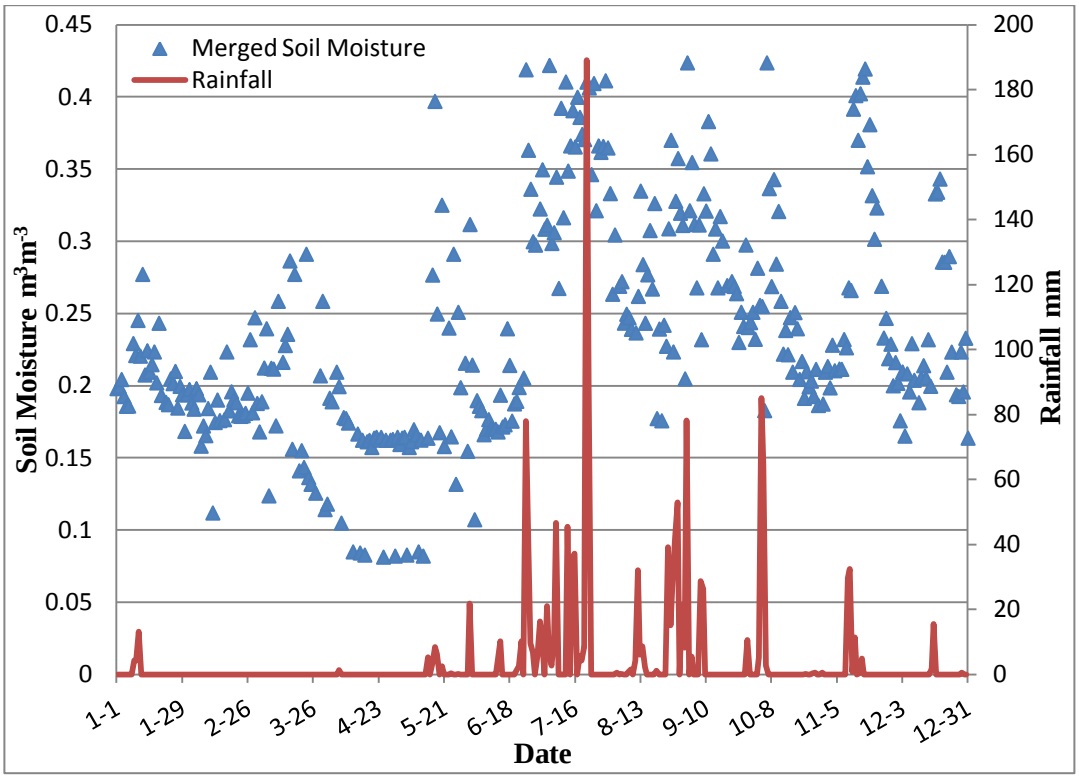

Fig. 5.25: Plot of time series between Blended soil moisture product and rainfall

The dominated climate in Hoshangabad is hot summer and dryness, except during the time of south west monsoon. From March to the middle of the June is characterized by summer season followed by southwest monsoon from middle of June till September. About 92.8% of the annual rainfall is received during monsoon season (source: hoshangabad). The maximum rainfall during the duration of May till November in 2009 is seen in July, with 608.3 mm rainfall in that month. Similarly the soil moisture is highest in the month of July, even though the soil moisture is constantly high after the end of May till the November-December time. The soil moisture during the period of May till December has raised upto value 0.4234m^3m^{-3} and lowest to 0.1 m^3m^{-3}.

The monsoon trend is an overall scenario, and by observing the rainfall trend in 2009 over the area it is depicting that at the mid of May that is from 14th May the monsoon season has initiated in this year (2009) and has goes upto first week of October with maximum rainfall of 189 mm on 21st September and similarly the soil moisture is high during that period. The information from the blended soil moisture data clearly signifies that during the three month duration of June, July and August the soil moisture is at its peak and very high especially in the month of July.

This region is experienced by a very hot summer with maximum temperature reaching high upto 42^{o}C in May and the driest month of the year is explicitly April (Source: District Ground Water Information Booklet, Hoshangabad District, Madhya Pradesh, Central ground Water Board). During the period of end of February till the mid off May, the soil moisture value is comparatively low as due to effect of high temperature in summer season. During the summer period the soil moisture value goes low to 0.08 m^3m^{-3}. In the winter season of December to February the soil moisture value is in the range 0.15 to 0.255 m^3m^{-3}, relatively lower than seen in the rainfall period.

This region is rich in production of Green Gram which is cultivated due to the presence of good source of irrigation and fertile alluvial soil, the Green Gram is sowed and harvested during the period of June-Aug to Oct-Dec. In between the period there is a surplus amount of water supply for the irrigation keeping the soil moisture value constantly high in the second half period of the year.

Thus, temperature, rainfall, and crop cycle all constantly affect the soil moisture value and this can be clearly visualized in the above mentioned plots.

In the Fig 5.24, there is un-availability of the data at various dates in the initial time of the year and the available values are showing comparatively lower values than expected. Thus providing ambiguous data for the time period and this caveat is nullified by deriving the blended product.

5.4.4 Bargarh

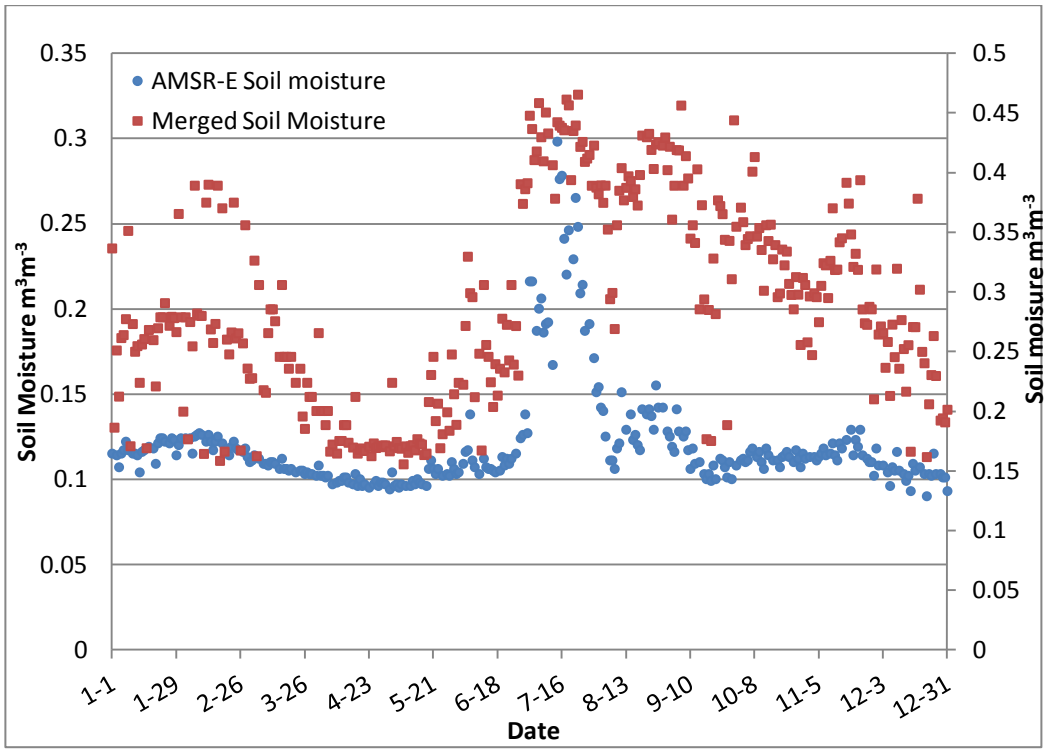

Fig 5.26: Plot of time series between Blended soil moisture product and AMSR-E product

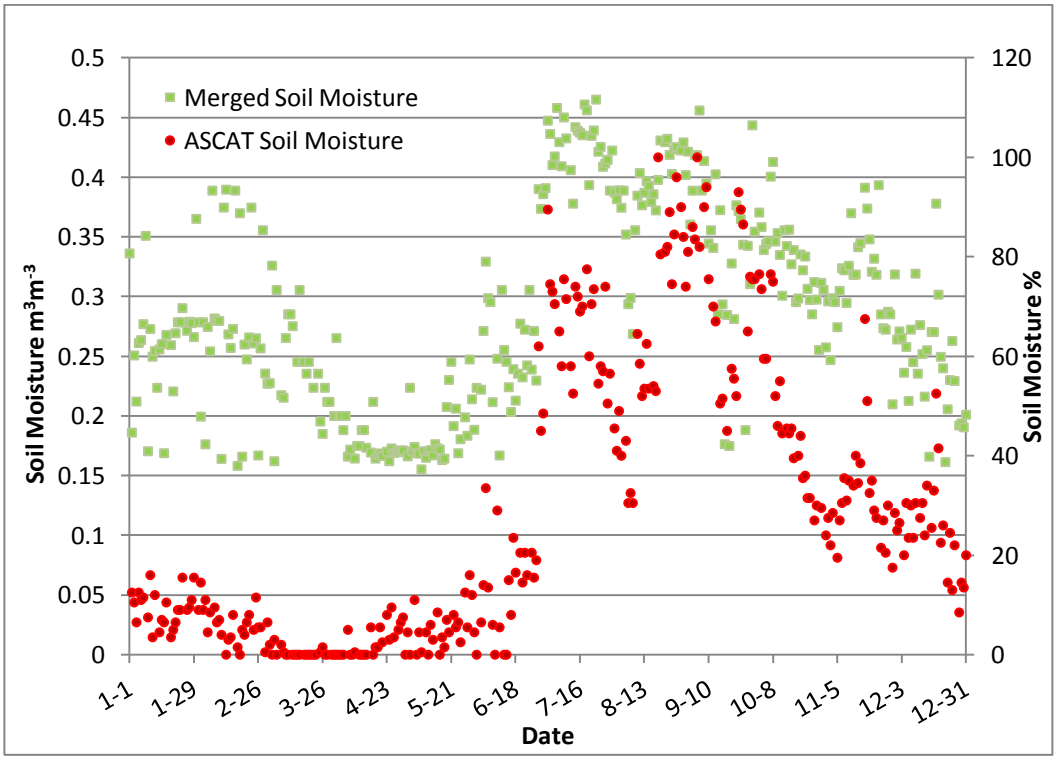

Fig. 5.27: Plot of time series between Blended soil moisture product and ASCAT product

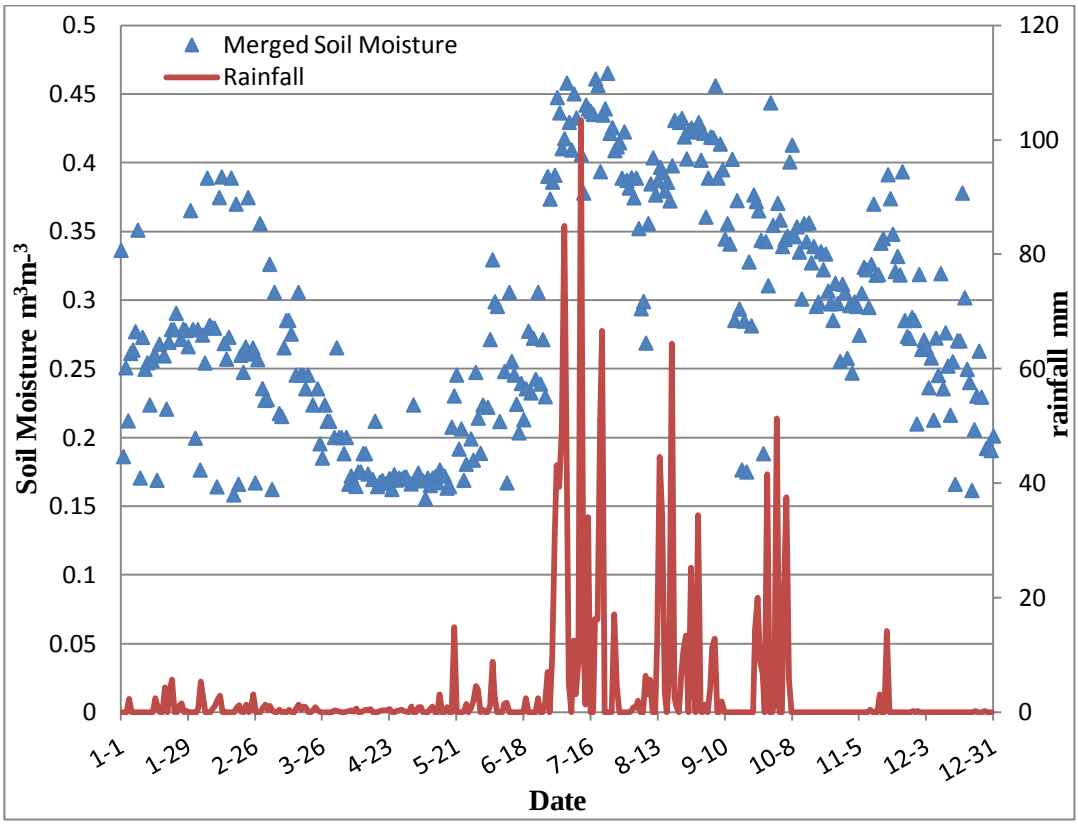

Fig. 5.28: Plot of time series between Blended soil moisture product and rainfall

Bargarh in Orissa is predominantly characterized for Paddy/Rice production. Climate wise Bargarh district experiences extreme type with hot and dry summer followed by humid monsoon and severe cold.

The monsoon is primarily by the south west monsoon setting up in start of July till end of October pouring showers with maximum rainfall of 943.7 mm in the month of July. The soil moisture eventually is quite high during the respective period. With the onset of monsoon the soil moisture value linearly increases to reach above 0.4 m^3m^{-3} and then decrease in the end of year, in the month of December.

The rainfall trend as seen in Fig 5.28 shows that, there is a heavy rainfall during the July till October, with maximum rainfall observed on 12th July of 103.432 mm and corresponding soil moisture value is 0.406 m^3m^{-3}. The soil moisture value after blending gives us the value range 0.3 to 0.5 m^3m^{-3} for the time period of Jul-Oct, which corresponds well with the rainfall statistics. In the complete series of soil moisture the maximum soil moisture goes to 0.465 m^3m^{-3} and minimum value as 0.1553 m^3m^{-3}.

The temperature effect is vividly shown in the above comparison, in the summer season of March till the end of June the rainfall is scantly and accordingly the soil moisture value is very low and it constantly stays low depicting a very clear relationship with that of rainfall and temperature. From the end of February till the second week of May there is no rainfall and temperature is also high reaching upto maximum of 46^{o}C in the month of June. There is a

decreasing trend in the soil moisture value in March month and constantly stays low until the first rainfall in the third week of May.

With Rice and Paddy cultivation dominating in the region, all the lands are occupied for this crop production where more area is kept for the rainfed rice production than for the irrigation. June and July is the sowing window for Paddy crop in the Kharif season and are harvested in the duration of December and January. Since the Kharif season requires plentiful rainfall which is there in the monsoon period the soil moisture value is always very high. Irrigation predominates if the rainfall water is not sufficient and this summarizes for the higher value of soil moisture in the blended product.

Deciphering information from the Fig 5.26, the AMSR-E soil moisture is showing peaks for a very short duration that is in the mid of June to start of August, but that is inaccurate as the rainfall period extends till October. In the Fig 5.27, it shows very low soil moisture from the start of year till June, with values in the range 0 to 16 % and there is large amount of unavailability of data due to the sensor characteristics. The blended soil moisture product relatively matches with that of rainfall pattern and shows significant values accordingly.

5.4.5 Haripur

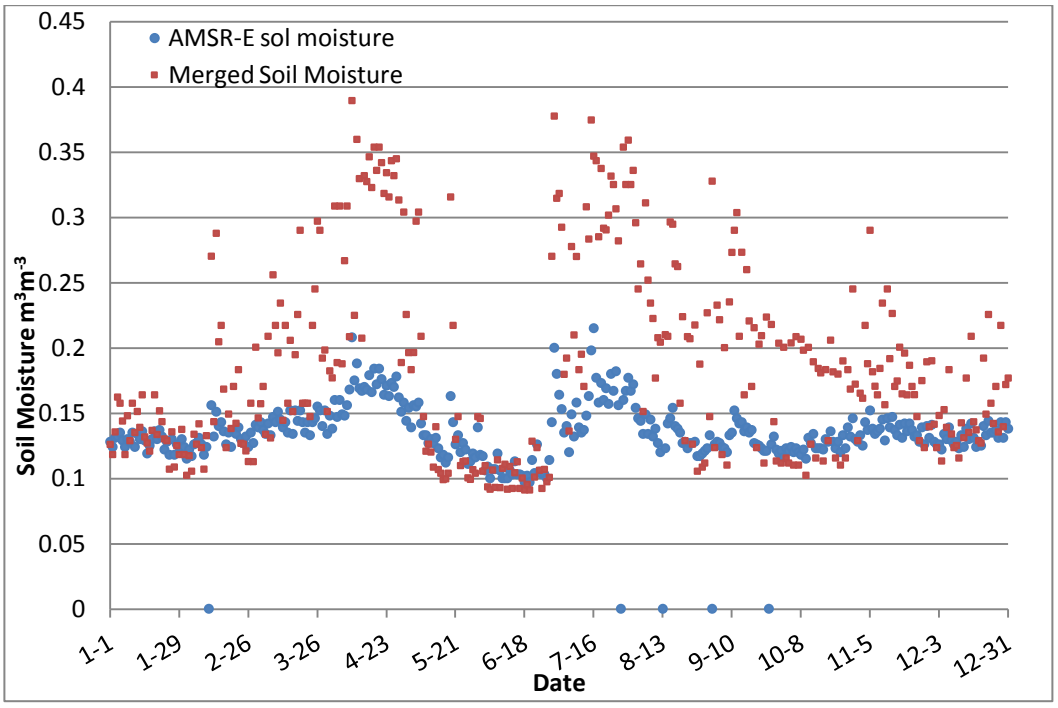

Fig. 5.29: Plot of time series between Blended soil moisture product and AMSR-E product

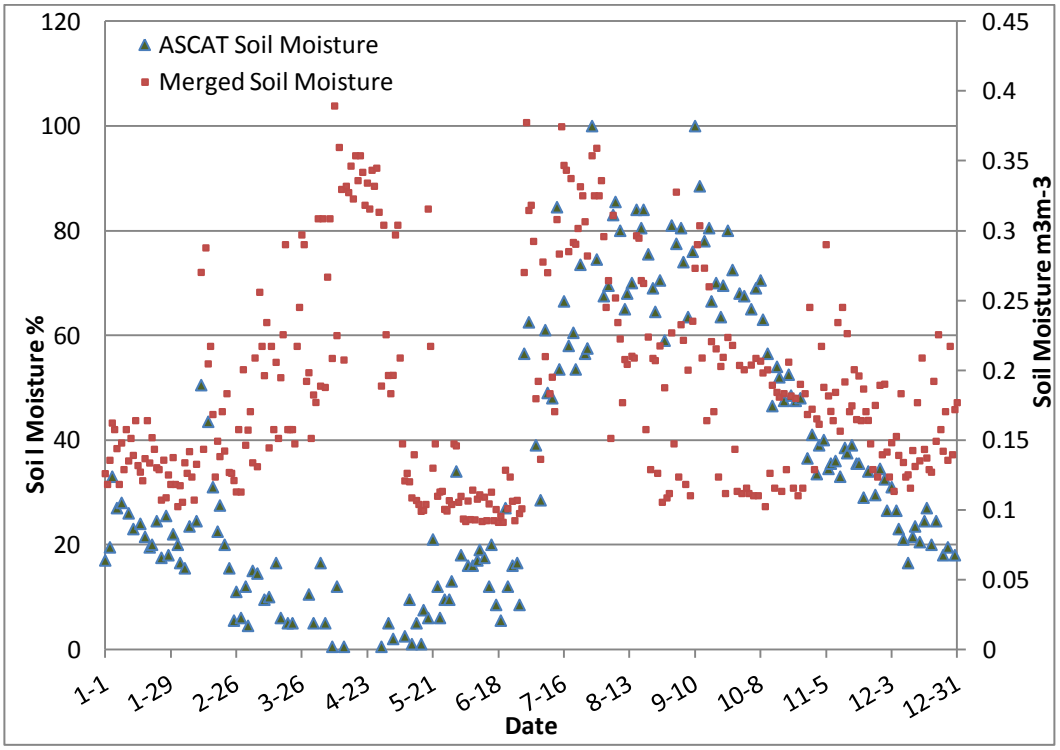

Fig. 5.30: Plot of time series between Blended soil moisture product and ASCAT product

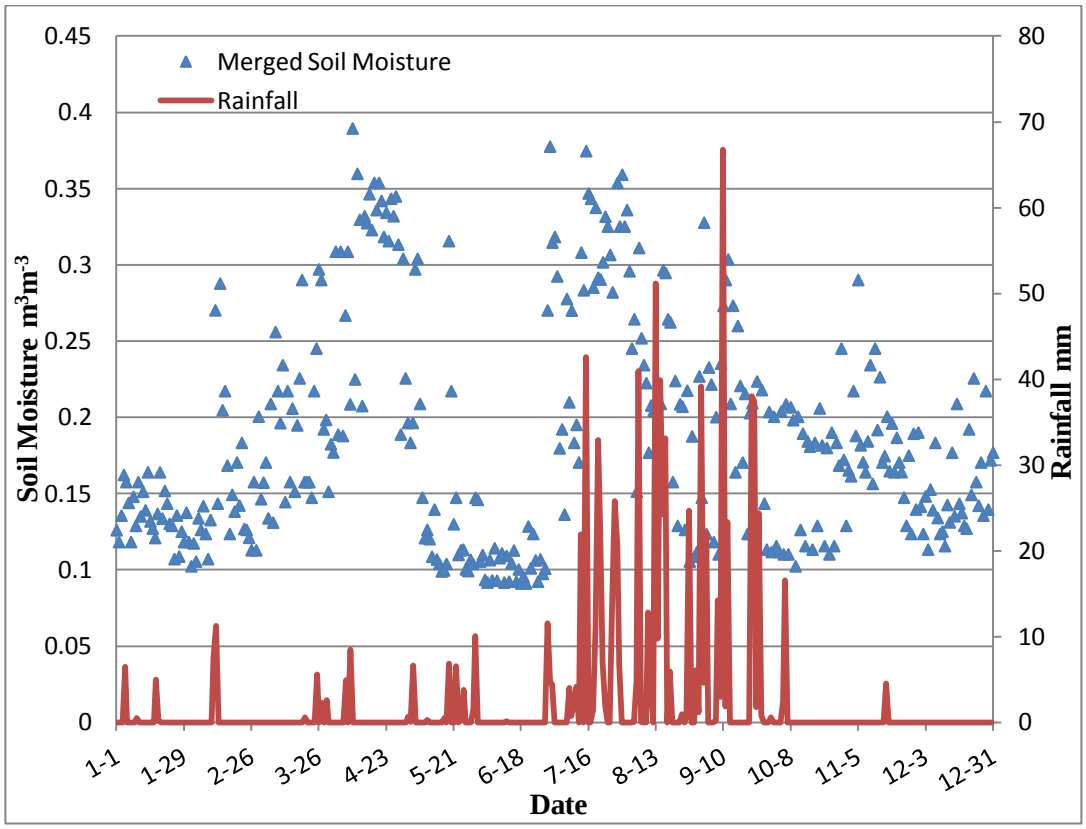

Fig. 5.31: Plot of time series between Blended soil moisture product and rainfall

The soil moisture pattern observed here is that there is a high value in the period of March and start of April and then very low value in the months of April to June. Prior to this there is a very low value in the initial two months of the year due to very low temperature in that time. During the monsoon period of July to October the soil moisture value is also varying with very high value in July and August and lowers in the coming months but it do not reaches the minimum value. The soil moisture value fluctuates in the monsoon period due to its terrain characteristics. Since the location is on the upper terrain the soil moisture values dips low and then again raises high. The upland phenomenon characteristics are shown in the soil moisture trend.

In mountainous or hilly terrains soil water distribution is controlled by vertical and horizontal water divergence and convergence, infiltration recharge and evapotranspiration which affects the soil moisture value especially in the place like Haripur in Uttarakhand. Soil moisture decreases with increasing hill slope, although there is a significant amount of rainfall.

In this entire section it must be take in to consideration that validating grid based soil moisture product with point based ground observations will not give any clear picture about the accuracy of derived soil moisture product (blended soil moisture product). As reported by many researchers the highest correlation coefficient achievable between points based ground observations and grid based soil moisture product is in the range of 0.4 to 0.7. So the attempt is made in above section to validate general nature/trend of blended soil moisture product with respect to agro-climatic information available of all the test sites. It is noteworthy that the

blended product follows the general soil moisture trend of all the test sites. Having proven the worthiness of blending of soil moisture, the methodology is extended on regional scale and the results are discussed in next section

5.4.6 Blended soil moisture dataset for the Ganga basin

The study area, Ganga basin has larger extent of snow covered area in the upper reaches of Himalaya. The soil moisture retrieval and molding algorithms cannot generally work for the snow and glacier covers, so a permanent snow mask for the basin is generated using MODIS snow cover product (Source: GLOVIS, MOD 10 Snow Cover product), the snow cover area is masked out of the further processing.

The CDF matching and blending approach as discussed in sections 5.3 and 5.4 are applied in the regional scale and the daily blended soil moisture product is generated.

The representative blended soil moisture products of each month are shown in Fig 5.32

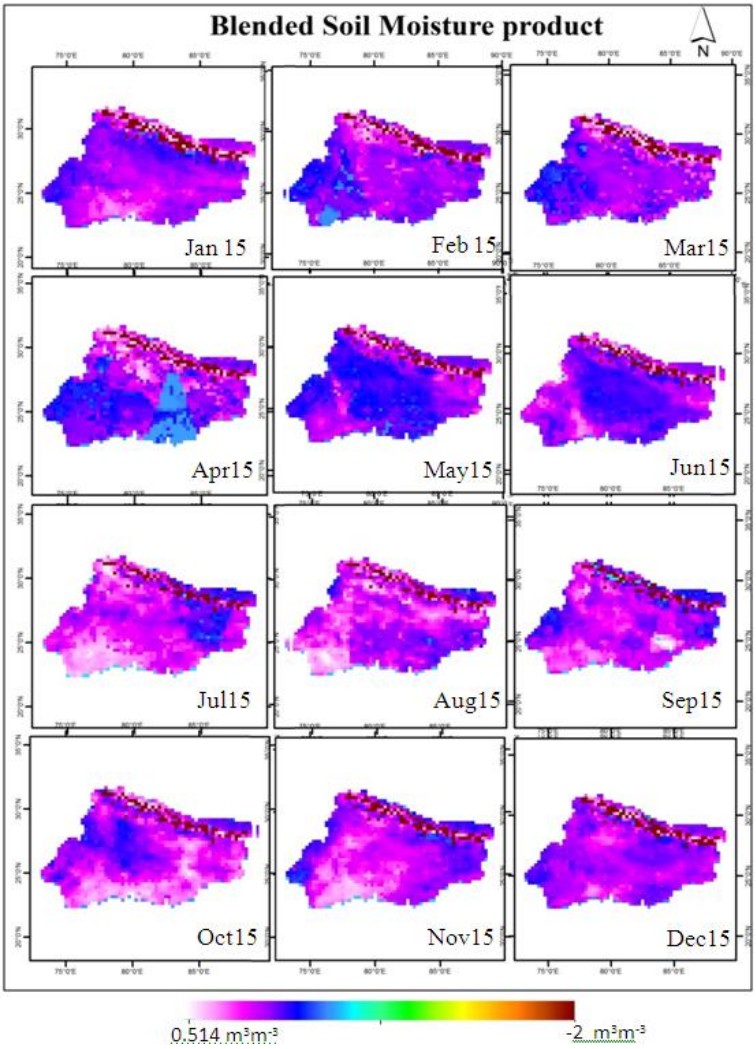

Fig. 5.32: Blended Soil Moisture product for the year 2009.

5.5 SOIL MOISTURE ANALYSIS WITH RESPECT TO RAINFALL IN THE MONSOON PERIOD

To analyze the blended soil moisture product with that of the rainfall pattern, first 15 days of the rainfall is added to get the 15 day rainfall amount for the two month period August and September, and the soil moisture is then compared with the rainfall (Fig 5.33).

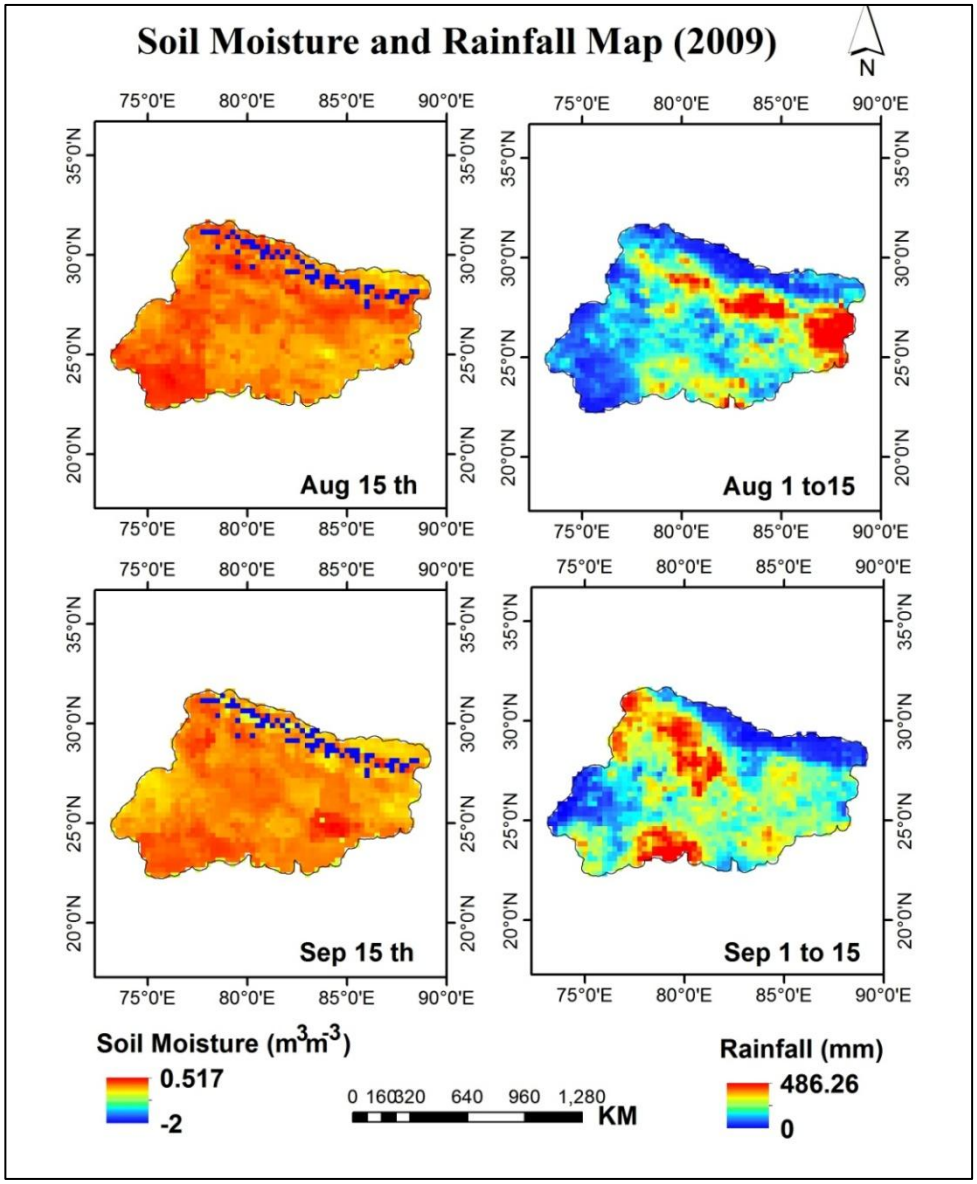

Fig. 5.33: Blended Soil Moisture product in comparison with 15 day rainfall for the month August and September in 2009.

The upper part of Ganga basin experiences heavy rainfall in the August, specifically in the area of Nepal and eastern part of Bihar with moderate rainfall in various parts of Uttar Pradesh, entire Bihar and some parts of Madhya Pradesh too. Similarly there is a high soil moisture value of a 0.24 m^3m^{-3} in the northern regions and central India. The Parts of Nepal in the upper Ganga basin also have relatively high soil moisture value as compared to the rest of the basin.
Whereas in the month of September the monsoon shifts towards North West, there is a heavy rainfall in Uttarakhand, central Uttar Pradesh, and central Madhya Pradesh covering almost all of MP. It is also providing the information that the southern part of Himachal Pradesh, touching Uttarakhand has experienced heavy rainfall too. There is very low rainfall in the western part that is the region of Rajasthan and upper part of Ganga basin that is in the Nepal. Following the rainfall trends there is a clear visibility of high soil moisture in the parts of Uttar Pradesh and Madhya Pradesh. The southern part of Bihar has also observed very high soil moisture due to the preceding 15 days rainfall.

Although the year 2009 has deficient rainfall almost all over the country (Source: IMD, Government of India) including the regions coming under Ganga basin, the soil moisture value is showing considerable value, corresponding to the amount of rainfall occurred in the respective area.

5.6 APPLICATION PERSPECTIVE OF BLENDING

The main motive in performing the blending of soil moisture is to improve the spatial and temporal resolution of the soil moisture dataset. The soil moisture data retrieved from passive remote sensor that is AMSR-E has various locations where there is lack of data or unavailability of data as seen as white portion in the AMSR-E map in the Fig 5.34, where there is either "no-data" and active sensor lacks the daily coverage for the retrieval of soil moisture.

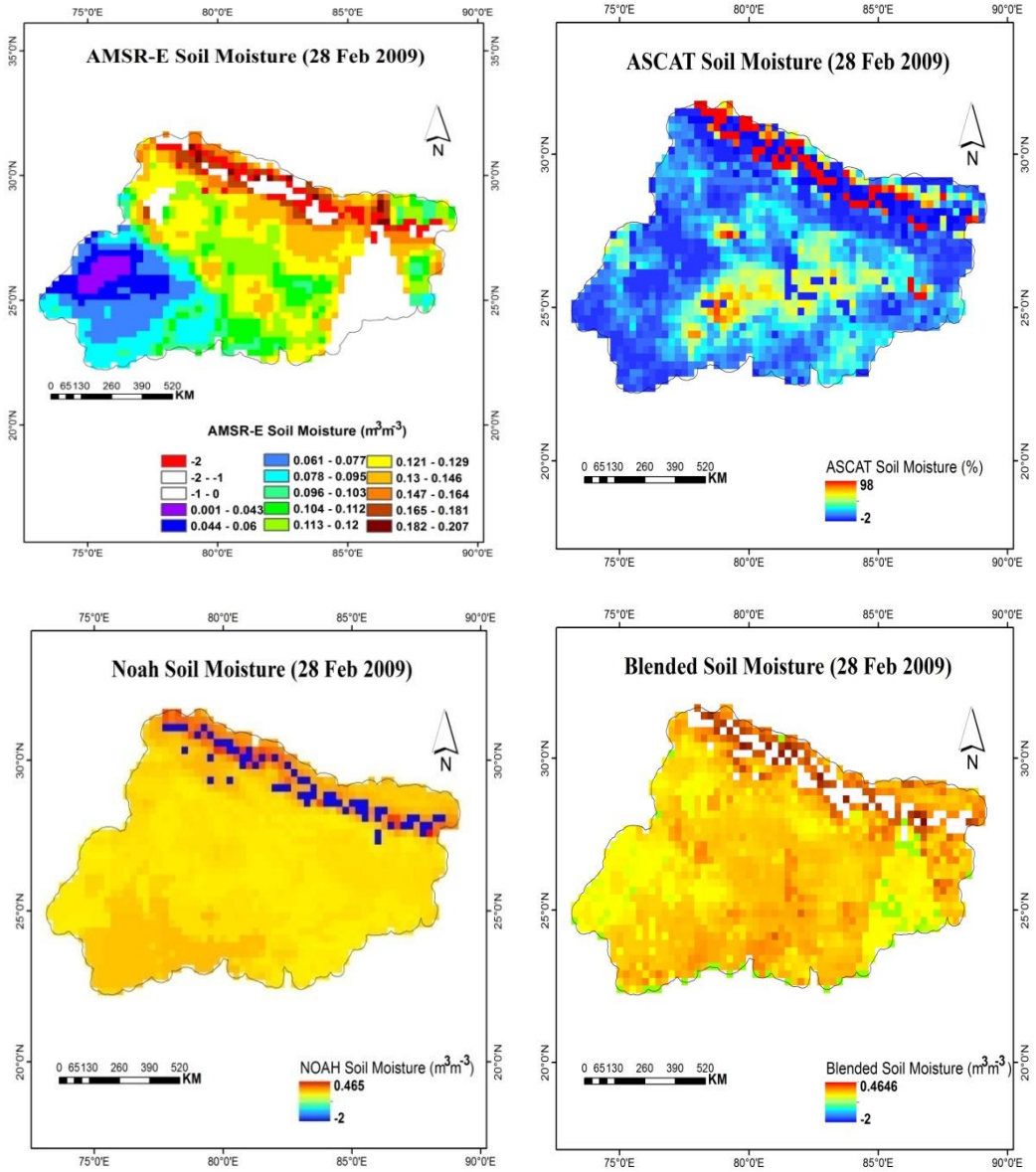

Fig. 3.34: Soil Moisture dataset of AMSR-E, ASCAT, Noah and Blended data.

The blended soil moisture data in Fig 5.34 overcomes this limitation by providing the soil moisture value at the location where the data was initially unavailable and ASCAT soil moisture data is not available on the daily basis. This limitation prevails if this kind of approach is not followed. The enhancement of the information by combining both products helps in understanding various aspects of the land and atmosphere and the interaction between both. For most application the reproduction of relative dynamics of soil moisture are important than the absolute values making this product more practically feasible in various end user applications.

In the legend of Fig 5.34, '-2' value indicates snow covered area and '-1' value represents "no-data" or unavailability of data.

5.7 VALIDATION OF SOIL MOISTURE MERGED DATA PRODUCT

The merged soil moisture product is correlated with the ground data as mentioned in the methodology for the chosen station location in China. The correlation value is *0.58* that is approximately equal to *0.6*. The Scatterplot of the ground data and the blended soil moisture dataset is shown in Fig 5.35 and the plot showing the trend of blended soil moisture product and the ground soil moisture product is shown in the Fig 5.36.

The correlation is estimated between the merged soil moisture dataset from AMSR-E and ASCAT and the ground soil moisture data. The correlation between the satellite and the *in-situ* data are usually not very high and the value range between 0.5 - 0.8 and a complete lack of correlation does not necessarily mean that the satellite data is wrong (Wagner et al., 2013b).

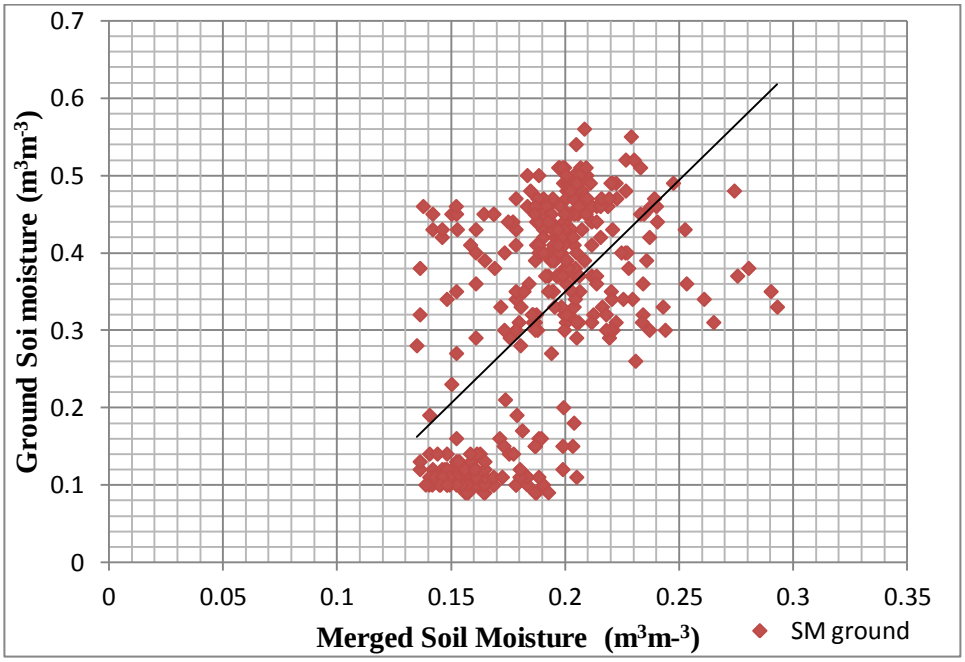

Fig. 5.35: Scatterplot of ground soil moisture dataset and blended soil moisture data.

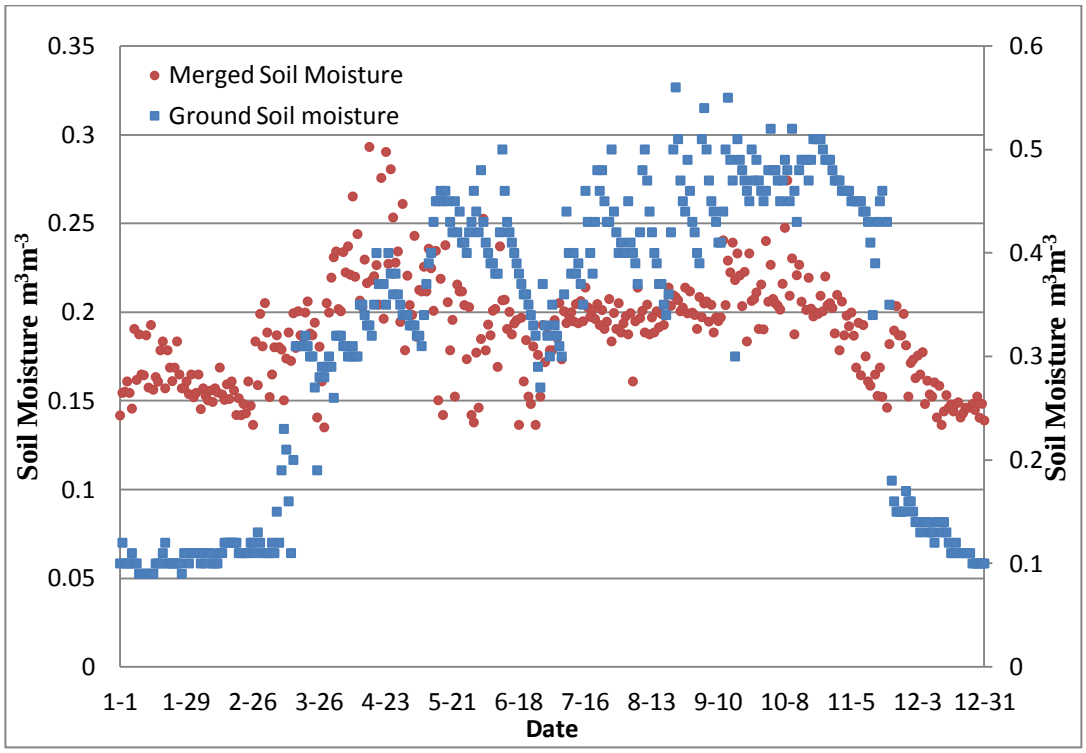

Fig. 5.36: Plot of comparison of blended soil moisture data and ground soil moisture.

The correlation coefficient values are different for the input data, rescaled AMSR-E, ASCAT soil moisture data and the blended data. The ground data have good correlation with the ASCAT data, initially with 0.8564 and reduces to value 0.792 after the rescaling procedure as in the Table 5.6. The higher correlation coefficient of ASCAT has provided an advantage that is, after the merging with lower correlated value of AMSR-E; the blended product has acceptable R value. Due to the spatial extent and sensor attributes, ASCAT has acquired a higher correlation value for the respective study area (Wagner et al., 2013b).

Table 5.6: Comparison chart of the correlation coefficient(R) value.

Jan 2009 to Dec 2009						
Ground Point	AMSR-E	ASCAT	Noah Model	Blended product	AMSR-E Rescaled	ASCAT Rescaled
MAQU - CST 02	0.3985	0.8564	0.112	0.5812(~0.6)	0.4534	0.7920

CHAPTER - 6
CONCLUSIONS AND RECOMMENDATIONS

6.1 SUMMARY AND CONCLUSION

Soil moisture, an essential hydrological parameter, varies with space and time. This parameter has influence on both hydrological and energy balance of our environment. Soil moisture is the key to comprehend the spatial variability and scale problems that are paramount in hydrology, meteorology and climatology. A time series soil moisture dataset for a region provides valuable information as climate change, crop water requirement and water resource management studies. Microwave remote sensing is recognized as a potential method for estimating soil moisture due to its low frequency observations at 5-7 GHz and high penetration capability. Soil moisture mapping using the passive microwave sensors have a limitation of spatial gaps, primarily existing due to the swath widths and the satellite orbits, whereas the active sensor have temporal voids, i.e. low temporal resolution. The process of blending is the technique to merge two or more different soil moisture dataset to improve the resolution, with higher spatial coverage over the entire study area. An attempt has been made in present study to improve the temporal and spatial quality of soil moisture product (RS derived) using three different soil moisture products. The broad conclusions drawn from this research are mentioned in this chapter.

Soil moisture has been derived using Radiative Transfer (RT) method from the AMSR-E brightness temperature (Tb) for the year 2009 respectively considering various sensor as well as soil and vegetation parameters. The parameters have been derived from the literature, whereas vegetation water content as a parameter is retrieved from the AMSR-E sensor. The soil moisture derived through an algorithm using Tb has a values nearer to the satellite soil moisture product, although it lacks the accuracy and closeness to the satellite product as Radio Frequency Interference (RFI) factor, vertical and horizontal heterogeneity factor is not considered while retrieval. Hence, the standard satellite derived soil moisture product available on global scale is utilized for the purpose of blending to derive an improved soil moisture dataset.

Varying microwave frequencies in the soil moisture retrieval are related with the different soil sampling depths and vegetation optical depths resulting in spatial and temporal errors and heterogeneities during retrieval from satellite sensors and different instruments and that propagates in the soil moisture product. Cumulative distribution frequency (CDF) matching approach considers the means of retrievals from sensors and resulting trend of the merged product is analyzed accordingly. Cumulative distribution frequency (CDF) matching technique has been applied for rescaling VUA-NASA AMSR-E and TU-Wein ASCAT C-band soil moisture dataset. The AMSR-E and ASCAT products are rescaled against GLDAS-Noah simulated soil moisture product. This method does not change the temporal pattern of the original soil moisture dataset. The time series trend of the original dataset is restored in the scaled dataset.

The blending is performed initially at the point scale basis for various locations. Each location selected has different land use land cover (LULC), meteorological and agricultural

characteristics, which have a profound effect on the soil moisture behavior. A yearly soil moisture trend is observed at these locations. Every location has a dominant characteristic and accordingly the soil moisture trend follows. In the location Mahendargarh, soil moisture value varies from 0.079 to 0.32 m^3m^{-3} during the monsoon period. In Sova the soil moisture for the year 2009 varies from 0.05 to not a very value of 0.125 m^3m^{-3}. In Hoshangabad soil moisture reaches maximum upto 0.4234 m^3m^{-3} and similarly in Bargarh the value reaches to 0.465 m^3m^{-3} in the period of monsoon.

The process of blending applied on a larger region (Ganga Basin) depicts the soil moisture variation on the daily as well as monthly scale. Soil moisture variation for a region depends on the monsoon period, crop cycle, and crop type. Soil moisture derived from AMSR-E and ASCAT lacks the spatial coverage and temporal resolution. There are many areas in the study area where unavailability of soil moisture is there; similarly the soil moisture value is not obtainable on the daily basis due to poor temporal resolution for the active sensor. The blended soil moisture dataset has covered the entire study area (Ganga Basin) with daily soil moisture estimations. The soil moisture observed at a specific location gives a yearly trend, while considering the region as a whole, soil moisture variation is observed in a larger domain.

In comparison with *in-situ* measurements, satellite products are well correlated with correlation coefficient (R) ≈ 0.6. The enhancement of information by the process of blending the passive and active microwave products help in understanding land surface atmospheric interactions and additionally improving the weather and climate prediction skills over the study area. Development of a dataset along these criteria enables better estimation of various hydrological parameters increases understanding of terrestrial hydrology and vegetation dynamics.

6.2 RECOMMENDATIONS

The following are the recommendations for the future scope and work,

1. The approach and the algorithm would be applicable to both past and current records, and also for the future missions that are expected to bring higher accuracy and improved merged product of the soil moisture, ,e.g. Soil Moisture and Ocean Salinity Mission (SMOS) and Soil Moisture Active Passive (SMAP), Radar Imaging Satellite (RISAT).
2. The scope of improvement is to reduce the effect of radio frequency interference (RFI) on the AMSR-E C-band retrievals observed in Indian subcontinent.
3. Fulfilling the gaps in the satellite based soil moisture products in a considerate manner is one of the highlight for the future analysis.
4. A higher need of ground soil moisture data for the Indian location is recommended vol validation and improvements.

References

Álvarez-Mozos, J., Verhoest, N.E.C., Larrañaga, A., Casalí, J., González-Audícana, M., 2009. Influence of Surface Roughness Spatial Variability and Temporal Dynamics on the Retrieval of Soil Moisture from SAR Observations. Sensors 9, 463–489.

Baghdadi, N., Zribi, M., Loumagne, C., Ansart, P., Anguela, T., 2008. Analysis of TerraSAR-X data and their sensitivity to soil surface parameters over bare agricultural fields. Remote Sens. Environ. 112, 4370–4379.

Barrett, B.W., Dwyer, E., Whelan, P., 2009. Soil Moisture Retrieval from Active Spaceborne Microwave Observations: An Evaluation of Current Techniques. Remote Sens. 1, 210–242.

Brocca, L., Melone, F., Moramarco, T., Morbidelli, R., 2009. Antecedent wetness conditions based on ERS scatterometer data. J. Hydrol. 364, 73–87.

Champagne, C., McNairn, H., Berg, A.A., 2011. Monitoring agricultural soil moisture extremes in Canada using passive microwave remote sensing. Remote Sens. Environ. 115, 2434–2444.

Chanasyk, D.S., Naeth, M.A., 1996. Field measurement of soil moisture using neutron probes. Can. J. Soil Sci. 76, 317–323.

Chauhan, N.S., 1997. Soil moisture estimation under a vegetation cover: Combined active passive microwave remote sensing approach. Int. J. Remote Sens. 18, 1079–1097.

Chauhan, N.S., Le Vine, D.M., Lang, R.H., 1994. Discrete scatter model for microwave radar and radiometer response to corn: comparison of theory and data. Geosci. Remote Sens. Ieee Trans. 32, 416–426.

Chen, K.S., Tzong-Dar Wu, Leung Tsang, Qin Li, Jiancheng Shi, Fung, A.K., 2003. Emission of rough surfaces calculated by the integral equation method with comparison to three-dimensional moment method simulations. Ieee Trans. Geosci. Remote Sens. 41, 90–101.

Chen, K.S., Yen, S.K., Huang, W.P., 1995. A simple model for retrieving bare soil moisture from radar-scattering coefficients. Remote Sens. Environ. 54, 121–126.

D'Urso, G., Minacapilli, M., 2006. A semi-empirical approach for surface soil water content estimation from radar data without a-priori information on surface roughness. J. Hydrol. 321, 297–310.

Dharssi, I., Bovis, K.J., Macpherson, B., Jones, C.P., 2011. Operational assimilation of ASCAT surface soil wetness at the Met Office. Hydrol. Earth Syst. Sci. 15, 2729–2746.

Dobriyal, P., Qureshi, A., Badola, R., Hussain, S.A., 2012. A review of the methods available for estimating soil moisture and its implications for water resource management. J. Hydrol. 458-459, 110–117.

Dobson, M.C., Ulaby, F.T., 1986. Active microwave soil moisture research. Geosci. Remote Sens. Ieee Trans. 23–36.

Dobson, M.C., Ulaby, F.T., Hallikainen, M.T., El-Rayes, M.A., 1985. Microwave dielectric behavior of wet soil-Part II: Dielectric mixing models. Geosci. Remote Sens. Ieee Trans. 35–46.

Dobson, M.C., Kouyate Fatou, Ulaby, F.T., 1984. A Reexamination of Soil Textural Effects on Microwave Emission and Backscattering, Geosci. Remote Sens. Ieee Trans. Vol. GE-22, No.6

Dubois, P.C., Van Zyl, J., Engman, T., 1995. Measuring soil moisture with imaging radars. Geosci. Remote Sens. Ieee Trans. 33, 915–926.

Dubois-Fernandez, P.C., Souyris, J.-C., Angelliaume, Sé., Garestier, F., 2008. The Compact Polarimetry Alternative for Spaceborne SAR at Low Frequency. Ieee Trans. Geosci. Remote Sens. 46, 3208–3222.

Famiglietti, J.S., Devereaux, J.A., Laymon, C.A., Tsegaye, T., Houser, P.R., Jackson, T.J., Graham, S.T., Rodell, M., Oevelen, P. van, 1999. Ground-based investigation of soil moisture variability within remote sensing footprints during the Southern Great Plains 1997 (SGP97) Hydrology Experiment. Water Resour. Res. 35, 1839–1851.

Fensholt, R., Sandholt, I., 2003. Derivation of a shortwave infrared water stress index from MODIS near- and shortwave infrared data in a semiarid environment. Remote Sens. Environ. 87, 111–121.

Ferranti, L., Viterbo, P., 2006. The European summer of 2003: Sensitivity to soil water initial conditions. J. Clim. 19, 3659–3680.

Fung, A.K., Dawson, M.S., Chen, K.S., Hsu, A.Y., Engman, E.T., O'Neill, P.O., Wang, J., 1996. A modified IEM model for: scattering from soil surfaces with application to soil moisture sensing, in: Geoscience and Remote Sensing Symposium, 1996. IGARSS'96.'Remote Sensing for a Sustainable Future.', International. pp. 1297–1299.

Fung, A.K., Li, Z., Chen, K.S., 1992. Backscattering from a randomly rough dielectric surface. Geosci. Remote Sens. Ieee Trans. 30, 356–369.

Gao, B.-C., 1996. NDWI—a normalized difference water index for remote sensing of vegetation liquid water from space. Remote Sens. Environ. 58, 257–266.

Gavin, H ., 2011, The Levenberg-Marquardt method for nonlinear least squares curve-fitting problems, Department of Civil and Environmental Engineering Duke University

Gupta, V.K., Jangid, R.A., 2011. The Effect of Bulk Density on Emission Behavior of Soil at Microwave Frequencies. Int. J. Microw. Sci. Technol. 2011, 1–6.

Hallikainen, M.T., Ulaby, F.T., Dobson, M.C., El-Rayes, M.A., Wu, L.-K., 1985. Microwave dielectric behavior of wet soil-part 1: empirical models and experimental observations. Geosci. Remote Sens. Ieee Trans. 25–34.

Hofer, R., Njoku, E.G., 1981. Regression techniques for oceanographic parameter retrieval using space-borne microwave radiometry. Geosci. Remote Sens. Ieee Trans. 178–189.

Hui Lu, Toshio Koike, Tetsu Ohta, David Ndegwa Kuria, Kun Yang, Hideyuki Fujii, Hiroyuki Tsutsui, Katsunori Tamagawa, 2009. Monitoring Soil Moisture from Spaceborne Passive Microwave Radiometers: Algorithm Developments and Applications to AMSR-E and SSM/I.

Jackson, T.J., Hsu, A.Y., O'Neill, P.E., 2002. Surface soil moisture retrieval and mapping using high-frequency microwave satellite observations in the Southern Great Plains. J. Hydrometeorol. 3, 688–699.

Jackson, T.J., Schmugge, T.J., 1991. Vegetation effects on the microwave emission of soils. Remote Sens. Environ. 36, 203–212.

Khanna, S., Palacios-Orueta, A., Whiting, M.L., Ustin, S.L., Riaño, D., Litago, J., 2007. Development of angle indexes for soil moisture estimation, dry matter detection and land-cover discrimination. Remote Sens. Environ. 109, 154–165.

Lacava, T., Cuomo, V., Di Leo, E.V., Pergola, N., Romano, F., Tramutoli, V., 2005. Improving soil wetness variations monitoring from passive microwave satellite data: The case of April 2000 Hungary flood. Remote Sens. Environ. 96, 135–148.

Le Vine, D.M., Karam, M.A., 1996. Dependence of attenuation in a vegetation canopy on frequency and plant water content. Geosci. Remote Sens. Ieee Trans. 34, 1090–1096.

Lee, K., 2004. A combined passive/active microwave remote sensing approach for surface variable retrieval using Tropical Rainfall Measuring Mission observations. Remote Sens. Environ. 92, 112–125.

Liu, Y.Y., Dorigo, W.A., Parinussa, R.M., de Jeu, R.A.M., Wagner, W., McCabe, M.F., Evans, J.P., van Dijk, A.I.J.M., 2012. Trend-preserving blending of passive and active microwave soil moisture retrievals. Remote Sens. Environ. 123, 280–297.

Liu, Y.Y., Parinussa, R.M., Dorigo, W.A., De Jeu, R.A.M., Wagner, W., van Dijk, A.I.J.M., McCabe, M.F., Evans, J.P., 2011. Developing an improved soil moisture dataset by blending passive and active microwave satellite-based retrievals. Hydrol. Earth Syst. Sci. 15, 425–436.

Liu, Y.Y., van Dijk, A.I.J.M., de Jeu, R.A.M., Holmes, T.R.H., 2009. An analysis of spatiotemporal variations of soil and vegetation moisture from a 29-year satellite-derived data set over mainland Australia. Water Resour. Res. 45.

Liu, Y.Y., McCabe, M.F., Evans, J.P., van Dijk, A.I.J.M., De Jeu, R.A.M., Su H., Comparison of Soil Moisture in GLDAS model Simulations and Satellite Observations over Murray Darling Basin.

Lourakis, M.I., 2005. A brief description of the Levenberg-Marquardt algorithm implemented by levmar. Inst. Comput. Sci. Found. Res. Technol. 11.

Martti, T., Hallikainen, Fawwaz ,T., Ulaby, Myron, C.,Ddobson, Mohamed, A., El-Rayes, Lin-Kun Wu, 1985. Microwave Dielectric Behavior of Wet Soil- art 1:Empirical Models and Experimental Observations, ieee Transactions on Geoscience and Remote Sensing, Vol. GE-23, NO. 1

Matgen, P., Fenicia, F., Heitz, S., Plaza, D., de Keyser, R., Pauwels, V.R.N., Wagner, W., Savenije, H., 2012. Can ASCAT-derived soil wetness indices reduce predictive uncertainty in well-gauged areas? A comparison with in situ observed soil moisture in an assimilation application. Adv. Water Resour. 44, 49–65.

McLauchlan, P.F., 2001. Levenberg-Marquardt minimisation. Univ. Surrey.

Molden, D.J., Sakthivadivel, R., Keller, J., International Irrigation Management Institute, 2001. Hydronomic zones for developing basin water conservation strategies. International Irrigation Management Institute, Colombo, Sri Lanka.

Montosi, E., Manzoni, S., Porporato, A., Montanari, A., 2012. An ecohydrological model of malaria outbreaks. Hydrol. Earth Syst. Sci. 16, 2759–2769.

Moran, M.S., Clarke, T.R., Inoue, Y., Vidal, A., 1994. Estimating crop water deficit using the relation between surface-air temperature and spectral vegetation index. Remote Sens. Environ. 49, 246–263.

Neusch, T., Sties, M., 1999. Application of the Dubois-model using experimental synthetic aperture radar data for the determination of soil moisture and surface roughness. Isprs J. Photogramm. Remote Sens. 54, 273–278.

Njoku, E.G., 1999. AMSR Land Surface Parameters.

Njoku, E.G., Entekhabi, D., 1996. Passive microwave remote sensing of soil moisture. J. Hydrol. 184, 101–129.

Njoku, E.G., Li, L., 1999. Retrieval of land surface parameters using passive microwave measurements at 6-18 GHz. Geosci. Remote Sens. Ieee Trans. 37, 79–93.

Oh, Y., Sarabandi, K., Ulaby, F.T., 1992. An empirical model and an inversion technique for radar scattering from bare soil surfaces. Geosci. Remote Sens. Ieee Trans. 30, 370–381.

Palacios-Orueta, A., Khanna, S., Litago, J., Whiting, M.L., Ustin, S.L., 2006. Assessment of NDVI and NDWI spectral indices using MODIS time series analysis and development of a new spectral index based on MODIS shortwave infrared bands. pp. 207–209.

Peplinski, N.R., Ulaby, F.T., Dobson, M.C., 1995. Dielectric properties of soils in the 0.3-1.3-GHz range. Geosci. Remote Sens. Ieee Trans. 33, 803–807.

Raney, R.K., 2007. Hybrid-Polarity SAR Architecture. Ieee Trans. Geosci. Remote Sens. 45, 3397–3404.

Ranganathan, A., 2004. The levenberg-marquardt algorithm. Tutoral Lm Algorithm.

Reichle, R.H., 2004. Bias reduction in short records of satellite soil moisture. Geophys. Res. Lett. 31.

Rodell, M., Houser, P.R., Jambor, U., Gottschalck, J., Mitchell, K., Meng, C.-J., Arsenault, K., Cosgrove, B., Radakovich, J., Bosilovich, M., Entin*, J.K., Walker, J.P., Lohmann, D., Toll, D., 2004. The Global Land Data Assimilation System. Bull. Am. Meteorol. Soc. 85, 381–394.

Schmugge, T., and Jackson T.J., 1993, Passive Microwave Remote Sensing of Soil Moisture, EARSeL Advances in remote Sensing, Vol.2, No.2 - VI.

Schmugge, T., Jackson T.J and McKIM H. L., 1980. Survey of Methods for Soil Moisture Determination, Water Resources Research, Vol. 16, No. 6, Pg- 961-979

Scott, A., Christopher., Bastiaanssen, G.M., Wimn., Ahmed, Mobin-ud-Din., 2003. Mapping root Zone Soil MOisture using remotely Sensed Optical Imagery, Journal of Irrigation and Drainage Engineering, ASCE.

Shi, J., Wang, J., Hsu, A.Y., O'Neill, P.E., Engman, E.T., 1997. Estimation of bare surface soil moisture and surface roughness parameter using L-band SAR image data. Geosci. Remote Sens. Ieee Trans. 35, 1254–1266.

Spans, G., 1978. An empirical model for the complex dielectric permittivity of soils as a function of water content.

Stafford, J.V., 1988. Remote, non-contact and< i> in-situ</i> measurement of soil moisture content: a review. J. Agric. Eng. Res. 41, 151–172.

Ulaby, F.T., Batlivala, P.P., 1976. Optimum radar parameters for mapping soil moisture. Geosci. Electron. Ieee Trans. 14, 81–93.

Ulaby, F.T., Batlivala, P.P., Dobson, M.C., 1978. Microwave backscatter dependence on surface roughness, soil moisture, and soil texture: Part I-bare soil. Geosci. Electron. Ieee Trans. 16, 286–295.

Ulaby, F.T., Moore, R.K., Fung, A.K., 1981a. Microwave Remote Sensing: Active and Passive. Microwave remote sensing fundamentals and radiometry. 1. Addison-Wesley Publishing Company, Advanced Book Program/World Science Division.

Ulaby, F.T., Moore, R.K., Fung, A.K., 1981b. Microwave Remote Sensing: From theory to applications. Addison-Wesley Publishing Company, Advanced Book Program/World Science Division.

Van Zyl, J.J., Kim, Y., 2001. A quantitative comparison of soil moisture inversion algorithms, in: Geoscience and Remote Sensing Symposium, 2001. IGARSS'01. IEEE 2001 International. pp. 37–39.

Verstraeten, W.W., Veroustraete, F., Wagner, W., Roey, T., Heyns, W., Verbeiren, S., Feyen, J., 2010. Remotely sensed soil moisture integration in an ecosystem carbon flux model. The spatial implication. Clim. Change 103, 117–136.

Wagner, W., Hahn, S., Kidd, R., Melzer, T., Bartalis, Z., Hasenauer, S., Figa-Saldaña, J., de Rosnay, P., Jann, A., Schneider, S., Komma, J., Kubu, G., Brugger, K., Aubrecht, C., Züger, J., Gangkofner, U., Kienberger, S., Brocca, L., Wang, Y., Blöschl, G., Eitzinger, J., Steinnocher, K., Zeil, P., Rubel, F., 2013. The ASCAT Soil Moisture Product: A Review of its Specifications, Validation Results, and Emerging Applications. Meteorol. Z. 22, 5–33.

Wagner, W., 2008. Remote Sensing of Soil Moisture in Support to Hydrological and Meteorological Modelling, METIER Training Course "Remote Sensing of the Hydrosphere" Finish Environment Institute, Helsinki, Finland.

Wardlow, B.D., Anderson, M.C., Verdin, J.P., 2012. Remote Sensing of Drought: Innovative Monitoring Approaches. CRC Press.

Wen, B., Tsang, L., Winebrenner, D.P., Ishimaru, A., 1990. Dense medium radiative transfer theory: comparison with experiment and application to microwave remote sensing and polarimetry. Geosci. Remote Sens. Ieee Trans. 28, 46–59.

Whiting, M.L., Li, L., Ustin, S.L., 2004. Predicting water content using Gaussian model on soil spectra. Remote Sens. Environ. 89, 535–552.

Wigneron, J.-P., Calvet, J.-C., Pellarin, T., Van de Griend, A.., Berger, M., Ferrazzoli, P., 2003. Retrieving near-surface soil moisture from microwave radiometric observations: current status and future plans. Remote Sens. Environ. 85, 489–506.

APPENDIX - I
PROGRAM STEP 1 OUTPUT

Notepad files are created for all the three dataset (AMSR-E, ASCAT and Noah), having cumulative distribution frequency (CDF) values at the defined interval with the help of python programming language. (Python 2.6.5)

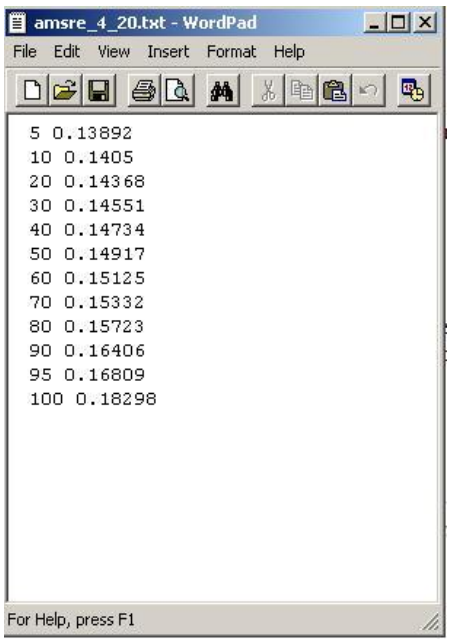

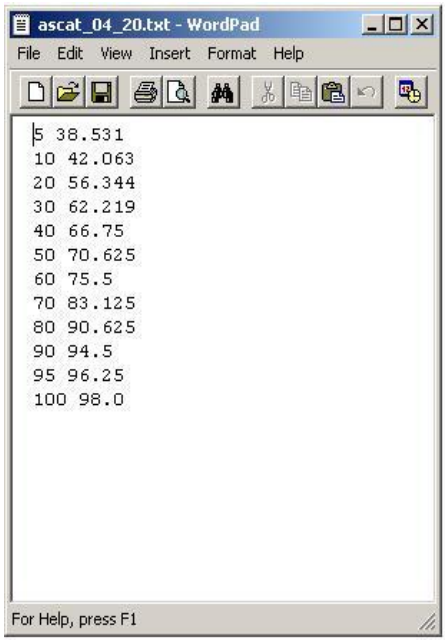

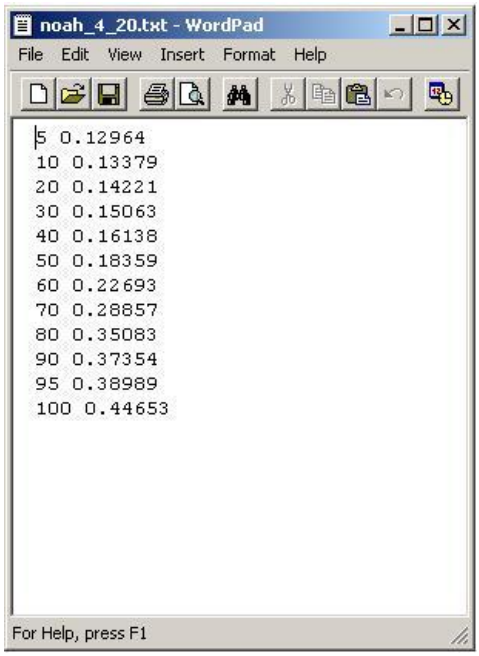

APPENDIX - II
PROGRAM STEP 2 OUTPUT

Slope (m) and intercept (c) values are calculated for all 11 segments for each pixel in the step II between the CDF plot of AMSR-E – Noah and ASCAT – Noah with the aid of coding.